EFFECTS OF TRANSVERSE SHEAR DEFORMATION ON MAXIMUM DEFLECTION OF COMPOSITE BEAMS WITH VARIOUS LAMINATE CONFIGURATIONS AND BOUNDARY CONDITIONS

by

WEI-TSEN LU

Presented to the Faculty of the Graduate School of

The University of Texas at Arlington in Partial Fulfillment

of the Requirements

for the Degree of

MASTER OF SCIENCE IN AEROSPACE ENGINEERING

THE UNIVERSITY OF TEXAS AT ARLINGTON

AUGUST 2015

Acknowledgements

I must express my appreciation and gratitude to my supervising professor, Dr. Wen Chan, for his guidance, support, and encouragement throughout my research in every aspect especially in composite fields. This thesis could not have been completed without his efforts. He also treats all students as his children. I will always consider him as my “Academic Father”.

In addition, I would like to express my sincere thanks to Dr. Ashfaq Adnan and Dr. Seiichi Nomura, committee members, for their valuable advice and assistance.

I would like to thank the entire faculty of Mechanical and Aerospace Engineering for their help in building by understanding of the subject.

I would like to thank my friend, Alistair and Ming Feng, for their assistance and encouragement at this thesis.

Finally, I would to thank my parents for their patience and encouragement. Without their support, I cannot fulfill my dream. I would like to express my special acknowledgment to my girlfriend, Ching Wen Hwang. She very supports me during the time of study. Without her support and understanding, this thesis would not have been completed.

August 7, 2015

Abstract

EFFECTS OF TRANSVERSE SHEAR DEFORMATION ON MAXIMUM DEFLECTION OF COMPOSITE BEAMS WITH VARIOUS LAMINATE CONFIGURATIONS AND BOUNDARY CONDITIONS

Wei-Tsen Lu, M.S.

The University of Texas at Arlington, 2015

Supervising Professor: Wen S. Chan

Analytical methods are developed for determining deflection of composite beams under transverse load with various boundary conditions and laminate configurations. The present methods include development of expression for 1-D equivalent bending stiffness with and without presence of twisting curvature and prediction of the beam deflection accounting for transverse shear effect. Finite element analysis of 3-D ANSYS models is conducted by using Solid186 elements. The present analytical model is executed by using MATLAB program. Both analytical and FEM models were first validated by using isotropic material in the model and comparing the existing solutions.

The composite beams with rectangular cross-section and small ratios of its length to its width and its width to its depth were selected for study. These conditions were chosen for enhancing the effect of the shear deformation. Various boundary conditions used for study include simply support, fixed at both ends, and cantilever beams under uniformly distributed or concentrated load, respectively. The maximum deflection of composite beams is investigated for transverse shear effects due to laminates with symmetric vs unsymmetrical layups and balanced vs unbalanced layups.

Among all of the case studies, the analytical results agree well with the results obtained from FEM.

It is found that for a given laminated beam under the same type of loading, effect of transverse shear on beam deflection is identical regardless with simply supported and fixed both ends but more pronounced for the case of cantilever beam. However, the effect of shear deformation on beam deflection due to stacking sequence is insignificant regardless of the type of loading.

Table of Contents

List of Illustrations

List of Tables

Chapter 1

Introduction

1.1 Overview of Composite Materials

In a broad sense the word “composite” means “made of two or more different parts”. A composite material contains two or more materials which are combined in a macroscopic scale to get the useful third material whose mechanical performance and properties are superior to those of the constituent material acting independently. There are two phases of the composite. One phase is continuous phase which is called *matrix*. The other phase is discontinuous phase which is called *reinforcement*, or *reinforcing material*. The properties of composite material result from properties of the constituent materials, their geometrical distribution, and their interaction. Thus, to describe a composite material, it will be necessary to specify the nature of the constituents and their properties, the geometry of the reinforcement and its distribution, and the reinforcement interface.

The phase of the composite system plays different roles, which depend on the type of the application of the composite material. The reinforcement, usually in the form of fibers, may provide some stiffening but only limited strengthening of the material in the case of low to medium performance composite materials. On the other hand, the matrix is the main load-bearing constituent governing in the mechanical properties of the material. In the case of high performance composite materials, continuous fiber reinforcement is the backbone of the material. The matrix phase provides protection for the sensitive fibers, bonding, support, and local stress transfer from one fiber to another. The interface can play an important role in controlling the failure mechanisms, failure propagation, fracture toughness, and the overall stress-strain behavior to failure of the material.

Advanced composites are becoming more widely used as alternative to metallic structures. Applications of composites have been used to the aircraft, marine, automotive, sporting goods, biomedical industries, civil construction, and aerospace structures because of following reasons.

- High specific stiffness
- High specific strength
- Low density
- Design flexibility
- Corrosion resistance
- Low thermal expansion
- Parts count reduction
- Easy fabrication

Aerospace structures, for example, have to operate in a very high degree of dimensional stability under environment conditions. Some composites can be applied in the aerospace structures because they can be designed to have nearly zero coefficient of thermal expansion.

The high specific stiffness, high specific strength, and low density characteristics makes composites highly desirable in primary and secondary structures of both military and civilian aircrafts. The strongest sign of acceptance of composites in civil aviation is using in Boeing 787, and the world largest airliner, Airbus A380. Composite materials account for approximately 50% of the weight of the Boeing 787, including most of the fuselage and wings.

One of the important advantages of composites is reducing in acquisition and life circle due to weight savings, lower tooling costs, reduced number of parts and joints, and reduced maintenance. These advantages are diluted when considering the high cost of raw materials, fiber, and auxiliary materials used in fabrication and assembly of composite structures.

Composite structure design can be validated by three different methods on their performance – closed form analytical solutions, finite element Method, and testing. In fact composite structures are normally certified by test not by the analysis although testing in nature is very tedious and expansive. In these cases, finite element method takes advantages because it can deal with large and complex structures with high accuracy. However, in design stage, parametric study is often performed to determine the optimal design of laminate configuration. Hence, it is not an efficient analysis tool. As a result, a simplified structure should be used to perform an initial analysis by using the theoretical or analytical solutions. Also, once the parameters are programmed into mathematical software, it is easily modified the changes and effects of each variables. It should be check for the validation between finite element method and theoretical solutions. Once the result can be validated, more complexities in modeling can be added. This will insure saving cost and time efficiently.

1.2 Issues Considered

Special considerations should be made on structural sectional property, finite element meshing, boundary conditions, and stacking sequences while designing and modeling of composite structure. As composite materials are inherently 2-dimensional orthotropic behavior, four material properties are needed for describing the structural response. These include Young's modulus in fiber and transverse directions, in plane shear modulus and in-plane Poisson's ratio. The 2-dimensional sectional property of

composite structures can be evaluated by using lamination theory. However, designing for 1-dimentional beam structure, the 1 dimensional sectional properties are required in order to have better evaluation of beam structural response.

Finite element meshing of pattern and size is also an important issue needed to be considered. The accuracy of the model depends on mesh pattern and size which includes the element numbers and its aspect ratio. The insufficient numbers of element will lead to inaccurate results. Moreover, if aspect ratio is too large, the error of the deflection will increase. Consequently, using proper meshing in modeling can decrease the error of the result.

Moreover, boundary condition used in structure modeling is one of the important issues that need special considerations. Unlike isotropic materials, composite material exhibits coupling behavior of in-plane coupling, out-of-plan coupling and between in-plane and out-of-plane coupling. The in-plane coupling is a structure under an axial load inducing shear deformation or vice versa. A structure under bending inducing twisting curvature is the out-plane-load coupling or vice versa. The coupling between in-plane and out-of-plane is a structure under in-plane load induces the out-of-plane deformation (curvature) or vice versa. Hence, if a structural boundary is constrained in certain direction, it may suppress the corresponding response. As a result, additional force/moment will be induced. In this case, the actual loading condition will not be the same condition that is intended to have. Hence,, boundary condition plays an important role when accurately modeling composite materials.

Lastly, the stacking sequence of composite materials has to be considered. If the laminate has symmetric and balanced stacking sequence, the behavior will react no coupling effect. However, unbalanced or un-symmetric laminates will have extension-shear coupling and extension-bending coupling while applying a tension load along the longitudinal axis. As a result, stacking sequence has to be considered carefully because it will affect the deflection of composite materials.

1.3 Literature Review

Composite beam structures have been extensively studied before. Several outstanding textbooks on composites include this subject [1, 2 and 3]. Among those books, the equivalent bending stiffness used in their beam analysis ignores the coupling effect. In finding the equivalent property, Chen and Chan [4] presented a method for calculating equivalent properties of the lumped layer. They stated that if un-symmetric and un-balanced laminas were lumped together, the effect of shear deformation on the effective moduli was ignored. Later, Lin, et al. [5] proposed a method for equivalent properties including thermal expansion coefficient of lumped layer.

Hu [6] proposed an analytical method to investigate the deformation of cantilever beams with various symmetric laminates. The method takes transverse shear effects and twisting coupling effects into account. Drummond and Chan [7] analytically and experimentally studied the bending stiffness of composites I-beam. Parambil et. al. [8] developed a non-conventional method to analyze composite laminated I-beam under bending. Closed form expressions for centroid and bending stiffness of I-beam were developed. The ply stress of I-beam under bending was also obtained and the results were in excellent agreement with finite element results.

Sanghavi and Chan [9] analytically studied the torsion behavior of composite I-beam. A closed-form expression for torsional and warping stiffness as well as shear

center is also developed.

Karama, Afaq, and Mistou [10] proposed the model of bending deformation under different types of loading and boundary conditions, showing that their approach is much closer to the finite element analysis than Sine model. Different stresses and displacements plotted with respect to the thickness and length for bending deformation, showing that this model is still trying to approach the finite element results. As a result, they concluded the present exponential model is more precise than other analytical models for multi-layered structures compared to finite element analysis.

Akavci et al. [11] analytically studied the bending analysis of cross-ply rectangular thick plates by using first order shear deformation theory. The results of examples showed that the mid-plane deflection and stresses of the laminate are significantly influenced by foundation stiffness. When thickness ratio a/h (length divided by thickness) decreases, the effect of foundation stiffness decreases. However, when length to thickness ratio L/h = 100, distribution of deflections and shear stresses for both of foundation stiffness are significantly different.

Schnabl, Saje, Turk, and Planinc [12] proposed a mathematical model for the analysis of geometrically and materially linear layered beams with different materials and geometric characteristics of each layer. This model took the transverse shear deformation of each layer of multi-layer into account. The shear deformation on vertical deflection increases with decreasing length to thickness ratio. Also, the influence of shear effects are significant for composite beams with $E/G \geq 16$ where the influence is about 15 % for L/h = 10, and about 250 % for short beams with L/h = 3.

Ascione, Feo, and Mancusi [13] presented a one-dimensional kinematical model for studying fiber reinforced beams. This model is able to take into account the transverse shear deformation. It is known that composite beams are significantly influence by shear

deformation because of their low shear moduli. In their work, they not only considered shear deformability within the context of a simplified one-dimensional model, but also overcome the difficulties related to a 3D analysis of these deformation. Consequently, the results of this model have more precious deflections than Vlaso's theory. Wu and Sun [14] developed a simple theory for thin-walled composite beams by allowing the deformation of beam cross-sectional contour and shearing stain of mid-axis.

1.4 Objective in this Thesis

Structural members are often idealized as beams in practical engineering analysis. It is known that shear deformation increases with decreasing length to thickness ratio for isotropic beams. However, for composite beams, large shear deformation will be produced due to different fiber orientations, stacking sequences, and boundary conditions.

In analyzing a composite structure, classical lamination theory is used to perform the laminate analysis by using finite element analysis. However, analyzing the composite structure by finite element method is still time consuming and expensive. As a result, it should need to develop a simply method that can accurately analyze composite behaviors.

The main purpose of the thesis is to investigate maximum deflections of composite beams with various boundary conditions and applied loads. Deflections due to normal and shear stresses will be discussed and total deflections will be compared to finite element results.

1.5 Outline of the Thesis

Chapter 2 is a review of composite beams starts from classical lamination theory. Then briefly introduces the effect of transverse shear deformation and shear stiffness. Lastly, composite beams with various boundary conditions have represented and maximum deflection in each case is derived. Chapter 3 describes the finite element

analysis including element type, mesh techniques, and convergent study. Chapter 4 presents results obtained by both analytical and finite element methods. A comparison between these two methods was conducted and discussed. Finally, conclusion and recommendations for the future work are presented in Chapter 5.

Chapter 2

Analysis of Composite Beams with Various Boundary Conditions

This Chapter includes brief description of the stress/strain relationship of lamina and the constitutive equation of laminated plate. Modification of constitutive equation of laminated plate into the equation for the laminated beam is also presented and the rationale of the structural behavior of 2D into 1D is explained. Closed-form expressions of the maximum deflection are developed for the beams under transversely concentrated and uniformly distributed loads with different boundary condition.

2.1 Lamina Constitutive Equation

Due to thin lamina in composite, a state of plane stress is assumed. For an orthotropic lamina, the stress-strain relationship in the principle material axis i.e. 1-2 direction shown in Figure 2.1 can be expressed in matrix from as follows:

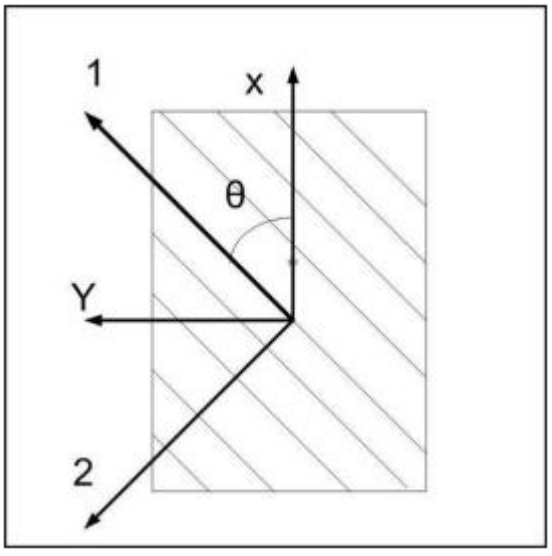

Figure 2.1 Coordinate System of Lamina

$$\begin{bmatrix}\sigma_1\\ \sigma_2\\ \tau_{12}\end{bmatrix}=\begin{bmatrix}Q_{11} & Q_{12} & 0\\ Q_{12} & Q_{22} & 0\\ 0 & 0 & Q_{66}\end{bmatrix}\begin{bmatrix}\varepsilon_1\\ \varepsilon_2\\ \gamma_{12}\end{bmatrix} \tag{2.1}$$

The elements of the stiffness [Q] are functions of the elastic constants and expressed as

$$Q_{11}=\frac{E_1}{1-\nu_{12}\nu_{21}} \tag{2.2}$$

$$Q_{12}=\frac{E_1\nu_{12}}{1-\nu_{12}\nu_{21}} \tag{2.2}$$

$$Q_{22}=\frac{E_2}{1-\nu_{12}\nu_{21}} \tag{2.2}$$

$$Q_{66}=G_{12} \tag{2.2}$$

where E_1 and E_2 are Young's moduli, G_{12} is the shear modulus, and ν_{12} is the Poisson's ratio of the lamina under a loading along the fiber direction.

The stiffness matrix $\left[\bar{Q}_{x-y}\right]$ for a lamina with fiber rotation of an arbitrary angle θ with respect to global axis can be obtained by rotating the stiffness matrix of a 0° lamina $[Q_{1-2}]$, as shown in the following equation

$$\left[\bar{Q}_{x-y}\right]=[T_\sigma(-\theta)][Q_{1-2}][T_\varepsilon(\theta)] \tag{2.3}$$

where

$$[T_\sigma(\theta)]=\begin{bmatrix}m^2 & n^2 & 2mn\\ n^2 & m^2 & -2mn\\ -mn & mn & m^2-n^2\end{bmatrix}$$

$$[T_\varepsilon(\theta)] = \begin{bmatrix} m^2 & n^2 & mn \\ n^2 & m^2 & -mn \\ -2mn & 2mn & m^2 - n^2 \end{bmatrix}$$

$[T_\sigma(\theta)]$ and $[T_\varepsilon(\theta)]$ are the stress and strain transformation matrices, respectively. and

m=cosθ and n=sinθ.

2.2 Laminate Constitutive Equation

A laminate consists of two or more laminas which are bonded together perfectly to perform as an integral structure element. Each layer has its own fiber orientation. Hence, it is convenient to choose a reference plane of the given laminate which the fiber orientation of each layer is based on. The integral structural behavior can be referred to the mid-plane of this laminate. It is assumed that the laminate does not slip over each other and the cross-section of the laminate remains unwrapped. These assumption do not take shear deformation γ_{xz} and γ_{yz} into account. As a result, the displacement of any given point at a distance z from the mid-plane can be expressed in terms of the mid-plane displacements as

$$\begin{aligned} u &= u_0 - z\frac{\partial w_0}{\partial x} \\ v &= v_0 - z\frac{\partial w_0}{\partial y} \\ w &= w_0 \end{aligned} \tag{2.4}$$

where u_0, v_0, and w_0 are the mid-plane displacements. The strain-displacement relationship can be expressed as

$$\varepsilon_x = \frac{\partial u}{\partial x}$$
$$\varepsilon_y = \frac{\partial v}{\partial y} \tag{2.5}$$
$$\gamma_{xy} = \frac{\partial u}{\partial y} + \frac{\partial v}{\partial x}$$

Substituting Equation (2.4) into Equation (2.5), the strains at any given z position can be obtained in terms of the mid-plane strains ${\varepsilon_x}^0$, ${\varepsilon_y}^0$, and ${r_{xy}}^0$ the plate curvatures k_x, k_y, and k_{xy} as

$$\begin{bmatrix} \varepsilon_x \\ \varepsilon_y \\ r_{xy} \end{bmatrix} = \begin{bmatrix} {\varepsilon_x}^0 \\ {\varepsilon_y}^0 \\ {r_{xy}}^0 \end{bmatrix} + z \begin{bmatrix} k_x \\ k_y \\ k_{xy} \end{bmatrix} \tag{2.6}$$

where

$$\begin{aligned} {\varepsilon_x}^0 &= \frac{\partial u_0}{\partial x} & k_x &= -\frac{\partial^2 w}{\partial x^2} \\ {\varepsilon_y}^0 &= \frac{\partial v_0}{\partial y} & k_y &= -\frac{\partial^2 w}{\partial y^2} \\ {r_{xy}}^0 &= \frac{\partial u_0}{\partial y} + \frac{\partial v_0}{\partial x} & k_{xy} &= -2\frac{\partial^2 w}{\partial x \partial y} \end{aligned} \tag{2.7}$$

The resultant forces and moments on laminate cross-section are defined as

$$N_x = \int_{-h/2}^{h/2} \sigma_x dz \qquad M_x = \int_{-h/2}^{h/2} \sigma_x z dz$$

$$N_y = \int_{-h/2}^{h/2} \sigma_y dz \qquad M_y = \int_{-h/2}^{h/2} \sigma_y z dz \tag{2.8}$$

$$N_{xy} = \int_{-h/2}^{h/2} \tau_{xy} dz \qquad M_x = \int_{-h/2}^{h/2} \tau_{xy} z dz$$

Substituting Equation (2.8) into Equation (2.6), the constitutive equation can be obtained as

$$\begin{bmatrix} N \\ M \end{bmatrix} = \begin{bmatrix} A & B \\ B & D \end{bmatrix} \begin{bmatrix} \varepsilon^0 \\ k \end{bmatrix} \tag{2.9}$$

where

$$A_{ij} = \sum_{k=1}^{n} \left(\bar{Q}_{ij}\right)_k (z_k - z_{k-1})$$

$$B_{ij} = \frac{1}{2} \sum_{k=1}^{n} \left(\bar{Q}_{ij}\right)_k ({z_k}^2 - {z^2}_{k-1})$$

$$D_{ij} = \frac{1}{3} \sum_{k=1}^{n} \left(\bar{Q}_{ij}\right)_k ({z_k}^3 - {z^3}_{k-1}) \qquad \text{i, j} = 1,2, \text{and } 6$$

where A_{ij} is called the extensional stiffness matrix, B_{ij} is called the coupling stiffness matrix as it contributes in the coupling effect in response to different kind of load, D_{ij} is called the bending stiffness matrix, and z_k is the distance from mid-plane to k-th lamina.

The presence of matrix B_{ij} induces a coupling between stretching and bending/twisting of laminate. That is, in-plane strains can be due to not only in-plane resultants but also the out plane bending moments in the laminates. Similarly, bending and/or twisting strains do not induce resultant moment only, but also induce in-plane resultants. For symmetric laminate, the coupling stiffness matrix B_{ij} is a zero matrix which implies that in-plane deformation and the moment resultants are decoupled. On the other hand, unsymmetrical laminates will produce bending/twisting of the laminate in additional to the extensional and shear deformation.

This relationship (Equation 2.9) is usually referred as “Laminated Plate Theory” or simply as “Classical Lamination Theory”.

2.3 Inverse of Load-Deformation Relations: Laminate Compliances

Since multidirectional laminates are characterized by stress discontinuities from ply to ply, it is preferable to work with strain because there are continuous through the thickness. For this reason, it has to invert the load-deformation relations from Equation (2.9), and to express strains and curvatures as a function of applied loads and moments. Equation (2.9) can be rewritten as

$$\begin{bmatrix} \varepsilon^0 \\ k \end{bmatrix} = \begin{bmatrix} a & b \\ b^T & d \end{bmatrix} \begin{bmatrix} N \\ M \end{bmatrix} \tag{2.10}$$

where $\begin{bmatrix} a & b \\ b^T & d \end{bmatrix} = \begin{bmatrix} A & B \\ B & D \end{bmatrix}^{-1}$

It should be noted that the stiffness matrices A_{ij}, B_{ij}, and D_{ij} are symmetric and the combined 6×6 stiffness matrix is also symmetric. It can be easily proved that the inverse

of a symmetric matrix is also a symmetric matrix. Hence, the 6×6 compliance matrix and its individual sub matrices a and d are also symmetric. However, b and b^T may not be symmetric nor equal to each other. In fact, b^T is the transpose of b obtained from it by interchanging columns and rows.

2.4 Effects of Transverse Shear

In the classical lamination theory discussed before, it was assumed that the laminate is thin compared to its lateral dimensions and that straight lines normal to the middle surface remain straight and normal to that surface after deformation. Under these assumptions, the transverse shear strains and stresses are considered as zero. However, these assumptions are not valid in the case of thick cross-section laminated beams, sandwich beams, and thin-walled beams. The assumption that planes of the cross-section remain planes may no longer be valid because cross-sections exhibit deformation. As a result, an additional angle will be induced. Beam theory based on these relaxed assumptions is known as shear deformation beam theory, most commonly known as the Timoshenko beam theory.

Although the Timoshenko beam theory takes the transverse shear effect into account, the coupling effects due to un-symmetry and balanced laminates on the structure response should be also included. As a result, through simulating different composite beams to investigate shear deformations of the beam, the composite beam equation of predicting the tip displacements can be developed.

According to Figure 2.2, the cross-sections may not necessarily remain perpendicular to the deformed middle surface of the core. The slop of the middle surface dw/dx differs from the magnitude of the rotation of the cross-section ψ_x.

$$\frac{dw}{dx} \neq \psi_x \tag{2.11}$$

where the rotation ψ_x is negative while the slope is shown positive.

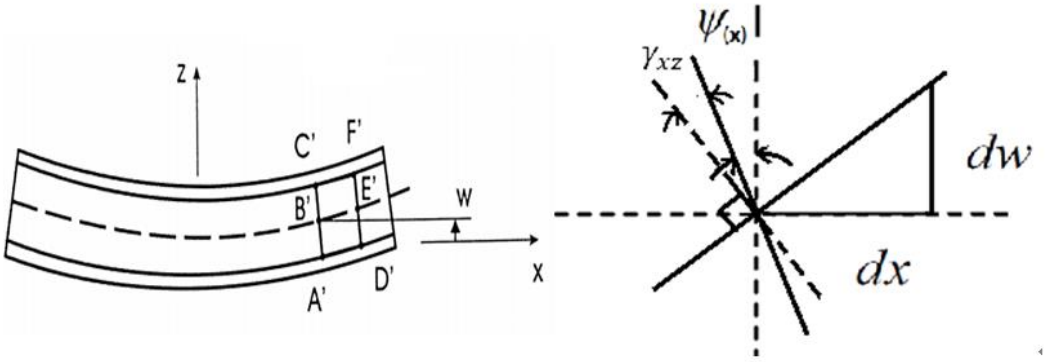

Figure 2.2 Deformation in x-z plane

Hence, the shear strain is

$$\gamma_{xz} = -\psi_x + \frac{dw}{dx} \tag{2.12}$$

The shear force resultant for composite element is obtained by integrating the stresses over the thickness.

$$Q_x = \int_{-h/2}^{h/2} \tau_{xz} dz \tag{2.13}$$

Notice that the in-plane normal and in-plane shear stresses are neglected.

For calculation of the transverse shear resultant Q_x defined in Equation (2.13), the shear stresses τ_{xz} is given in terms of the shear strain γ_{xz} by

$$\tau_{xz} = \overline{G_{xz}}\gamma_{xz} \tag{2.14}$$

where $\overline{G_{xz}}$ is the equilibrium transverse shear modulus of the composite laminate introduced in the section 2.6.

Since the shear stress distribution is not a constant across the laminate thickness, an average shear approach was often used in analysis of beam with isotropic material. In shear deformation theory, it is customary to use a correction factor k introduced as a multiplicative parameter in the constitutive relations between transverse shear forces and transverse shear strains. The need for a correction factor in the first-order theory originates from the fact that transverse shear strains and shear stresses are uniform through the thickness instead of the classical parabolic shear stress distribution with zero shear stresses on the surface of the laminates. The correction factor k is determined from exact solution for the shear stresses at the center of the laminate in terms of the transverses shear forces. For the rectangular cross-section of the isotropic material, the value of the shear correction factor k is determined as 1.2. However, for the composite field, transverse shear stresses are varied with stacking sequences and fiber orientations of the laminates. Since there is no closed-form expression for shear stress distribution available, the shear correction factor is chosen to be 1.2 used in isotropic material for this study.

With shear correction factor k, integration of the shear stress given by Equation (2.12) into Equation (2.14) over the laminate thickness h (Equation (2.13)) yields

$$Q_x = \frac{hG_{xz}}{k}\left(-\psi_x + \frac{dw}{dx}\right)$$
$$Q_y = \frac{hG_{yz}}{k}\left(-\psi_y + \frac{dw}{dy}\right) \qquad (2.15)$$

2.5 Equivalent Bending Stiffness of Composite Beam

The material of composites is inherent a 2-dimensional property. However, analysis of a beam is based upon a 1-dimensional structural response. The equivalent bending stiffness of one-dimensional beam is the proportional constant of the bending moment to the corresponding curvature of the beam. To evaluate the 1-dimensional equivalent bending stiffness, the structural response is needed to be taken into consideration. The structural response of the beam structure can be observed as induced the twisting curvature due to the bending. For isotropic beam, no twisting curvature will be induced as a beam is subjected to bending. For a composite beam under bending, the induced twisting curvature can be negligible if the ratio of the beam width to its depth is small.

Hence, two approaches in determining the equivalent bending stiffness of a composite beam will be discussed.

Case A: Twisting curvature is suppressed

For a beam under a bending moment M across b, the width of the beam, no other loadings are applied. Since the twisting curvature is suppressed, M_{xy} is induced. Since the loads per unit width is employed in the lamination theory, we have

$$M_x = \frac{M}{b}\ , M_{xy} \neq 0 \tag{2.16}$$

$$N_x = N_y = N_{xy} = M_y = 0,\ \ k_{xy} = 0 \tag{2.17}$$

where b is the width of the beam.

Under these assumptions, Equation (2.9) becomes

$$\begin{bmatrix} {\varepsilon^0}_x \\ k_x \\ 0 \end{bmatrix} = \begin{bmatrix} a_{11} & b_{11} & b_{16} \\ b_{11} & d_{11} & d_{16} \\ b_{16} & d_{16} & d_{66} \end{bmatrix} \begin{bmatrix} N_x \\ M_x \\ M_{xy} \end{bmatrix} \tag{2.18}$$

M_{xy} can be in terms of N_x and M_x presented in Equation (2.19)

$$M_{xy} = \frac{-b_{16}}{d_{66}} N_x - \frac{d_{16}}{d_{66}} M_x \tag{2.19}$$

Substituting Equation (2.19) into Equation (2.18) obtains

$$\varepsilon^0{}_x = \left(a_{11} - \frac{{b_{16}}^2}{d_{66}}\right) N_x + \left(b_{11} - \frac{b_{16} d_{16}}{d_{66}}\right) M_x \tag{2.20}$$

$$k_x = \left(b_{11} - \frac{{b_{16}}^2}{d_{66}}\right) N_x + \left(d_{11} - \frac{{d_{16}}^2}{d_{66}}\right) M_x \tag{2.21}$$

For the bending case, only M_x is applied which means N_x = 0. Equation (2.20) and (2.21) becomes

$$\varepsilon^0{}_x = \left(b_{11} - \frac{b_{16} d_{16}}{d_{66}}\right) M_x \; and \; k_x = \left(d_{11} - \frac{{d_{16}}^2}{d_{66}}\right) M_x \tag{2.22}$$

Hence, the equivalent bending stiffness can be written as $\frac{\mathrm{b}}{\hat{d}_1}$ and is shown below

$$\hat{d}_1 = d_{11} - \frac{{d_{16}}^2}{d_{66}} \tag{2.23}$$

Case B: Twisting curvature is allowed but M_{xy} does not exist.

With this assumption, Equation (2.10) becomes

$$\begin{bmatrix} {\varepsilon^0}_x \\ k_x \end{bmatrix} = \begin{bmatrix} a_{11} & b_{11} \\ b_{11} & d_{11} \end{bmatrix} \begin{bmatrix} N_x \\ M_x \end{bmatrix} \tag{2.24}$$

For the bending case, N_x is equal to zero. Because moments describe in Lamination theory are per unit width, the equivalent bending stiffness of the laminated beam can be written as

$$k_x = d_{11} M_x \quad and \quad beam\ bending\ stiffness = \frac{b}{d_{11}}. \tag{2.25}$$

where d_{11} is the flexural compliance of the composite beam.

To summary, there are two expressions of equivalent bending stiffness for a composite beam developed in this study. One takes twisting effect into account and the other does not. The results of beam deflection by using different bending stiffness will be discussed and presented in Chapter 4.

2.6 Equivalent Transverse Shear Modulus $\overline{G_{xz}}$

The constitutive equation of laminates including the effect of transverse shear deformation is, by Equation (2.15), the superposition of Equation (2.9) from the classical laminate theory and the equation that involves the transverse shear resultants Q_x and Q_y can be expressed as

$$\begin{bmatrix} Q_y \\ Q_x \end{bmatrix} = \sum_{k=1}^{n} \int_{h_k}^{h_{k-1}} \begin{bmatrix} \sigma_{yz} \\ \sigma_{xz} \end{bmatrix} dz \tag{2.26}$$

Equation (2.26) can be rewrite as

$$\begin{bmatrix} Q_y \\ Q_x \end{bmatrix} = \begin{bmatrix} F_{44} & F_{45} \\ F_{45} & F_{55} \end{bmatrix} \begin{bmatrix} \gamma_{yz} \\ \gamma_{xz} \end{bmatrix} \tag{2.27}$$

with

$$F_{ij} = \sum_{k=1}^{n} (h_k - h_{k-1})(C'_{ij})_k \,, \quad \mathrm{i,j,} = 4,5. \tag{2.28}$$

The stiffness constant, $(C'_{ij})_k$ referred to laminates' reference direction is a functions of the constants referred to the layer's principal directions as shown.

$$\begin{aligned} C'_{44} &= C_{44}\cos^2\theta + C_{55}\sin^2\theta \\ C'_{55} &= C_{44}\sin^2\theta + C_{55}\cos^2\theta \\ C'_{45} &= (C_{55-}C_{44})\sin\theta\cos\theta \end{aligned} \tag{2.29}$$

with

$$C_{44} = \frac{1}{G_{yz}}$$

$$C_{55} = \frac{1}{G_{xz}}$$

Thus, the equivalent shear modulus $\overline{G_{xz}}$ can be presented as follow

$$\overline{G_{xz}} = \frac{F_{55}}{h} \tag{2.30}$$

where h is the thickness of the laminate.

The detail information can be found in Berthelot [15].

2.7 Beam Deflection

The bending strain and transverse shear strain along the x-direction are given by

$$\varepsilon_x = \varepsilon^0{}_x + zk_x \tag{2.31}$$

$$\gamma_{xz} = -\psi_x + \frac{dw}{dx} \tag{2.32}$$

The curvature k_x is given in Equation (2.7) as

$$k_x = -\frac{d\psi_x}{dx} \tag{2.33}$$

where ψ_x is the rotation of cross-section which is not perpendicular to the mid-axis.

The shear force resultants are obtained by integrating the shear stresses over the layer thickness. Therefore, the constitutive equation for transvers shear along the x-direction is

$$Q_x = \frac{h\bar{G}_{xz}}{k}\left(-\psi_x + \frac{dw}{dx}\right) \tag{2.34}$$

Substituting Equation (2.25) with k_x which is given by Equation (2.33), and the shear force given by Equation (2.34) substituted into the equilibrium equation yields a different equation for bending

$$\frac{dw}{dx} = \psi_x + \frac{k}{h\bar{G}_{xz}}\frac{dM_x}{dx} \tag{2.35}$$

where

$$M_x = -\frac{b}{d_{11}}\frac{d\psi_x}{dx}$$

This equation is convenient for several beam-bending cases where the variation of moment along the beam is known from static equilibrium considerations. The detail derived equation can be found in Carlsson and Kardomateas [16].

2.8 Cases Study

Laminated composite beams with three different boundary conditions such as simply support, fixed end at both side, and cantilever beams were investigated the effect of shear deformation on the beam deflection under uniform distributed and concentrated loads, respectively. The boundary conditions and moment M_x of different type structural problems are presented in Table 2.1. The detail derived equations are list in APPENDIX A.

Case 1 Simply Support Beam – Uniform Distributed Load

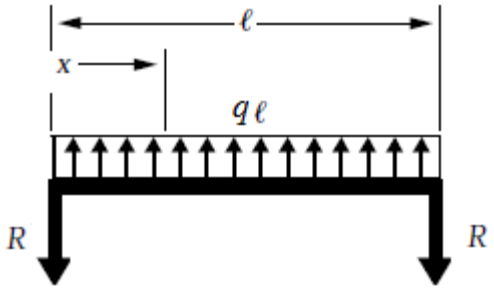

Figure 2.3 Simply Beam Under Uniform Distribution Load

The bending moment in the left half of the beam is

$$M_x = \frac{-qx}{2b}(\ell - x) \tag{2.36}$$

where b is the width, and ℓ is the length of the beam.

Table 2.1 Moments and Boundary Conditions in 1 to 6 Cases

case	End Condition	Load	Moment	Boundary Conditions
1	Simply Support Beam	Uniform Distributed Load	$M_x = \frac{-qx}{2b}(\ell - x)$	$\psi_x\left(\frac{\ell}{2}\right) = 0$ $w\,(0) = 0$ $w\,(\ell) = 0$
2		Concentrated Load	$M_x = \frac{-Px}{2b}$	$\psi_x\left(\frac{\ell}{2}\right) = 0$ $w\,(0) = 0$ $w\,(\ell) = 0$
3	Beam Fixed at Both Ends	Uniform Distributed Load	$M_x = \frac{-q}{12b}(6\ell x - \ell^2 - 6x^2)$	$\psi_x(0) = 0$ $\psi_x(\ell) = 0$ $w\,(0) = 0$ $w\,(\ell) = 0$
4	Beam Fixed at Both Ends	Concentrated Load	$M_x = \frac{-P}{8b}(4x - \ell)$	$\psi_x(0) = 0$ $\psi_x(\ell) = 0$ $w\,(0) = 0$ $w\,(\ell) = 0$
5	Cantilever Beam Free end at x=0	Uniform Distributed Load	$M_x = -\frac{qx^2}{2b}$	$\psi_x(\ell) = 0$ $w\,(\ell) = 0$
6		Concentrated Load	$M_x = -Px$	$\psi_x(\ell) = 0$ $w\,(\ell) = 0$

Thus, combined with Equations (2.25) and (2.33) into Equation (2.36) yields

$$\frac{d\psi_x}{dx} = d_{11}\frac{q}{2b}(x\ell - x^2) \tag{2.37}$$

which integrates to

$$\psi_x(x) = d_{11}\frac{q}{2b}\left(\frac{1}{2}x^2\ell - \frac{1}{3}x^3\right) + C_1 \tag{2.38}$$

The boundary condition, $\psi_x\left(\frac{\ell}{2}\right) = 0$, provides the constant of integration

$$C_1 = -d_{11}\frac{q\ell^3}{24b} \tag{2.39}$$

Thus, the rotation of cross-section originally perpendicular to the x axis ψ_x becomes

$$\psi_x(x) = d_{11}\frac{q}{2b}\left(\frac{1}{2}x^2\ell - \frac{1}{3}x^3\right) - d_{11}\frac{q\ell^3}{24b} \tag{2.40}$$

Substituting of Equation (2.40) into Equation (2.35), yields

$$\frac{dw}{dx} = -d_{11}\frac{q}{2b}\left(\frac{x^2\ell}{2} - \frac{x^3}{3}\right) + d_{11}\frac{q\ell^3}{24b} + \frac{kq(\ell - 2x)}{2A\overline{G_{xz}}} \tag{2.41}$$

where A is the cross-section area of the beam. (A=b×h)

The displacement *w* can be integrated from Equation (2.41).

$$w = -d_{11}\frac{q}{2b}\left(\frac{x^3\ell}{6} - \frac{x^4}{12}\right) + d_{11}\frac{q\ell^3x}{24b} + \frac{kq}{2A\overline{G_{xz}}}(\ell x - x^2) + C_2 \tag{2.42}$$

The boundary condition *w* (0) = 0, provides the constant of integration

$$C_2 = 0 \tag{2.43}$$

Hence, the beam deflection is given by

$$w = -d_{11}\frac{q}{2b}\left(\frac{x^3\ell}{6} - \frac{x^4}{12}\right) + d_{11}\frac{q\ell^3 x}{24b} + \frac{kq}{2A\overline{G_{xz}}}(\ell x - x^2) \tag{2.44}$$

In this case, the magnitude of deflection of the beam at the point of load application is of particular interest

$$\delta = |w(\ell/2)| = \frac{5}{384}\frac{d_{11}q\ell^4}{b} + \frac{kq\ell^2}{8A\overline{G_{xz}}} \tag{2.45}$$

where δ is the deflection of the beam.

When the bending moment distribution along the x-direction is known, the deflection may be obtained. The deflection due to both bending and shear deformation can be expressed as

$$w = w^B + w^s \tag{2.46}$$

For the case of simply beam under uniform distributed load,

$$w^B = \frac{5}{384}\frac{d_{11}q\ell^4}{b} \tag{2.47}$$

$$w^s = k\frac{q\ell^2}{8A\overline{G_{xz}}} \tag{2.48}$$

$$\frac{w^B}{w^s} = \frac{5d_{11}\ell^2 A\overline{G_{xz}}}{48kb} \tag{2.49}$$

where k = 1.2

By using the same derived method, case 2 to 6 can be derived by applying moments and boundary conditions presented in Table 2.2. The detail derived moments are presented in APPENDIX A and derived beam equations are presented in APPENDIX B.

Table 2.2 List of Bending Deformation and Shear Deformation for Various Boundary Conditions

case	End Condition	Load	w^B	w^s	$\frac{w^B}{w^s}$
1	Simply Support Beam	Uniform Distributed Load	$\frac{5}{384}\frac{d_{11}q\ell^4}{b}$	$\frac{kq\ell^2}{8A\overline{G_{xz}}}$	$\frac{5d_{11}\ell^2A\overline{G_{xz}}}{48kb}$
2		Concentrated Load	$\frac{1}{48}\frac{d_{11}P\ell^3}{b}$	$\frac{kP\ell}{4A\overline{G_{xz}}}$	$\frac{d_{11}\ell^2A\overline{G_{xz}}}{12bk}$
3	Beam Fixed at Both Ends	Uniform Distributed Load	$\frac{1}{384}\frac{d_{11}q\ell^4}{b}$	$\frac{kq\ell^2}{8A\overline{G_{xz}}}$	$\frac{d_{11}\ell^2A\overline{G_{xz}}}{48bk}$
4		Concentrated Load	$\frac{1}{192}\frac{d_{11}P\ell^3}{b}$	$\frac{kP\ell}{4A\overline{G_{xz}}}$	$\frac{d_{11}\ell^2A\overline{G_{xz}}}{48bk}$
5	Cantilever Beam free end at x=0	Uniform Distributed Load	$d_{11}\frac{q\ell^4}{8b}$	$\frac{kq\ell^2}{2A\overline{G_{xz}}}$	$\frac{d_{11}\ell^2A\overline{G_{xz}}}{4bk}$
6		Concentrated Load	$\frac{1}{3}\frac{d_{11}P\ell^3}{b}$	$\frac{kP\ell}{A\overline{G_{xz}}}$	$\frac{d_{11}\ell^2A\overline{G_{xz}}}{3bk}$

Chapter 3

Finite Element Analysis

3.1 Overview

Due to the various reasons such as geometry, boundary conditions, and environmental conditions, the real-problems are too complicated to be solved analytically. Once the material changes from the isotropic material to the orthotropic material, the complexity of the problem increases. If all these problems are considered as the analytical process, the solutions are practically unreachable. As a result, computer aided engineering (CAE) have been developed by translating analytical methods into convenient computer software to simulate problems effectively. These computer aided engineering can help to insure that the model features will be operate as designed in real conditions and to validate the theoretical results.

To divide the whole structural body into many small and geometrically simple bodies, which are called elements, is a basic concept of finite element methods. These elements have finite sizes so the method is named “Finite Element Methods (FEM)”. Large numbers of commercial programs exist with many finite element analysis capabilities for different engineering disciplines. They help to solve problems from a simple linear analysis to a nonlinear transient analysis. Some CAE have special capabilities to analyze composite material because these methods accept user programmed element formulations and custom constitutive equations such as $ANSYS^{TM}$ and $ABAQUS^{TM}$. These types of systems are commonly categorized into three parts: the pre-processor, the processor, and the post processor. In this study, $ANSYS^{TM}$ 15.0 is used to investigate behaviors of composite materials under various boundary conditions and configurations. The main propose of the study in this Chapter is to obtain the results by finite element

method that are used for comparison with results from analytical method developed in Chapter 2.

3.2 Element Types

Many different element types are contained in the element library of $ANSYS^{TM}$ 15.0. The element type determines the used element formulation such as degree of freedom, the interpolation functions, and the dimensions. Two – dimensional elements and three – dimensional elements must to be used for the composite structures due to its orthotropic behaviors. Through using the $ANSYS^{TM}$ 15.0 help files, proper element types for laminated composite structures are considered and listed below as a reference.

3.2.1 Two – Dimensional Elements

2-D elements are widely implemented and differentiated by elements types, which are called shell elements. The element types should be chosen based on the problems and desired results. Classical Lamination Theory of composite is based on Kirchhoff theory that inter-lamina shear strain is assumed to be zero. However, the shear effect in the composite structure is significant. As a result, the Mindlin theory, which takes the transverse shear deformation into account, is used in $ANSYS^{TM}$ 15.0. Hence, the Shell elements listed below have included the transverse shear deformation in their stiffness matrix.

SHELL181 (Finite strain layered shell):

- Suitable for analyzing thin to moderately thick shell structures
- Four-node element with six degrees of freedom at each node
- Well-suited for linear, large rotation and has large strain capabilities
- Highly accurate, even with coarse meshes
- Includes the effects of transverse shear deformation

SHELL281 (Finite strain layered shell):

- Suitable for analyzing thin to moderately thick shell structures
- Eight-node element with six degrees of freedom at each node
- Well-suited for linear, large rotation and has large strain capabilities
- Includes the effects of transverse shear deformation

3.2.2 Three – Dimensional Elements

Sometimes it is not suitable to use the shell element in specific cases such as woven fabric and thick laminates. Because plane stress conditions are applied shell elements, the stress in the third direction cannot be obtained. If studying localized phenomena likes free edge effects due to the inter-laminar stresses, the composite should be analyzed as solid instead of plane. However, using 3D elements should be done wisely because they need high computer space to store the data and usually cost time.

SOLID185:

- Layered elements with eight nodes having three degrees of freedom at each node
- Has plasticity, stress stiffening, large deflection, and large strain capabilities
- Prevent mesh volumetric locking in nearly incompressible cases

SOLID186:

- Layered elements with twenty nodes having three degrees of freedom at each node
- Has mixed formulation capability for simulating deformations of nearly

incompressible elastoplastic materials

- Allow up to 250 layers with large strain capabilities

3.2.3 Element Type in this Study

Solid186 element which exhibits quadratic displacement behavior is selected in this study. The element is defined by 20 nodes. Each node has three degree of freedom, translations in the nodal x, y, and z directions. This element can be simulate thick solids.

3.3 Meshing

One of the more frequently asked questions concerns the generation and selection of the proper mesh size in order to analyze a problem. Each problem is different and there are no definite rules to develop the proper mesh size. As a result, engineering judgment and intuition are called for to know where the regions of excessive stress or strain will be located. The problem geometry will dictate the areas where prominent changes in geometry occur, requiring a finer mesh in that particular area. In general, rectangular mesh should be used and triangular mesh should be avoided for composite structures because triangular mesh has fewer lines of symmetry compared to rectangular mesh.

The node displacements are single valued which means each node has a unique value. The displacement fields are continuous but not necessarily smooth. Using the continuous shape function guarantees the displacements fields are piecewise smooth but not necessarily smooth across the element boundaries. The reason is that the stress values are calculated from strain element by element. Therefore, nodes may have multiple stress values. By default, stresses are averaged in the nodes and the stress fields are recalculated. After that the stress values are continuous. In general, solution is more accurate and stress discontinuity is less for mesh.

It is normally preferred to have finer mesh in the region where load is applied, the region in which we are interested to get the stress and strain results. On the other hand, coarse mesh is acceptable in the other region of the structure. This can reduce the element numbers and increase operated time of the model.

Aspect ratio issues are very critical, if aspect ratio is more than 15, it will lead to inaccurate results. Therefore, $ANSYS^{TM}$ 15.0 recommends that aspect ratio should less than 10. In this study, aspect ratio is allowed in x to z direction for 8:1 and in y to z direction for 3:1. The model is built and shown in Figure 3.1.

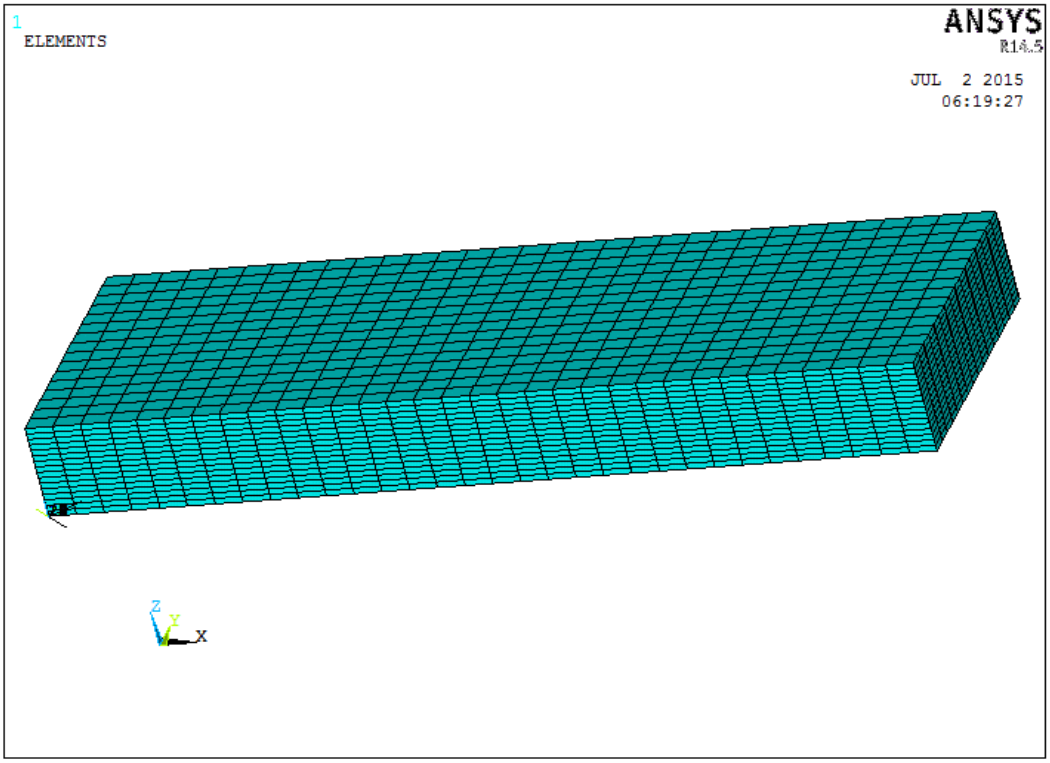

Figure 3.1 Typical Mesh of the 3-D Model

3.4 Boundary and Loading Conditions

This section describes what types of loading and their corresponding boundary conditions used in this study. In this study, six cases of composite beams with various types of loading and boundary conditions are used to investigate shear deformation presented in Table 3.1.

Table 3.1 Boundary Condition with Varied Applied Load

Case	End Condition	Load
1	Simply Supported Beam	Uniform Distributed Load
2		Concentrated Load
3	Beam Fixed at Both Ends	Uniform Distributed Load
4		Concentrated Load
5	Cantilever Beam	Uniform Distributed Load
6		Transverse Load

The dimensions of the beam are given in Table 3.2.

Table 3.2 Dimensions of the Beam

Length	Width	Height
0.72 in	0.24 in	0.08 in

The material used in this study is AS4/3501-6 laminate. The unidirectional layer orthotropic properties are taken from [17] as

$$E_1 = 21.3\ Msi \qquad E_2 = 1.5\ Msi \qquad E_3 = 1.5\ Msi$$

$$G_{12} = 1\ Msi \qquad G_{23} = 0.54\ Msi \qquad G_{13} = 1\ Msi$$

$$v_{12} = 0.27 \qquad v_{23} = 0.54 \qquad v_{12} = 0.27 \qquad t_{ply} = 0.005\ inch$$

where $E_1, E_2, and\ E_3$ are the Young's moduli of the composite lamina along the material coordinates. $G_{12}, G_{23}, and\ G_{13}$ are the shear moduli and $v_{12}, v_{23}\ and\ v_{13}$ are Poisson's ratio with respect to the 1-2, 2-3, and 1-3 planes, respectively and t_{ply} is the cured ply thickness.

3.5 Composite Beam Modeling in ANSYS

ANSYS Classic (APDL) version 15.0 is used to carry out all the FEM modeling and solution in this thesis. Simply step are used to model the composite/isotropic beam with varied boundary conditions and applied loads. Details are as follows:

Define Element Type

3-D Solid186 is used for modeling the composite beam. 2-D elements are not selected because out-plane shear deformation is considered.

Define Material type

Orthotropic properties are defined so the same model can be both verified isotropic and composite model by adjusting the material properties.

Boundary and loading conditions are problems dependent. In this study, there are three applied loads – uniform distributed load, concentrate load, and transverse load. For the cases of uniform distributed load, the force would be $(\frac{1}{\text{Number of nodes on the upper surface}})$ has shown in Figure 3.2.

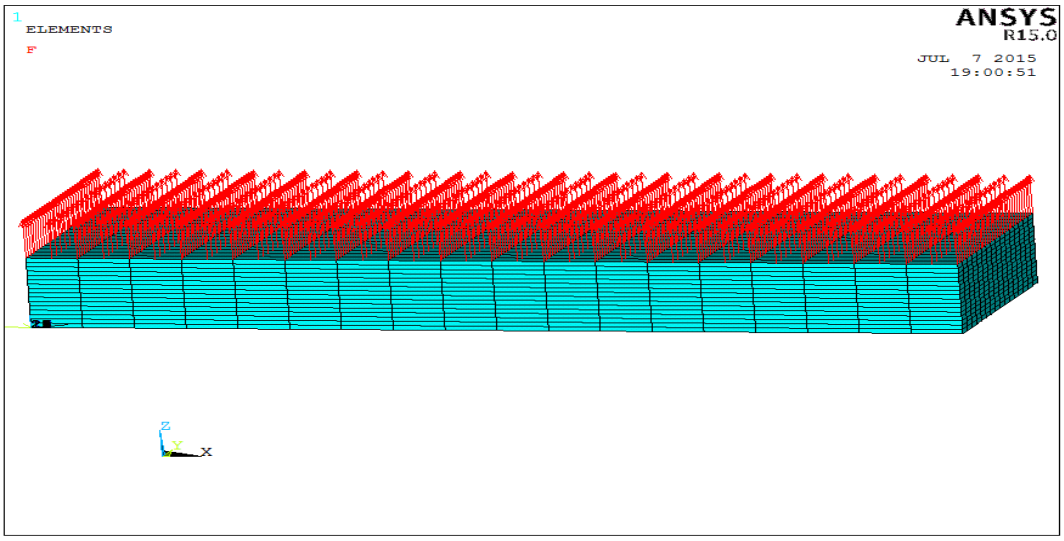

Figure 3.2 Uniform Distributed Load on Top Surface of the Laminate

For the cases of concentrated, the force would be

$\left(\frac{1}{\text{Number of nodes on the middle line of the upper surface}}\right)$ which has shown in Figure 3.3.

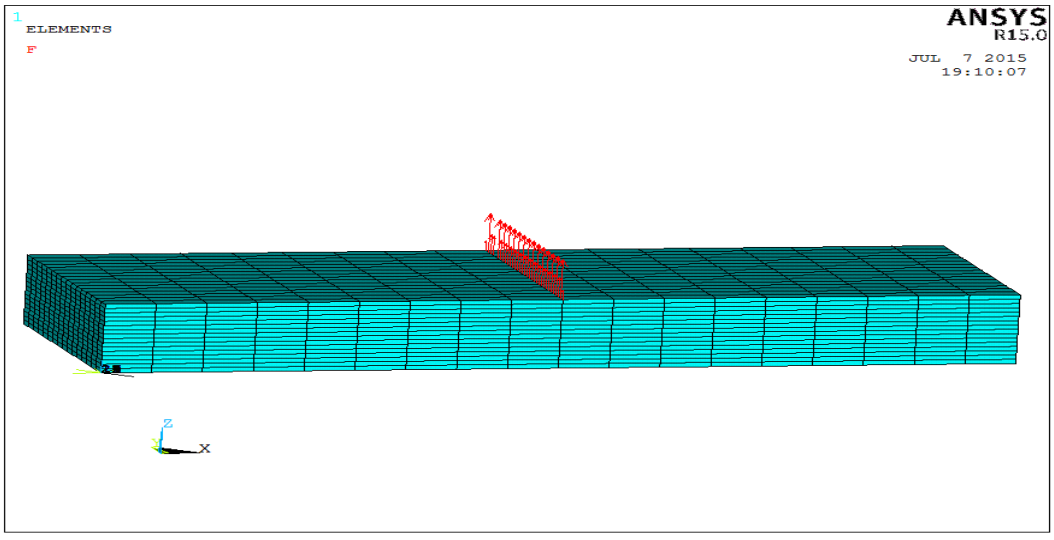

Figure 3.3 Concentrated Loads on Middle Line of Top Surface of the Laminate

For the case of cantilever beam with transverse load at the free end, the force would be ($\frac{1}{\text{Number of nodes on the cross-section}}$) which has shown in Figure 3.4

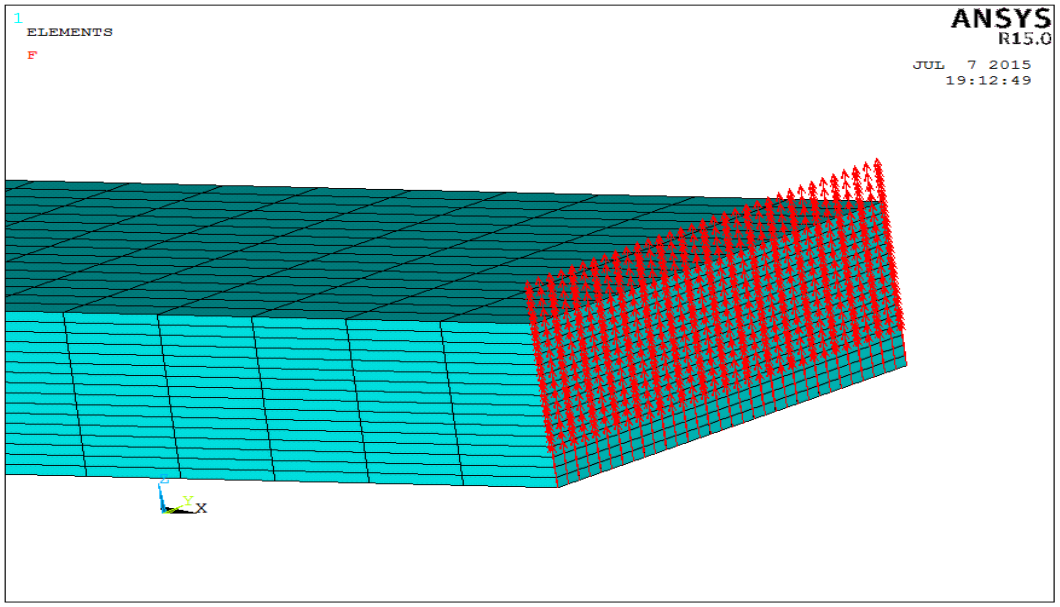

Figure 3.4 Transverse Loads on the Cross-section at the Free End

However, this condition cannot ensure uniform deformation for the surface because each node applies the same amount of load. Therefore, according to the shape function of 20 nodes element, the element weight distribution in each line of the block is 1:4:1. Take the line consisting node number 1, 9, and 2 according to Figure 3.5 for example. Node 9 contains $^4/_6$ element weight on that line and node 1 and 2 both contain $^1/_6$ element weight on that line. Because elements are bonded together on the line which applied the concentrated load, it has to accumulative the nodal forces of adjacent nodes to ensure uniform deformation on that line.

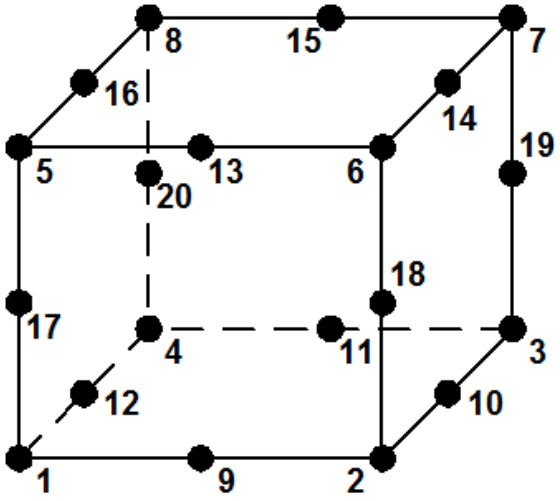

Figure 3.5 Solid186 Element

For the cases of simply supported beam, the right end only has $u_z = 0$ and the left end has u_x, u_y, and $u_z = 0$ which are shown in Figure 3.6 and Figure 3.7. In this case, no rotations restrain to maintain moment free at the both ends.

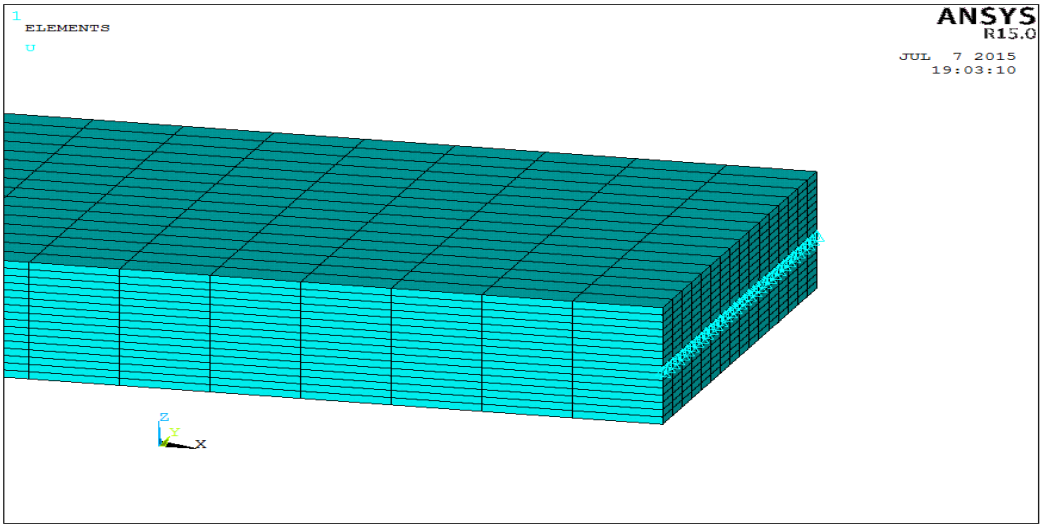

Figure 3.6 $u_z = 0$ on the Middle Line of Right Cross-section of Simply Supported Beam

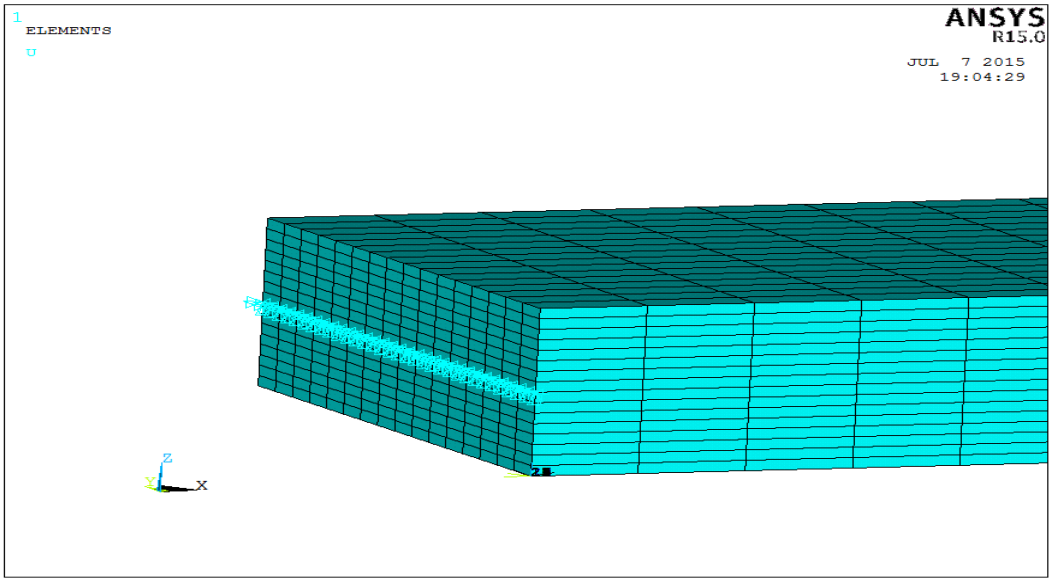

Figure 3.7 u_x, u_y, and $u_z = 0$ on the Middle Line of Left Cross-section of Simply Supported Beam

For the cases of beam fixed at the both ends, all degrees of freedom are equal to zero at the both end which is presented in Figure 3.8 and Figure 3.9

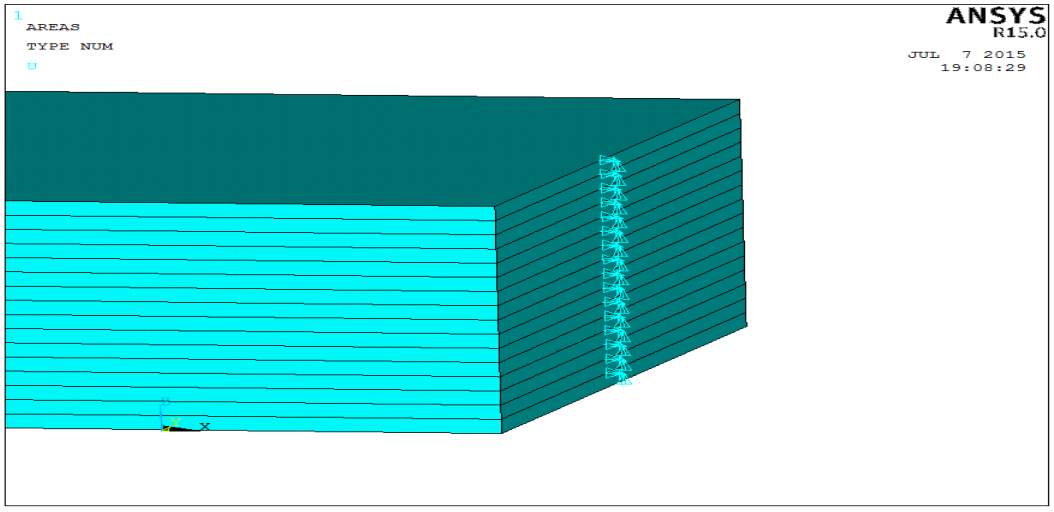

Figure 3.8 All Degrees of Freedom Constrained on the Nodes of the Fixed Right End Cross-section

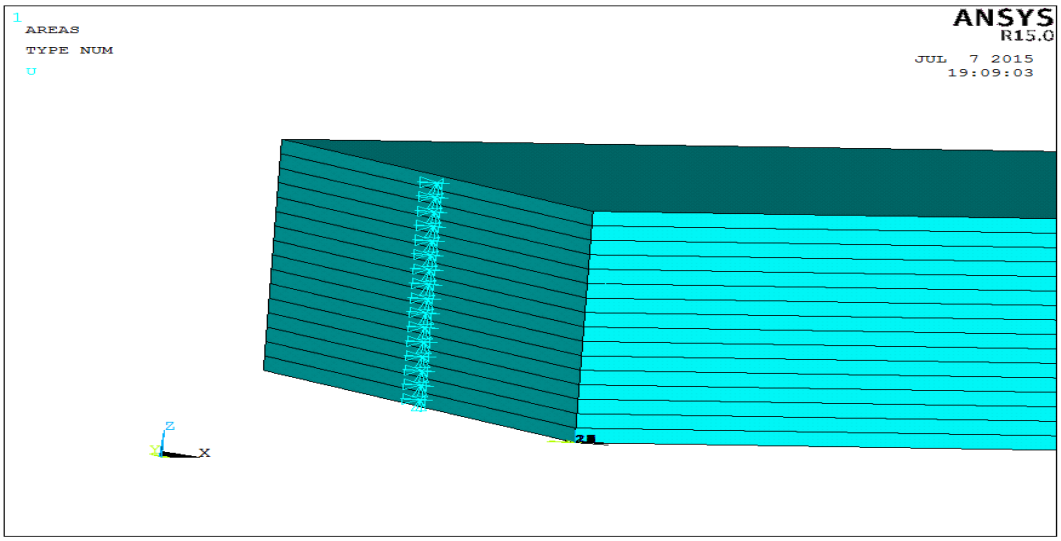

Figure 3.9 All Degrees of Freedom Constrained on the Nodes of the Fixed Left End Cross-section

For the cases of cantilever beam, all degrees of freedom are equal to zero in one end and the other end is free as shown in Figure 3.10.

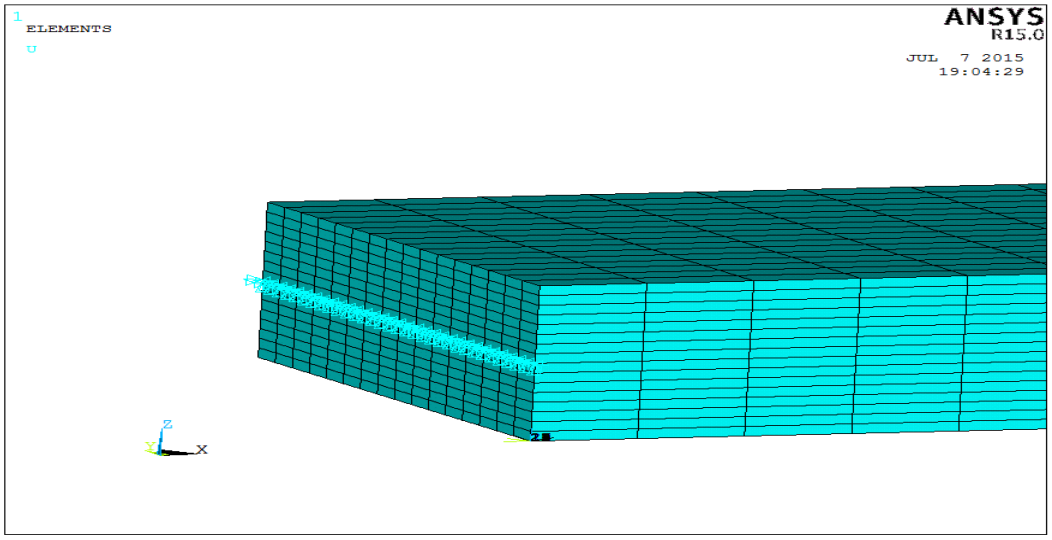

Figure 3.10 All Degrees of Freedom Constrained on the Nodes of the Fixed End of the Cantilever Beam

3.6 Verification of Finite Element Model

It is important to verify the accuracy of the model before employing composite models. Verification of the finite element model is based on comparison between the maximum deflection of the isotropic beam which is obtained from the finite element model and the results derived from the classical beam equations with shear deformation are shown in Table 3.3. The isotropic material used in this study is aluminum. The material properties, beam geometry, and load magnitude are given as follow.

$$E = 10\ Msi \quad v = 0.33$$

$$length\ (\ell) = 0.72 \quad width\ (b) = 0.24 \quad thickness\ (h) = 0.08 \qquad unit: inch$$

$$\mathrm{P} = 1\ lb \qquad q = \frac{P}{\ell}\ {}^{lb}/_{in}$$

where *E* is the Young's modulus , and v is Poisson's ratio.

Since all finite element results agree with theoretical isotropic beam equations with shear deformation, the present models are valid for investigating the composite beams.

Becker [18] stated that there are several errors would influence the accuracy of the model. First of all, modelling errors occur if the geometry is not exactly modelled or the boundary conditions are not accurately interpreted. Moreover, mesh errors may occur in "not good" mesh. If the element is thin and long, inaccuracy results will be obtained. Lastly, numerical errors may occur due to round-off in the computations, where numbers are truncated due to insufficient digits being used in the calculations. Some problems are very sensitive to small changes which are called ill-conditioned. This will occur when the stiffness matrix contains coefficients of varying orders of magnitudes in the same row,

due to large variation in element sizes or modulus of elasticity between elements. To prevent inaccuracy results, several steps are presented in the next section.

Table 3.3 Comparison of Deflection Results between Isotropic Material of Finite Element Model and Theoretical Beam Equations with Shear Deformation

Case	Theoretical Equation	Theoretical Result	FEM Result	Error %
Case 1	$\frac{5}{384}\frac{q\ell^4}{EI}+1.2\frac{q\ell^2}{8AG}$	4.90E-05	4.92E-05	**0.54**
Case 2	$\frac{1}{48}\frac{P\ell^3}{EI}+1.2\frac{P\ell}{4AG}$	7.89E-05	8.07E-05	**2.29**
Case 3	$\frac{1}{384}\frac{q\ell^4}{EI}+1.2\frac{q\ell^2}{8AG}$	1.10E-05	1.06E-05	**-3.53**
Case 4	$\frac{1}{192}\frac{P\ell^3}{EI}+1.2\frac{P\ell}{4AG}$	2.20E-05	2.17E-05	**-2.19**
Case 5	$\frac{1}{8}\frac{q\ell^4}{EI}+1.2\frac{q\ell^2}{2AG}$	4.62E-05	4.50E-04	**-2.49**
Case 6	$\frac{1}{3}\frac{P\ell^3}{EI}+1.2\frac{P\ell}{AG}$	1.23E-03	1.20E-03	**-2.39**

unit: inch

3.7 Convergence of FE Solutions

For a given problem, the FE solution should approach the exact solution. Convergent solutions can be obtained only if using right approach methods which are given below:

- Choose the correct element type.
- Use a good mesh
- Avoid long thin elements

- Check stress accuracy
- Prevent rigid body motion
- Check reaction forces
- Ensure inter-element connectivity
- Check the text output of the FE software

The detail information can be found from Becker [18].

Cantilever beam under concentrated load at the free end with $[\pm 45/0/90]_{2s}$ laminate is selected for this convergence study, where the material properties, beam geometry are presented in section 3.4, and load magnitude is presented in section 3.6.

It is often difficult to establish the optimum mesh refinement needed for an FE model. One way of checking that the FE mesh used is a reasonable one to start from a relatively coarse mesh, and then refine it. If solutions display large errors, further mesh refinement may be needed. According to Table 3.4, the maximum displacement of cantilever beam with transverse load at the free end is close to 1.745 with increasing element numbers. The model is validated by convergence study.

The interesting observation is that the convergent speed is faster when aspect ratio in thickness direction decreases. On the other hand, even though the aspect ratio in longitudinal direction decreases, the convergent speed of the result is still slower than the speed in decreasing aspect ratio in thickness. Due to large transverse shear deformation induced in composite laminates when applying the bending moment M_x, decreasing the aspect ratio in thickness direction will influence the result significantly. On the other hand, if the axial load is applied, then the aspect ratio in longitudinal direction will influence the convergent speed quickly.

Table 3.4 Convergence Study for Case 6 (Cantilever Beam with Concentrated Load at the Free End)

Model	Element number	Nodes number	Aspect ratio	Maximum Deflection (inch)
A	320	1823	x-z: 32 y-z: 12	1.736E-03
B	576	3095	x-z: 16 y-z: 12	1.738E-03
C	1152	5707	x-z: 16 y-z: 6	1.742E-03
D	2403	10981	x-z: 8 y-z: 6	1.743E-03
E	4608	21029	x-z: 8 y-z: 3	1.746E-03
F	9216	41225	x-z: 4 y-z: 3	1.745E-03
G	110592	472737	x-z: 1 y-z: 1	1.745E-03

Chapter 4

Results and Discussion

In this chapter, different laminated composite beams with different stacking sequences, boundary conditions, and applied loads were conducted to investigate effects of transverse shear deformation. In addition, two different expressions of bending stiffness for composite laminated beams are used. The comparison between the maximum deflections of the finite element results and analytical solutions are presented.

4.1 Effects of Boundary Conditions

In this part, the beam laminate is allowed to twist when the load is applied. If the laminates can be twisted, there exists no the moment M_{xy}. For this case, the bending stiffness of the laminate is $\frac{b}{d_{11}}$.

The deflection equations of the beams are listed in Table 2.2. The corresponding boundary conditions of each beam are tabulated in Table 2.1. In this part, shear deformations divided by total deformations for different laminates and boundary conditions are investigated. In addition, comparisons between theoretical and ANSYS results are presented below.

Figure 4.1 through 4.15 shows a comparison of the total beam deflection results obtained by analytical model and ANSYS method. Case 1 through case6 used in this study is referred as, simply supported beam (case 1 and 2), beam fixed both end (case 3 and 4) and the cantilevered beam (case 5 and 6). Each beam is subjected to uniformly and concentrated transverse load. These are listed in Table 3.1. The results indicate that both results agree well each other. The result discussion will be given at the end of the figures.

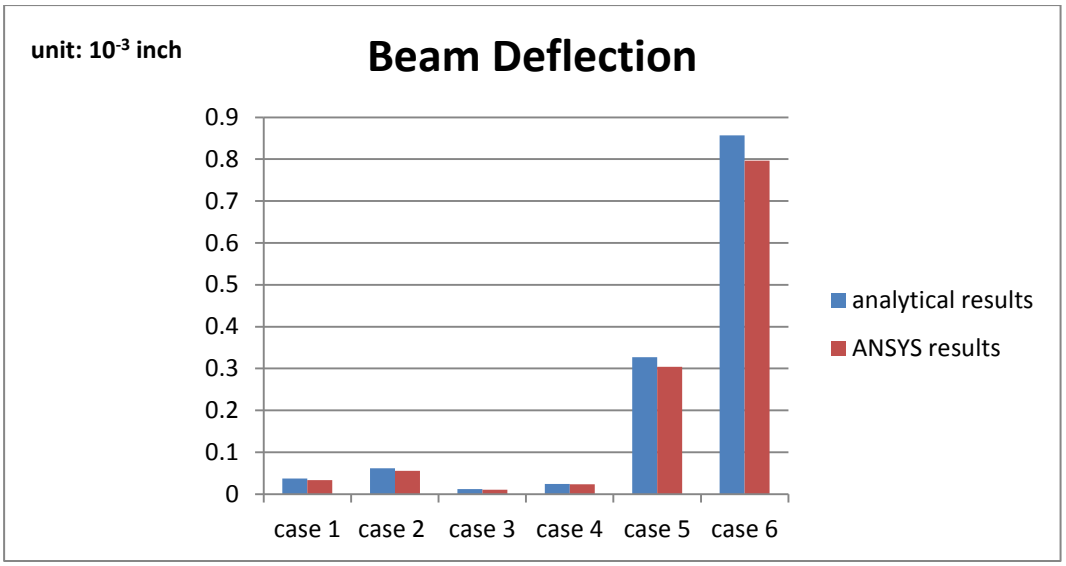

Figure 4.1 Comparison between Analytical and ANSYS Results for $[15/0]_{4s}$.

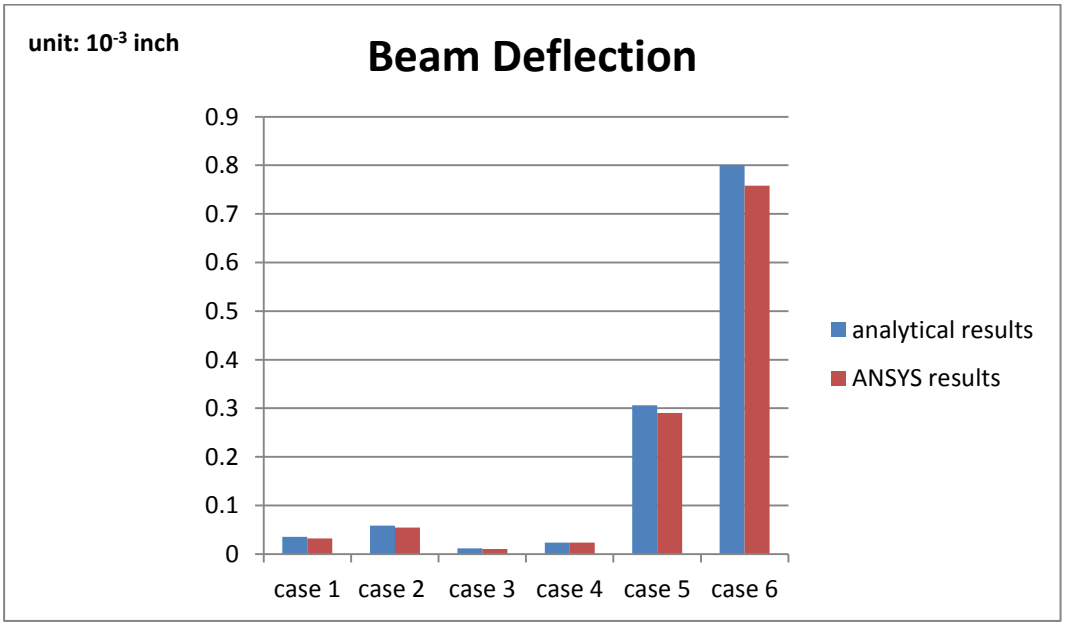

Figure 4.2 Comparison between Analytical and ANSYS Results for $[15/0]_{8T}$

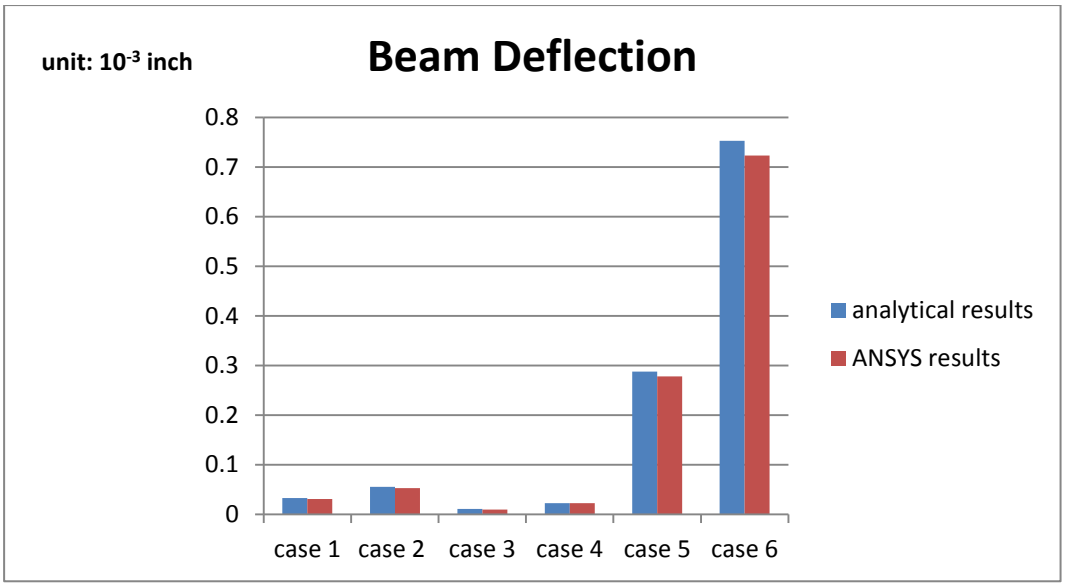

Figure 4.3 Comparison between Analytical and ANSYS Results for $[0/15]_{4s}$

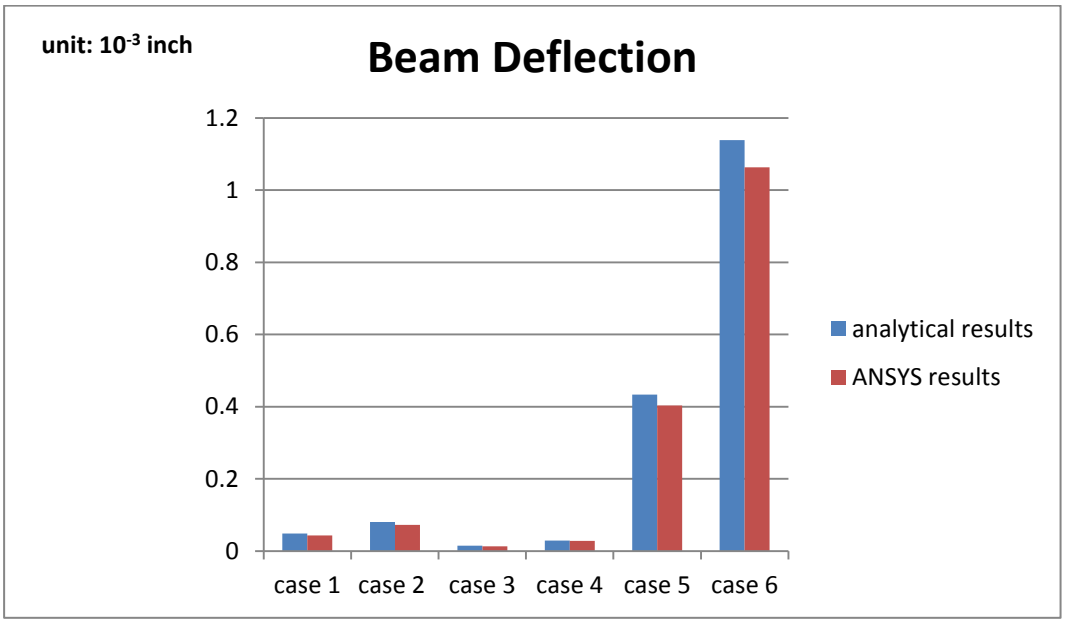

Figure 4.4 Comparison between Analytical and ANSYS Results for $[30/0]_{4s}$

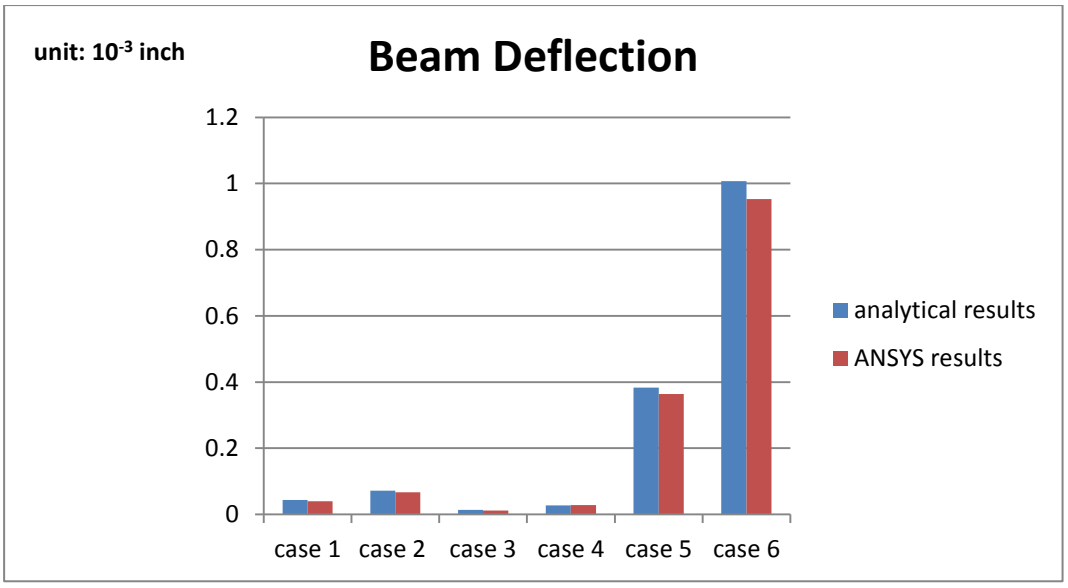

Figure 4.5 Comparison between Analytical and ANSYS Results for $[30/0]_{8T}$

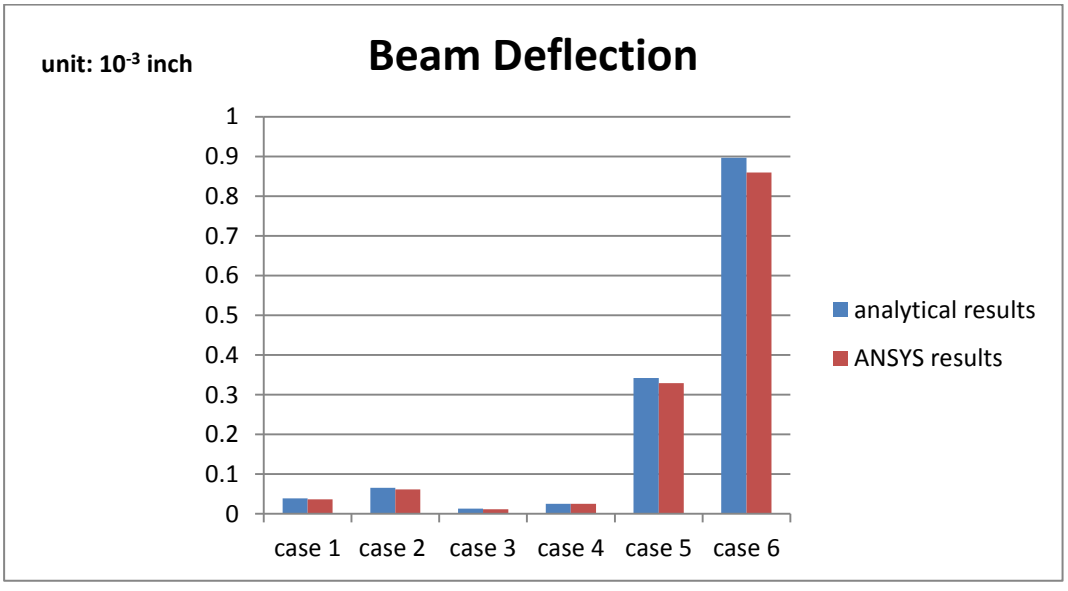

Figure 4.6 Comparison between Analytical and ANSYS Results for $[0/30]_{4s}$

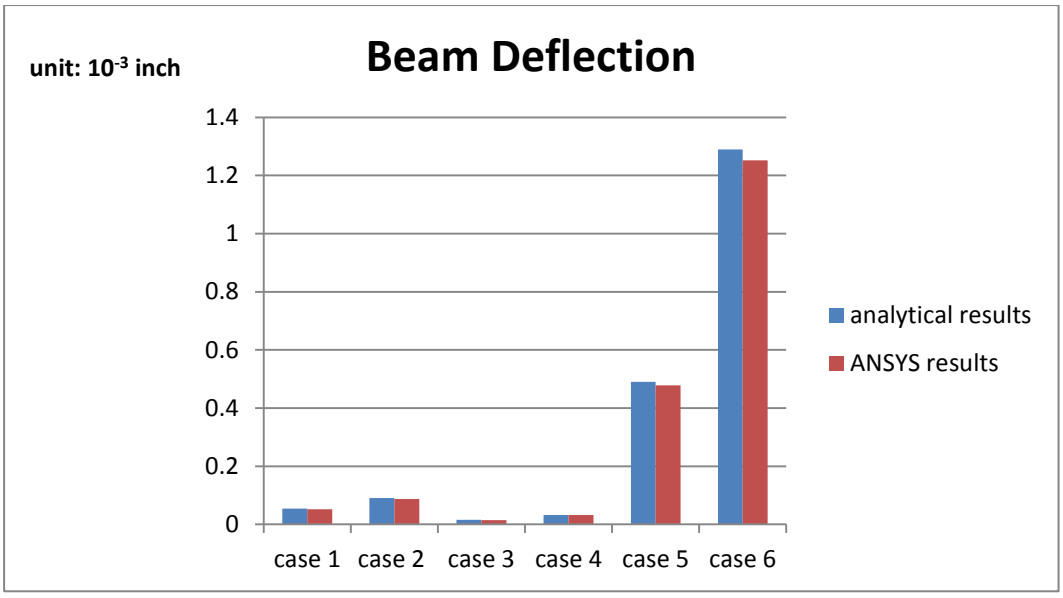

Figure 4.7 Comparison between Analytical and ANSYS Results for $[45/0]_{4s}$

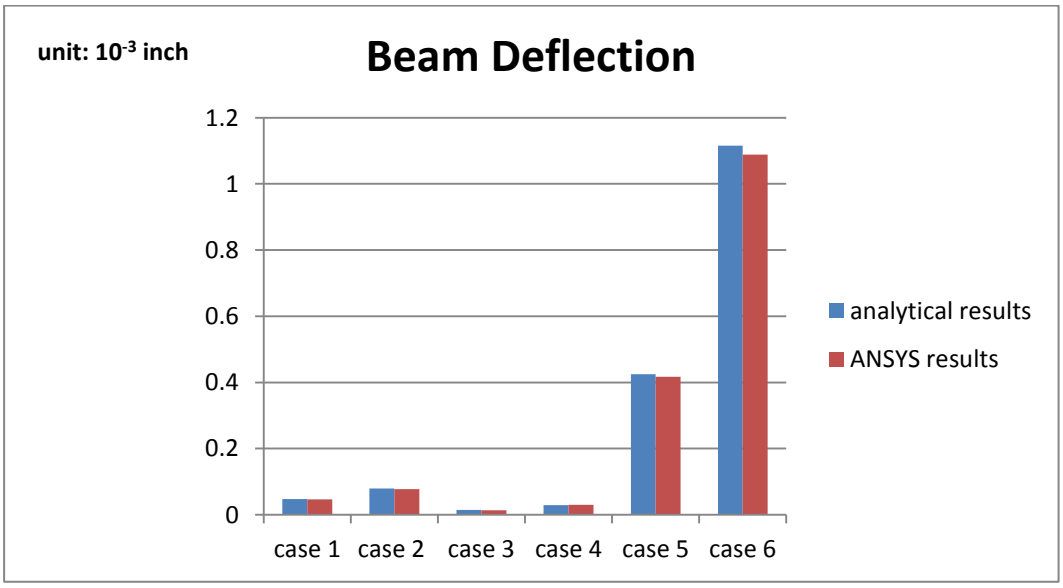

Figure 4.8 Comparison between Analytical and ANSYS Results $[45/0]_{8T}$

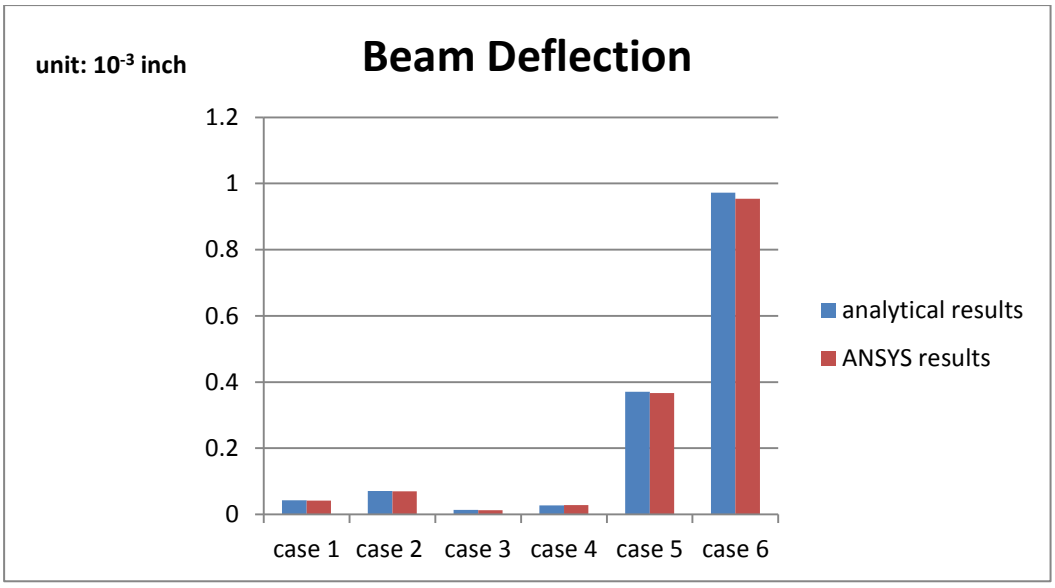

Figure 4.9 Comparison between Analytical and ANSYS Results $[0/45]_{4s}$

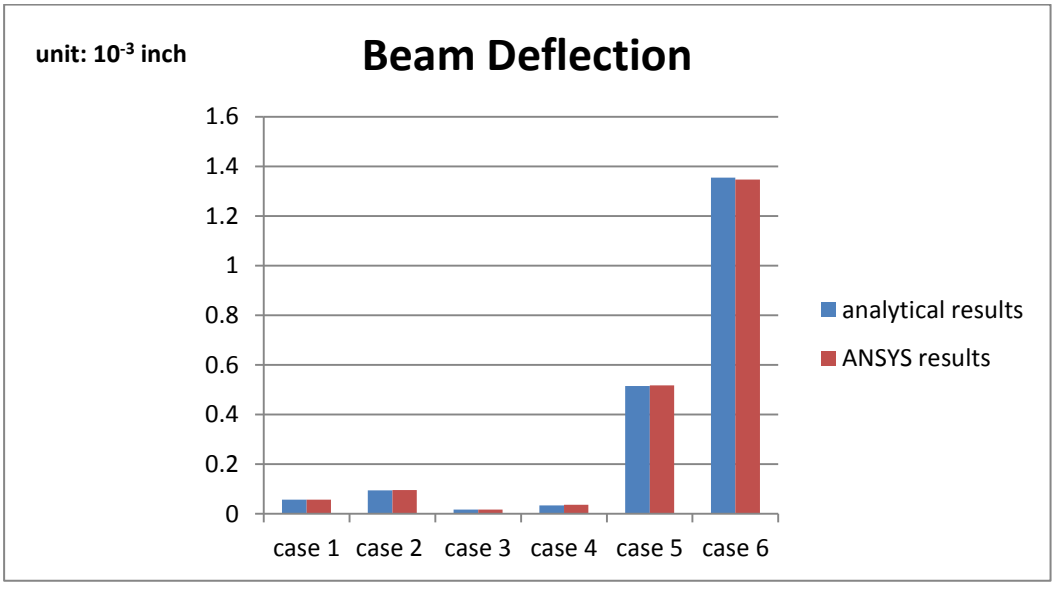

Figure 4.10 Comparison between Analytical and ANSYS Results $[60/0]_{4s}$

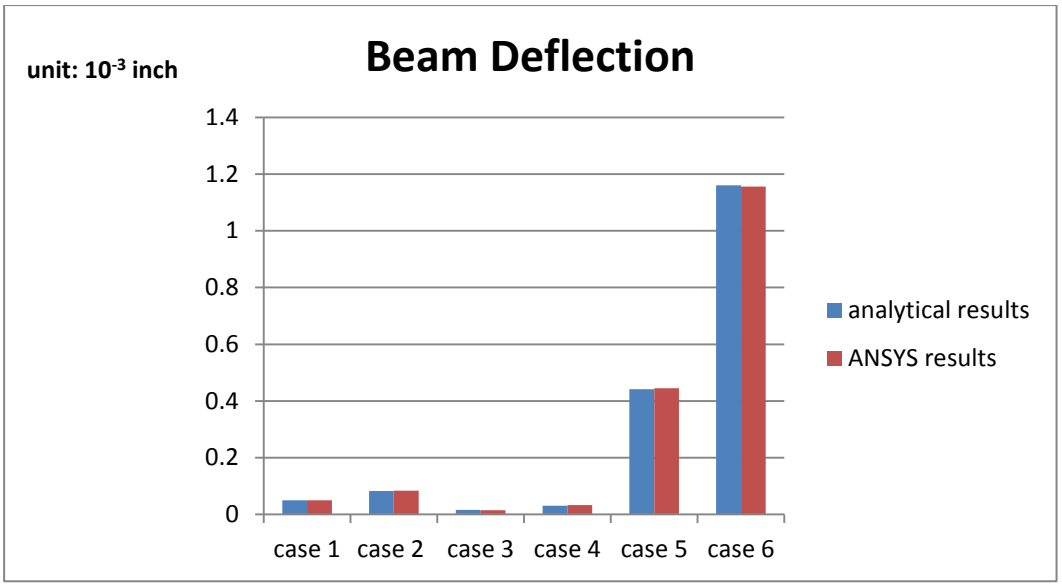

Figure 4.11 Comparison between Analytical and ANSYS Results $[60/0]_{8T}$

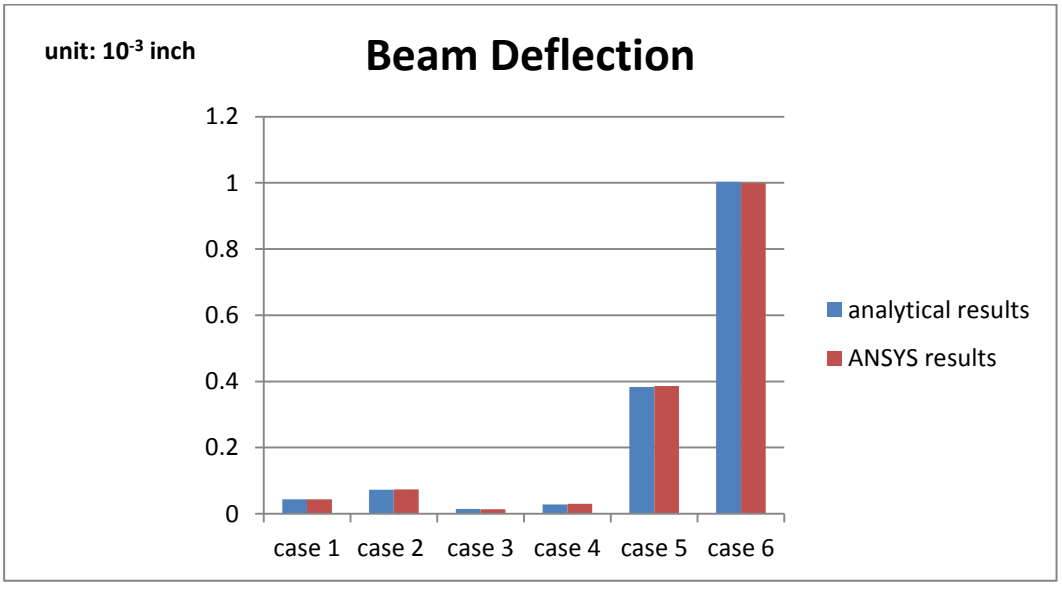

Figure 4.12 Comparison between Analytical and ANSYS Results $[0/60]_{4s}$

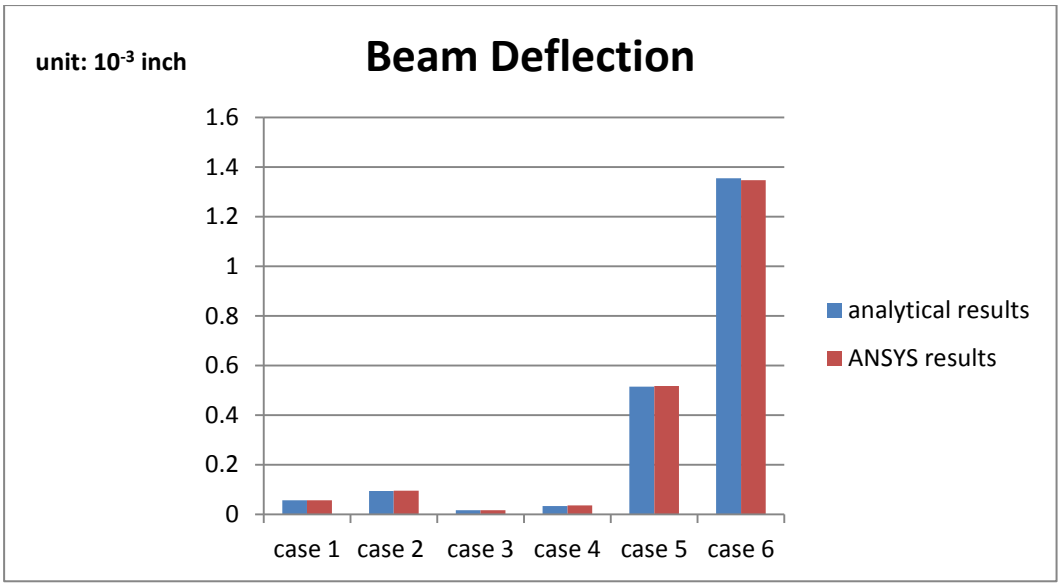

Figure 4.13 Comparison between Analytical and ANSYS Results $[75/0]_{4s}$

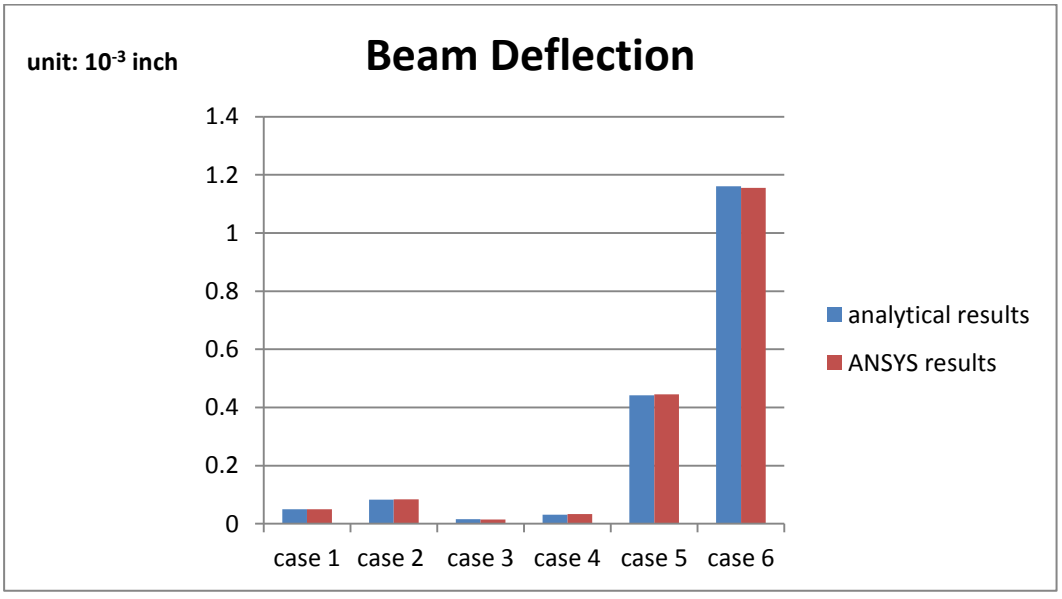

Figure 4.14 Comparison between Analytical and ANSYS Results $[75/0]_{8T}$.

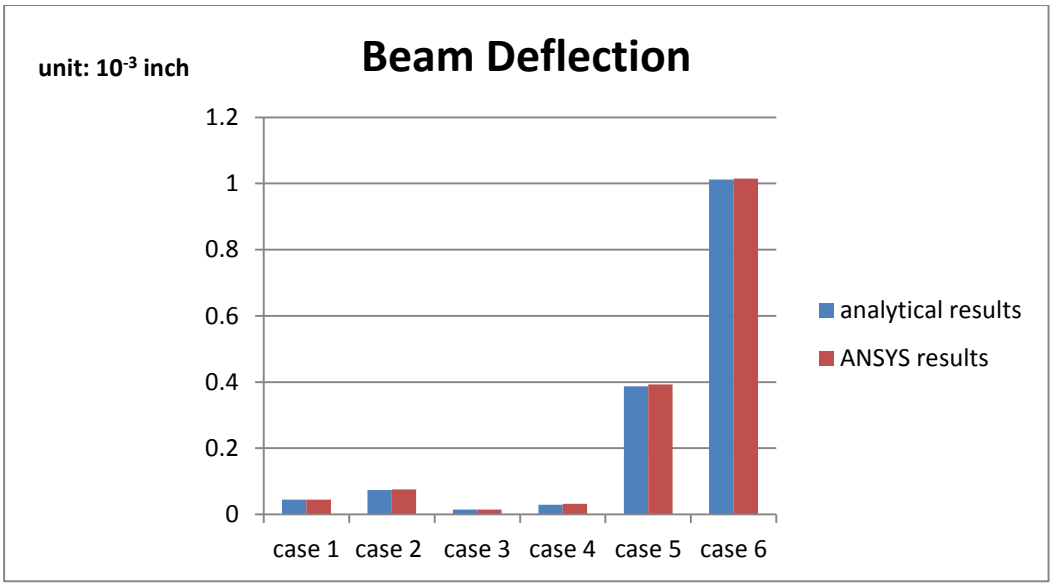

Figure 4.15 Comparison between Analytical and ANSYS Results $[0/75]_{4s}$.

Observations:

1. As expected, the cantilevered beams exhibit high largest deflection among those cases. It is also found that the results obtained by ANSYS are in general, a little slightly smaller than the results obtained from ANSYS.
2. According to Figure 4.1 to 4.15, for a given laminate under a certain load, W_s in case 6 (cantilever beam with transverse load at the free end) $>$ W_s in case 5 (cantilever beam with uniform distributed load) $>$ W_s in case 4 (beam fixed at both ends with concentrated load) = W_s in case 2 (simply support beam with concentrated load)$>$ W_s in case 3 (beam fixed at both ends with uniform distributed load) = W_s in case 1 (simply support beam with uniform distributed load). That is, for a given boundary condition, laminate and fiber orientations, W_s in concentrated load cases (2, 4 and 6) are larger than distributed cases (1, 3, and 5).
3. According to Figure 4.1 to 4.15, for a given laminate under a certain load, W_B in case

6 (cantilever beam with transverse load at the free end) > W_B in case 5 (cantilever beam with uniform distributed load) > W_B in case 2 (simply support beam with concentrated load) > W_B in case 1 (simply support beam with uniform distributed load) > W_B in case 4 (beam fixed at both ends with concentrated load) > W_B in case 3 (beam fixed at both ends with uniform distributed load).

4. Even though the total deflection W_{total} in case 6 > case 5 > case 2 > case 1 > case 4 > case 3, $\frac{W_s}{W_{total}}$ in case 4 = case 3 > case 2 > case 1 > case 5 > case 6 for a given laminate under a certain load.

4.2 Effects of Stacking sequences

When a laminate is constructed by stacking layers in an arbitrary sequence, the laminate stiffness matrix has the general form given by Equation (2.9). If the laminate is symmetric and balanced, a number of terms in the stiffness matrix will be zero, avoiding undesirable coupling between stretching, bending, and/or twisting.

Table 4.1 lists the percentage of total beam deflection due to shear for various layer stacking sequence of the beam of Case 6. Figure 4.16 through 4.18 shows the percentage of the shear deflection out of the total deflection. Detail discussion is given at the end of these figures.

Table 4.1 $\frac{W_s}{W_{total}}$ with Various Stacking Sequences

$\frac{W_s}{W_{total}}$	$[\pm\theta/0_2]_{2s}$	$[\pm\theta/0_2]_{4T}$	$[0_2/\pm\theta]_{2s}$	$[\theta/0_2/-\theta]_{2s}$	$[\theta/0_2/-\theta]_{4T}$
θ =15	0.063	0.066	0.068	0.063	0.065
θ =30	0.046	0.054	0.062	0.052	0.053
θ =45	0.035	0.047	0.06	0.046	0.046
θ =60	0.033	0.046	0.061	0.046	0.046
θ =75	0.034	0.048	0.064	0.047	0.047

As indicated in the table, smaller θ of the family laminate of $[\pm\theta/0_2]_{2s\ or\ 4T}$ gives a larger percentatge of shear deflection. For symmetrical laminate, placing θ lamina near the mid-plane of the laminate gives the largest shear contribution to the total beam deflection. For unsymmetrical laminate, shear deflection is immaterial to the ply stacking sequence.

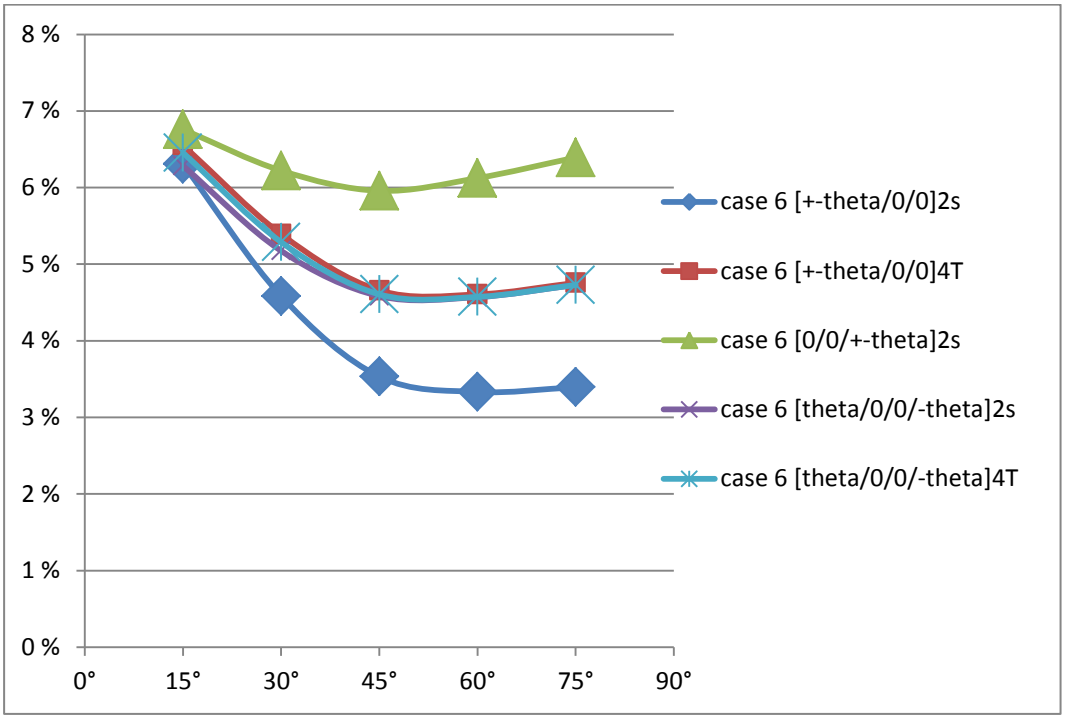

Figure 4.16 Variation of $\frac{W_s}{W_{total}}$ in Different Laminates with respect to the Fiber Orientations

For unbalanced laminates, Figure 4-17 and 4-18 shows the shear deflection and the deflection due to shear and bending respectively. It indicates that the shear deflections remain constant regardless of their stacking sequence. However, the bending stiffness strongly depends on the position of 0^0 ply in the laminate.

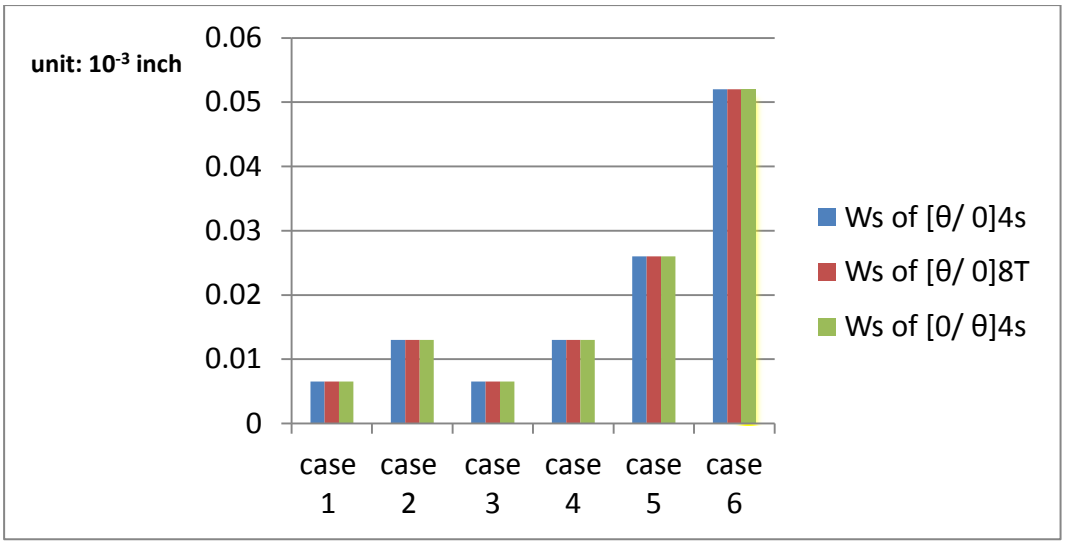

Figure 4.17 Comparison of Ws Deflection due to Shear between $[\theta/\ 0]_{4s}$, $[\theta/\ 0]_{8T}$, and $[0/\ \theta]_{4s}$ for θ = 45°

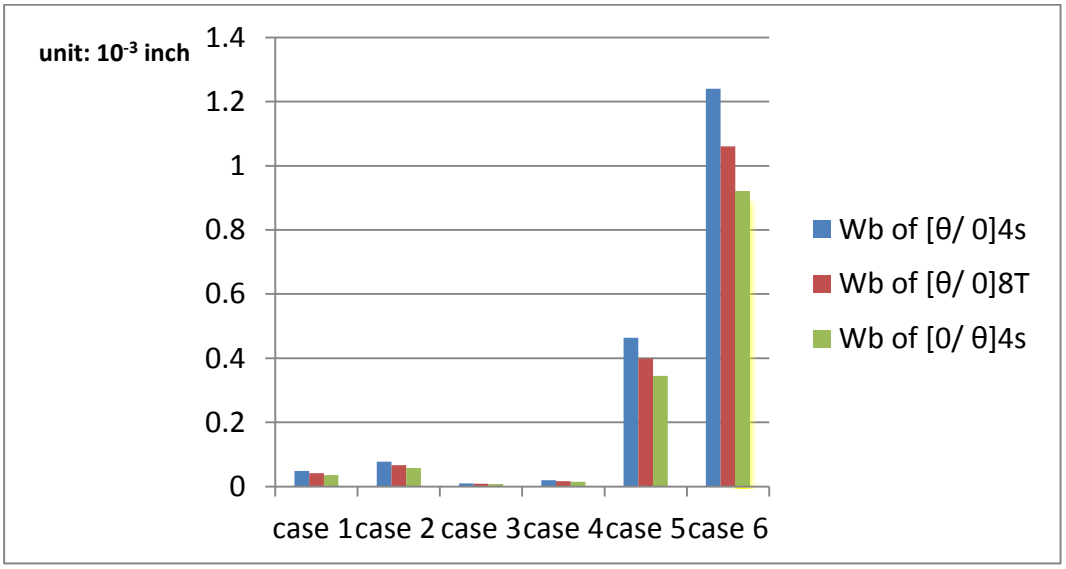

Figure 4.18 Comparison of W_b Deflection due to Bending between $[\theta/\ 0]_{4s}$, $[\theta/\ 0]_{8T}$, and $[0/\ \theta]_{4s}$ for θ = 45

Observations:

1. According to Figure 4.17, for a given load and fiber orientation, shear deformations W_s are the same for all cases. The reason is that the equivalent shear moduli $\bar{G}_{xz}$ for all laminate are the same, result in the same shear deformations for a certain fiber orientation.
2. According to Figure 4.16, symmetric laminates $[\pm\theta/0_2]_{2s}$ have larger shear deformations and total deflections for a certain fiber orientation compared to the symmetric laminates $[0_2/\pm]_{2s}$. The reason is that $[0_2/\pm\theta]2s$ has larger bending stiffness than $[\pm\theta/0_2]2s$.
3. According to Figure 4.16, symmetric laminates $[\pm\theta/0_2]2s$ have larger shear deformation and total deflection for a certain fiber orientation compared to the un-symmetric laminates $[\pm\theta/0_2]_{4T}$. The reason is that $[0_2/\pm\theta]2s$ has larger bending rigidity than $[\pm\theta/0_2]_{4T}$.
4. According to Figure 4.18, the bending stiffness is larger when zero degree lamina subjects to outer surfaces.

4.3 Effects of Fiber Orientations

The fiber orientation plays important role on the beam deflection not only of deflection due to bending but also deflection due the shear. It is noted that $\eta_{xy,x}$ an induced shear strain due to normal strain application is an important parameter of affecting the shear deflection. Figure 4.19 is plotted of $\eta_{xy,x}$ vs. θ . It is also awarded that once transverse load is applied, the bending moment M_x will be induced. This results in not only normal strains but also shear strains will be induced. According to Figure 4.19, maximum shear strain γ_{xy} will be induced by normal strain ϵ_x when fiber orientation is equal to 15°.

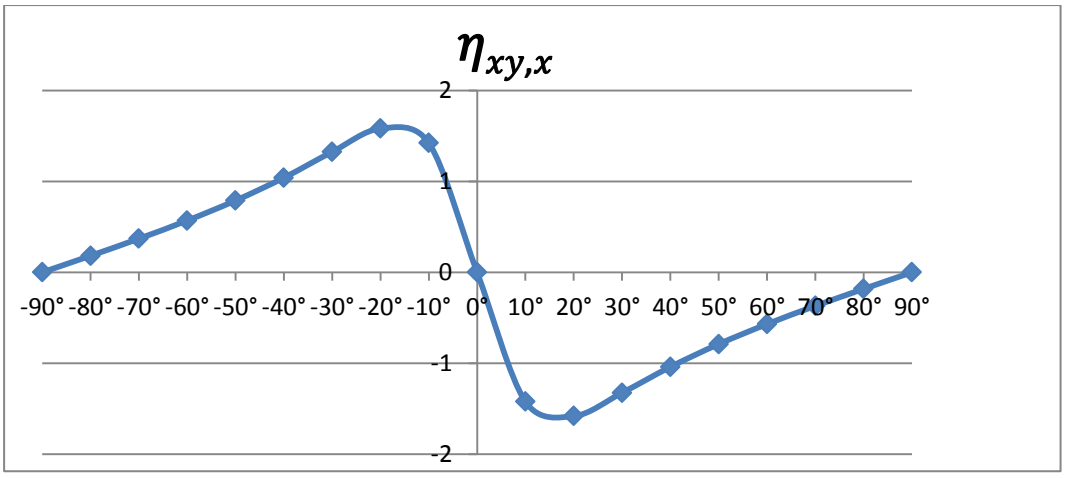

Figure 4.19 Variation of $\eta xy,x$ with respect to Fiber Orientations

For this part, shear and bending deformations varied with fiber orientations can be investigated by cases. Figure 4.20 through Figure 4-28 shows the percentage of the total deflection due to shear is significant at $\theta=15^0$. This coincides with the maximum value of $\eta_{xy,\,x}$occurring at this angle shown in Figure 4.19.

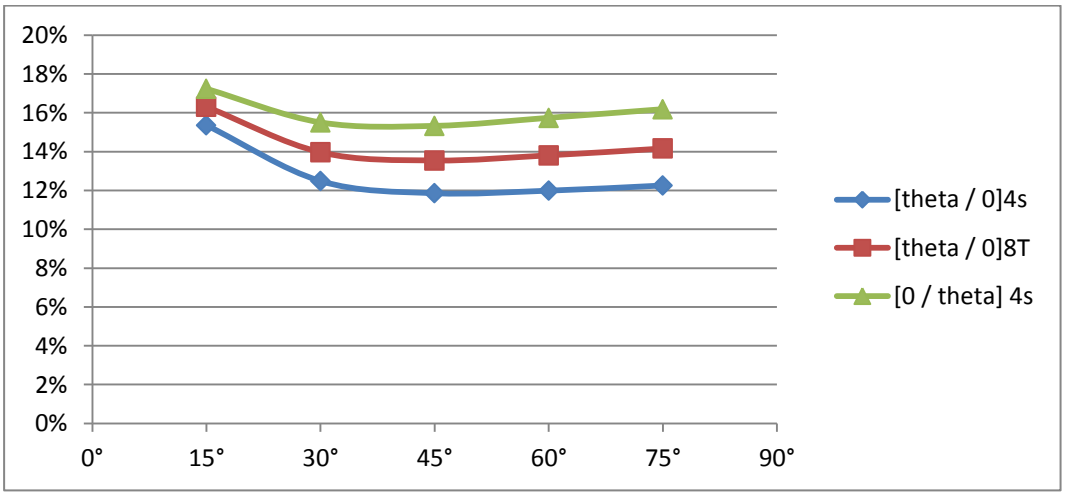

Figure 4.20 Variation of $\frac{W_s}{W_{toral}}$ in Different Laminates with respect to the Fiber Orientation for Case 1.

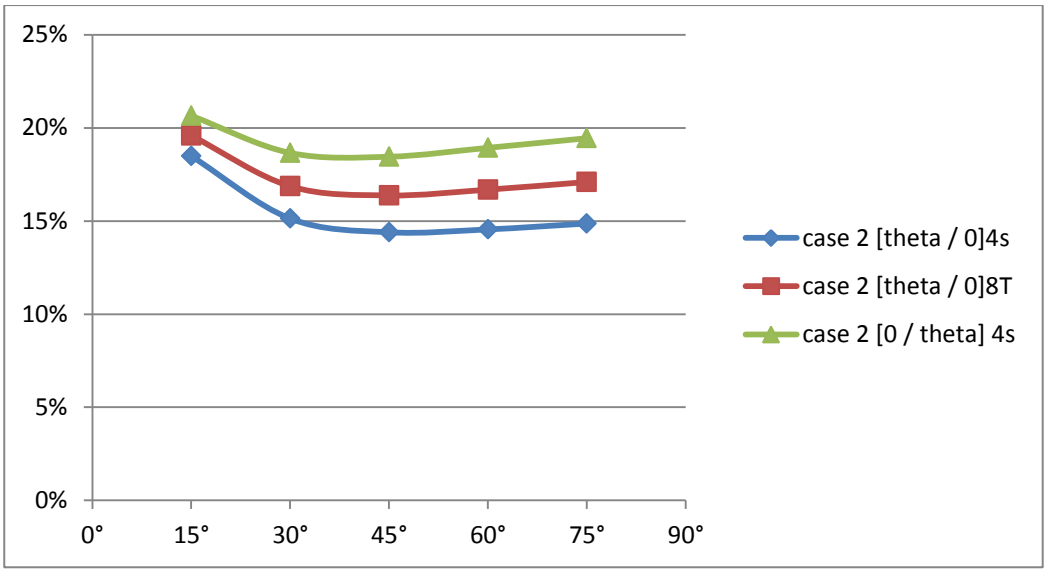

Figure 4.21 Variation of $\frac{W_s}{W_{total}}$ in Different Laminates with respect to the Fiber Orientation for Case 2

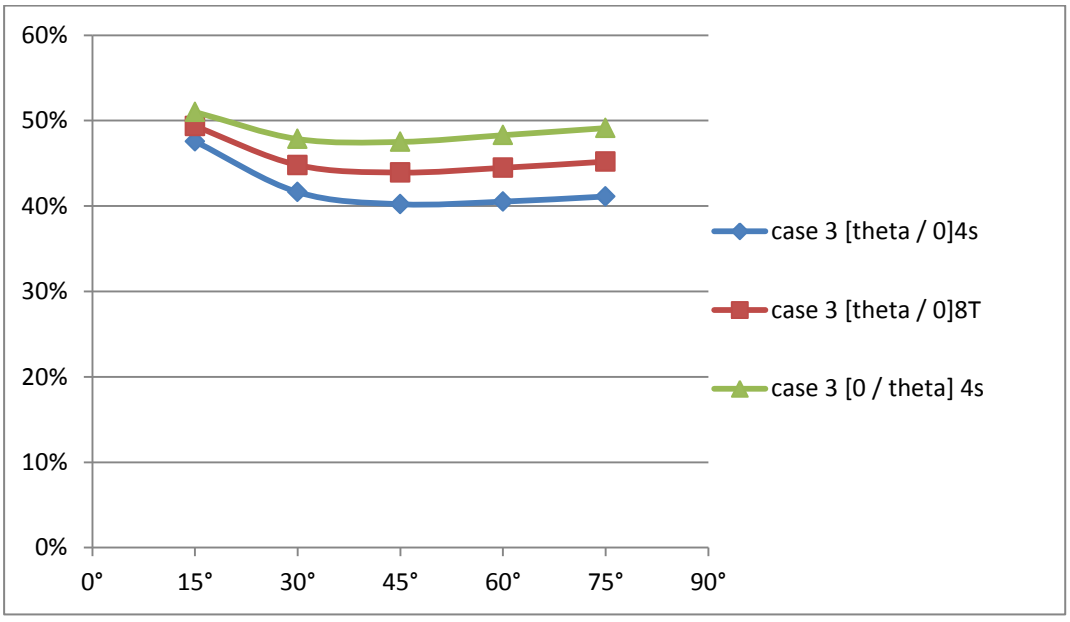

Figure 4.22 Variation of $\frac{W_s}{W_{total}}$ in Different Laminates with respect to the Fiber Orientation for Case 3

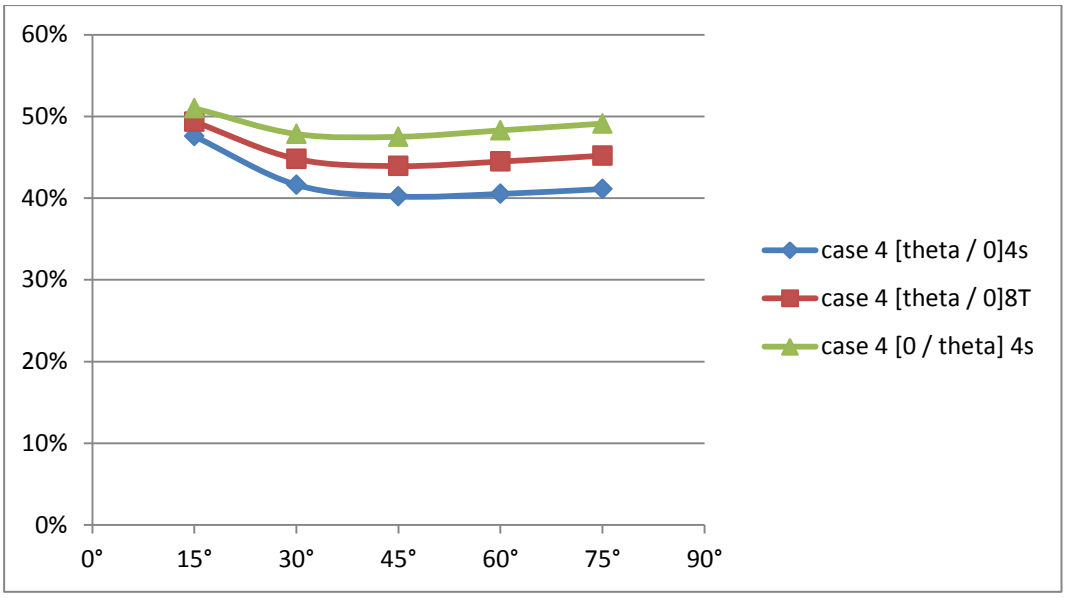

Figure 4.23 Variation of $\frac{W_s}{W_{total}}$ in Different Laminates with respect to the Fiber Orientation for Case 4

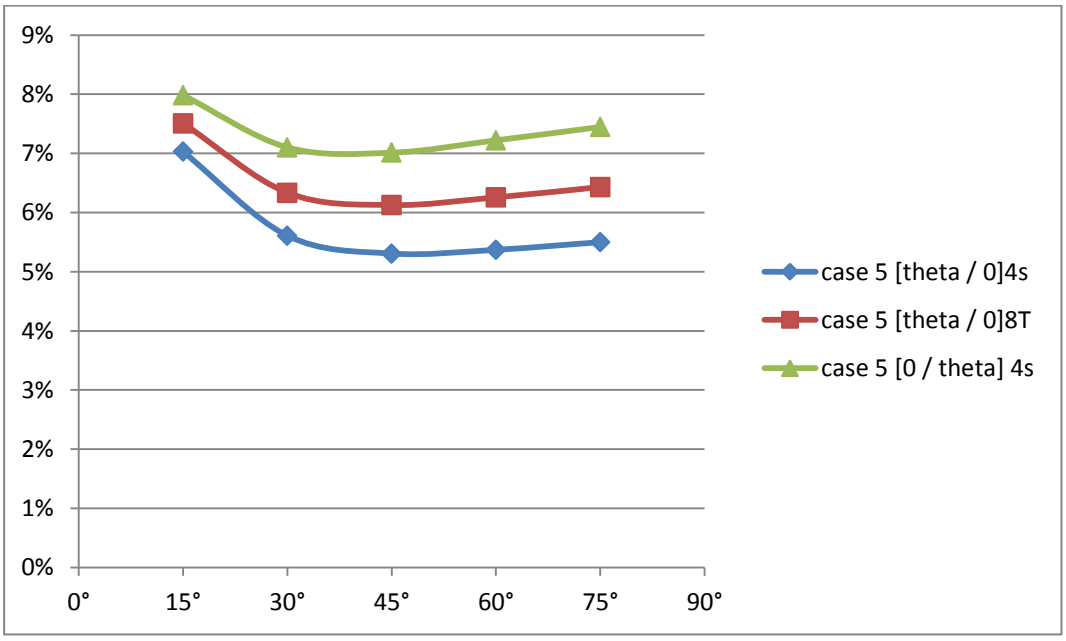

Figure 4.24 Variation of $\frac{W_s}{W_{total}}$ in Different Laminates with respect to the Fiber Orientation for Case 5

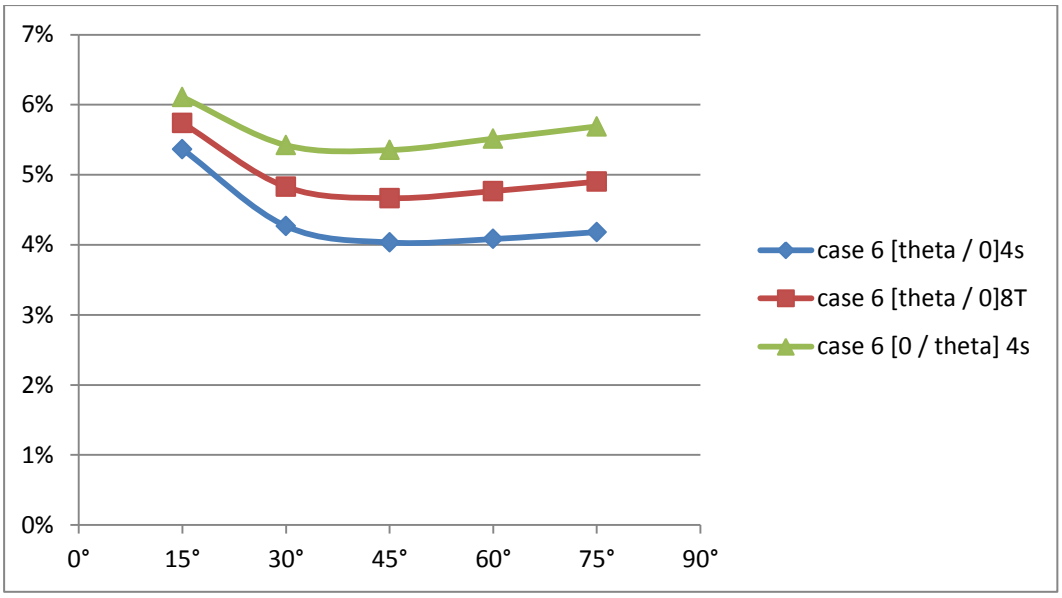

Figure 4.25 Variation of $\frac{W_s}{W_{total}}$ in Different Laminates with respect to the Fiber Orientation for Case 6

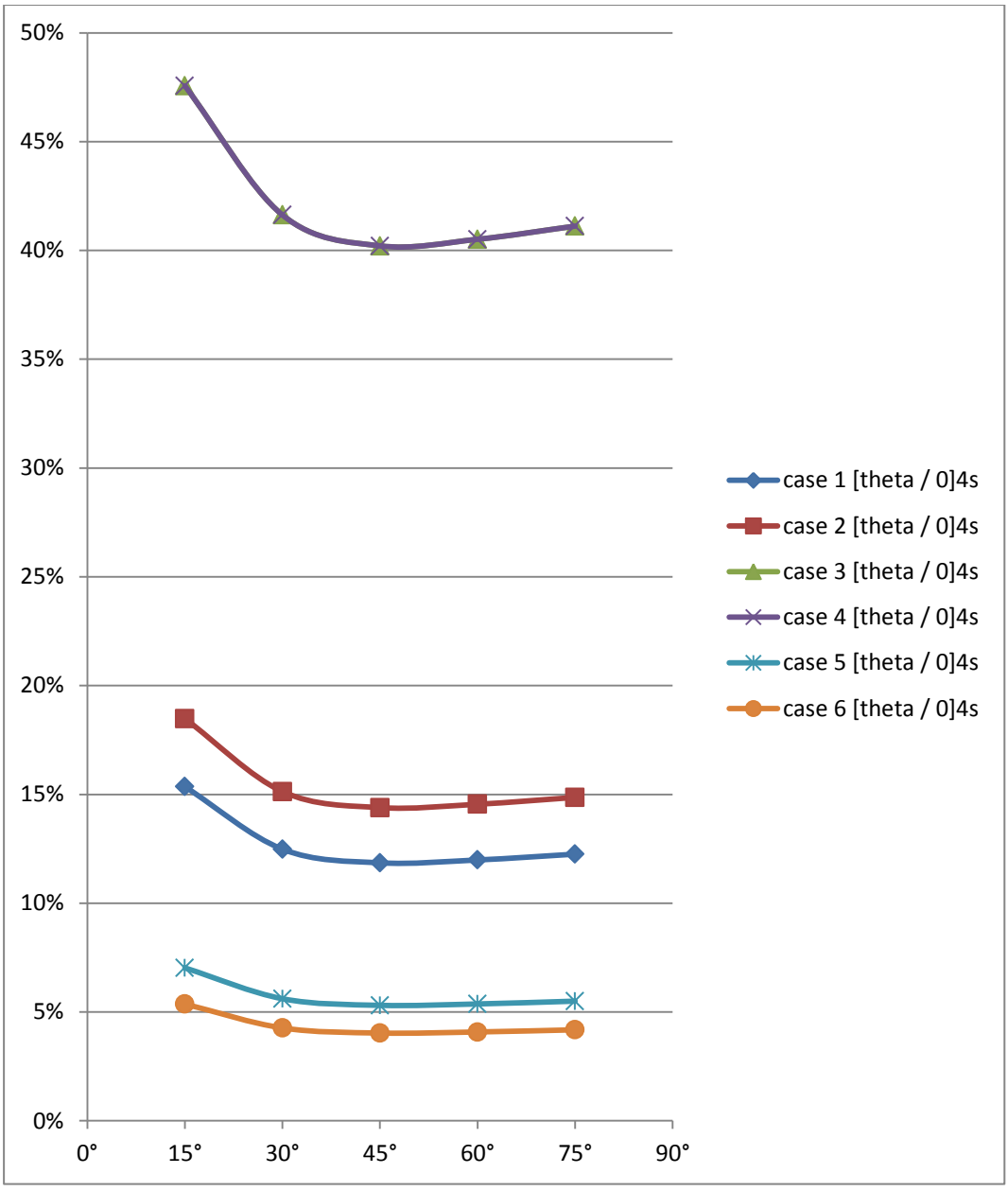

Figure 4.26 Variation of $\frac{W_s}{W_{total}}$ for Laminates $[\theta / 0]_{4s}$ in Different Cases.

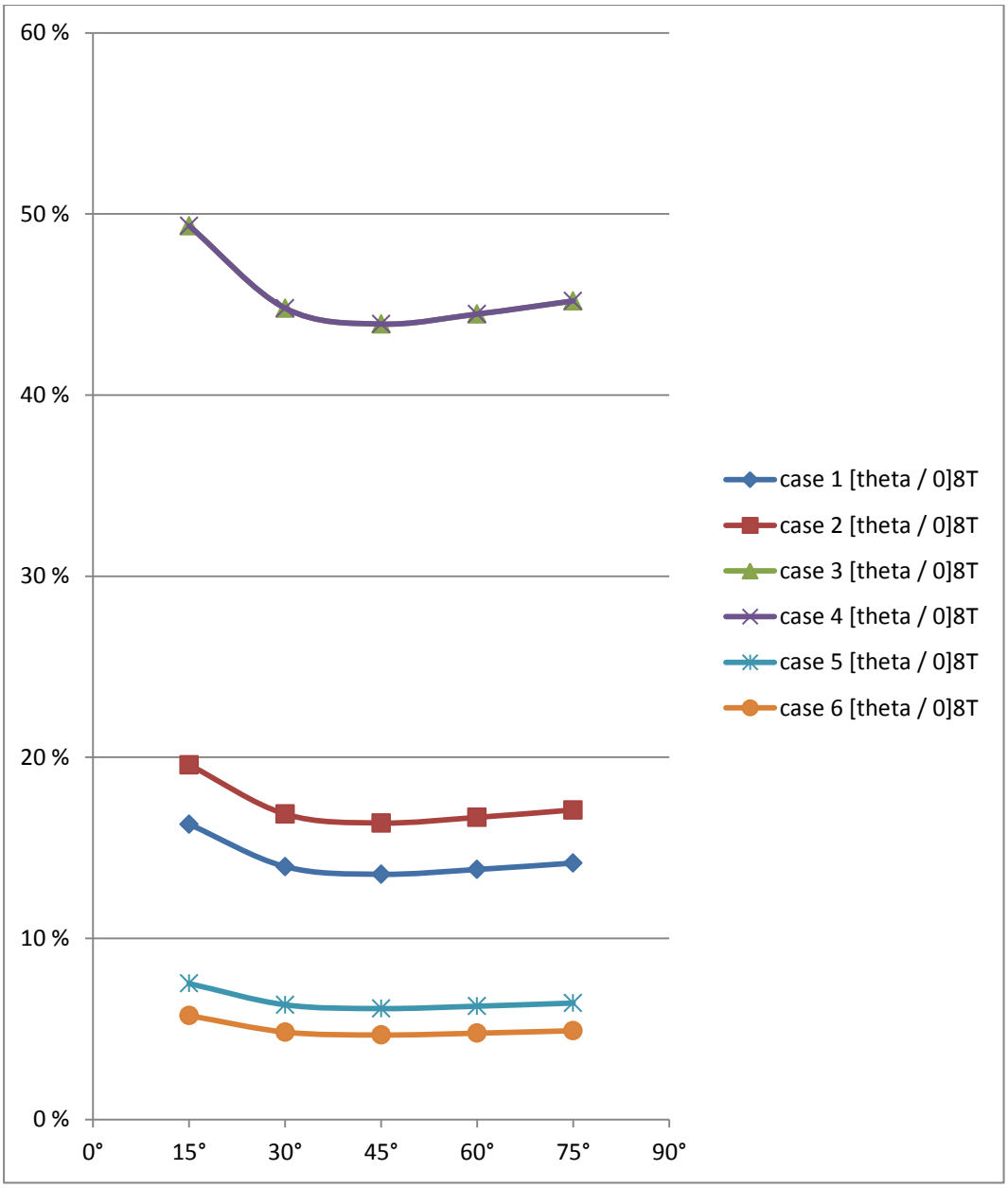

Figure 4.27 Variation of $\frac{W_s}{W_{total}}$ for Laminates $[\theta / 0]_{8T}$ in Different Cases.

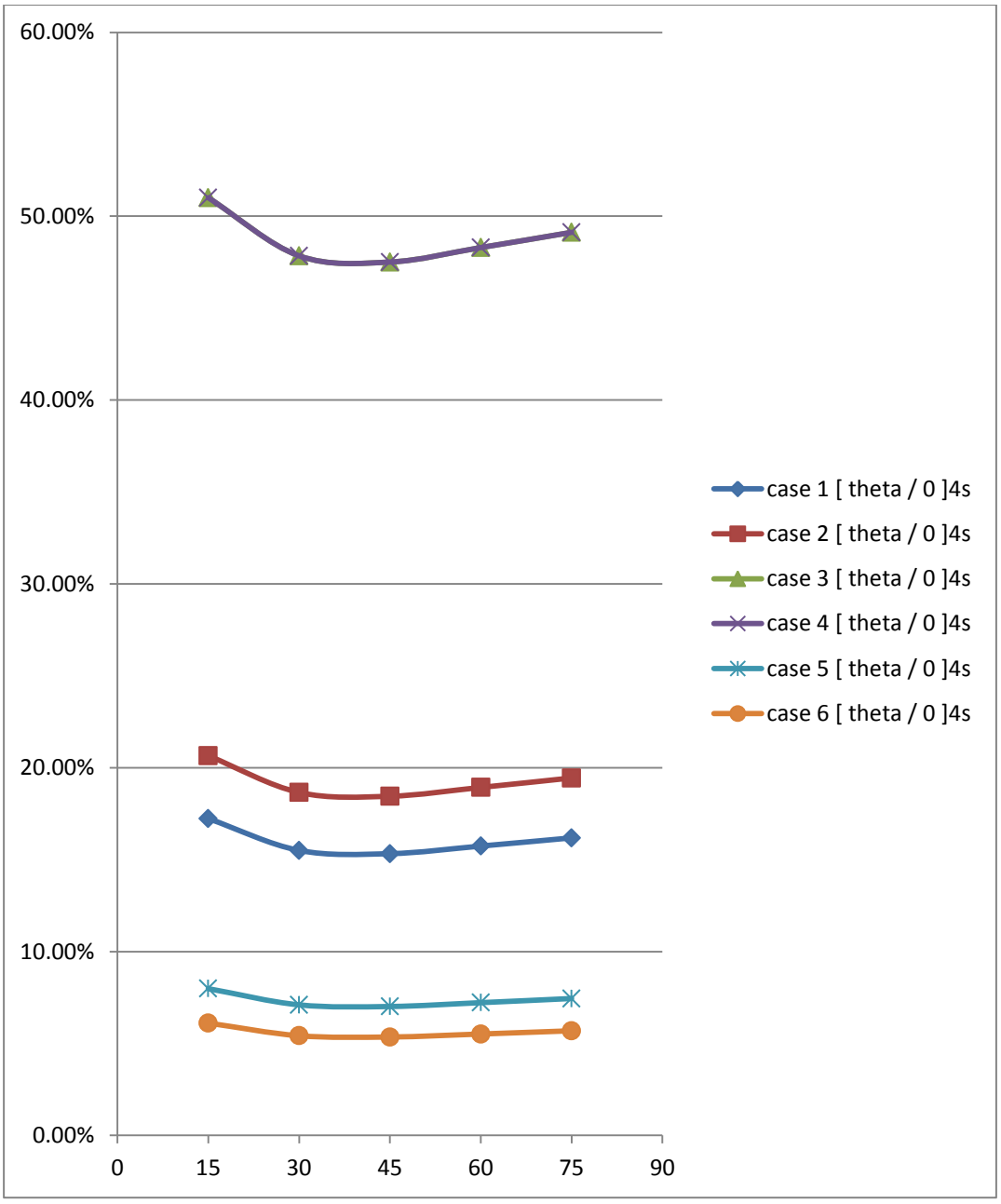

Figure 4.28 Variation of $\frac{W_s}{W_{total}}$ for Laminates $[0 / \theta]_{4s}$ in Different Cases.

Observation:

According to Figure 4.19 to 4.25,

1. Shear deformation W_s increases with increasing fiber orientations.
2. Bending deformation W_b increases with increasing fiber orientations. This is due to decreasing of bending stiffness.
3. Total deformation increases with increasing fiber orientations.
4. Fiber orientation $15°$ will have larger induced shear strain than others fiber orientations. However, the increased speed of W_b will larger than W_s when fiber orientation increases.

4.4 Comparisons of Error % Between Two Bending Stiffness

In this section, error % between theoretical and ANSYS results which are varied with fiber orientations are presented by cases. The bending stiffness $\frac{b}{d_{11}}$ in CASE B allows laminate twist by setting $M_{xy} = 0$. On the other hand, the bending stiffness in CASE A suppresses the curvature $k_{xy} = 0$. That is, bending moment in x-y plane M_{xy} will be induced. M_{xy} can be presented in terms of N_x and M_x. The detail information is included in Chapter 2. Figure 29 through Figure 40 show a comparison of the beam deflection with ANSYS results by using two different bending stiffness of the beam with and without twist. Table 4.2 and Table 4.3 tabulate the calculated results of beam deflection using two different expressions of bending stiffness.

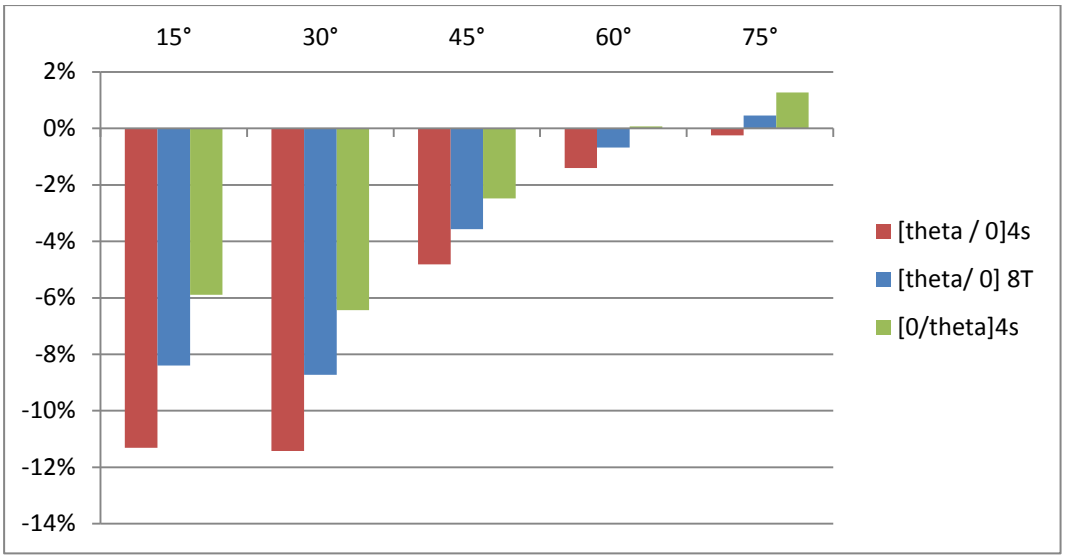

Figure 4.29 Error % in Case 1 by Using Bending Stiffness in Case B

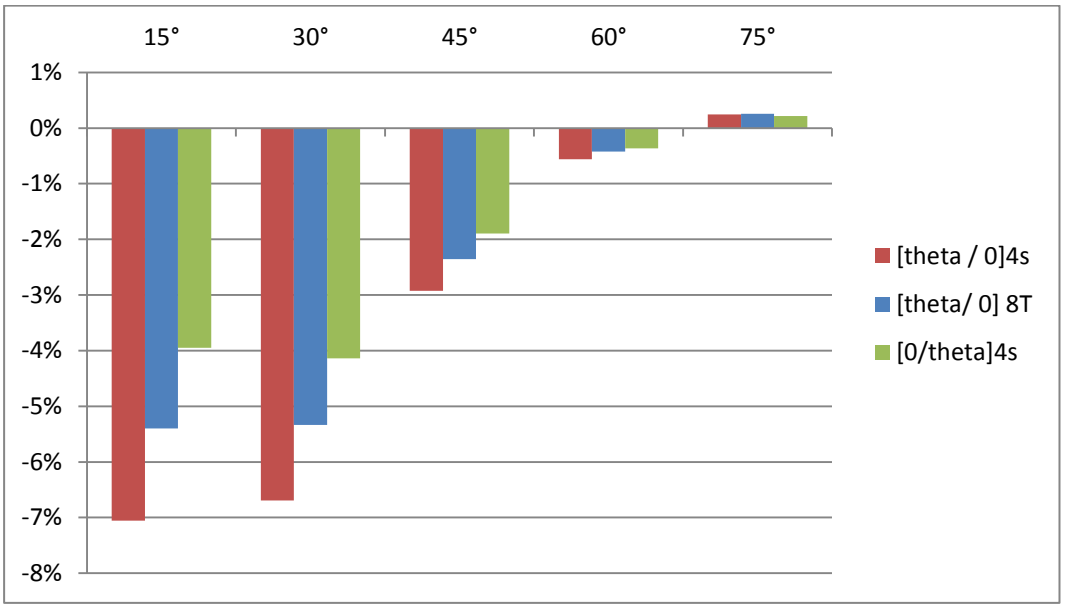

Figure 4.30 Error % in Case 1 by Using Bending Stiffness in Case A

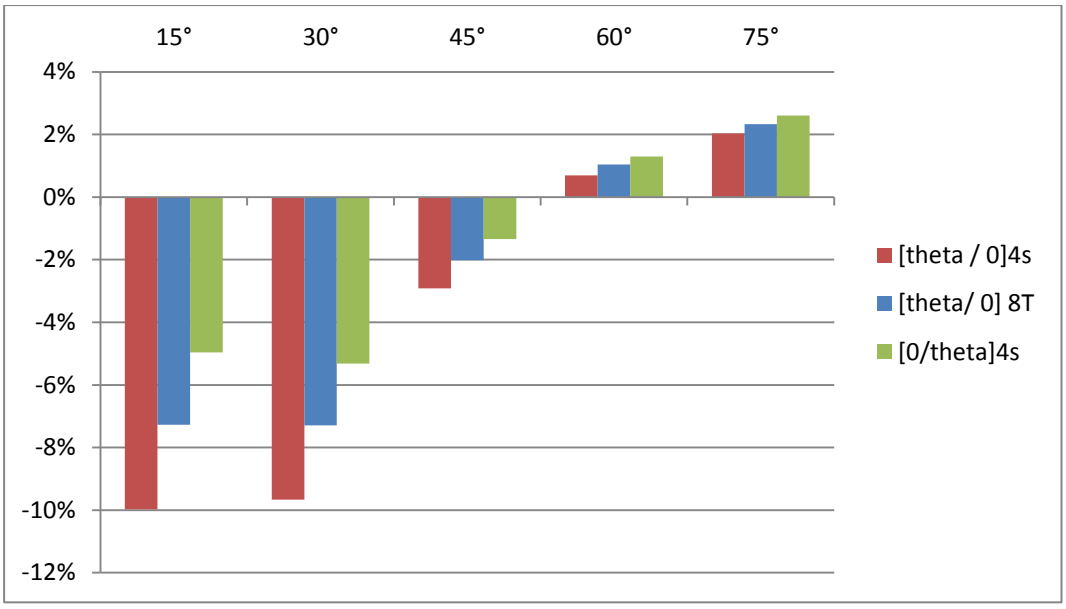

Figure 4.31 Error % in Case 2 by Using Bending Stiffness in Case B

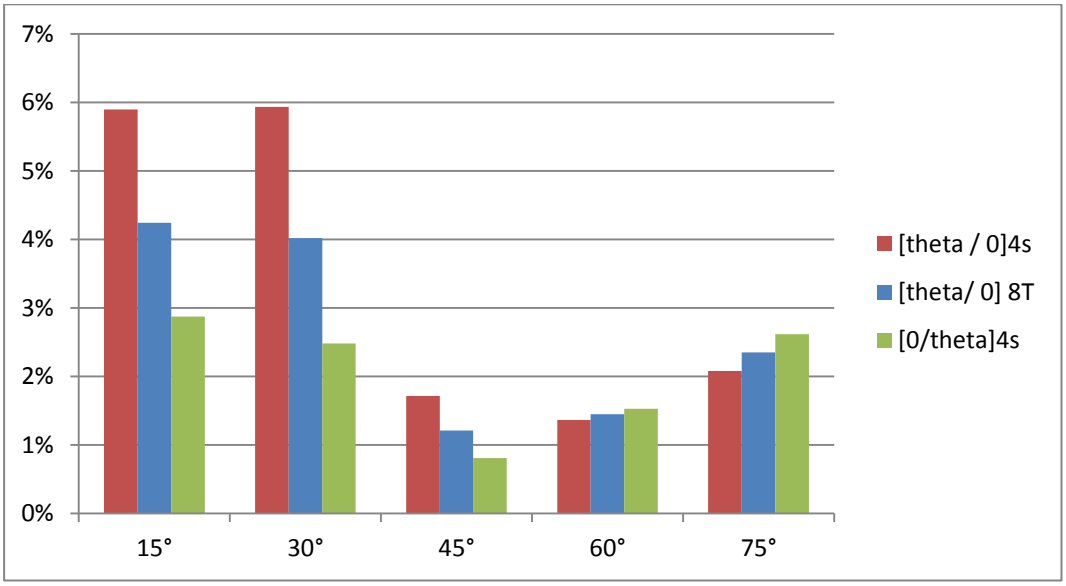

Figure 4.32 Error % in Case 2 by Using Bending Stiffness in Case A

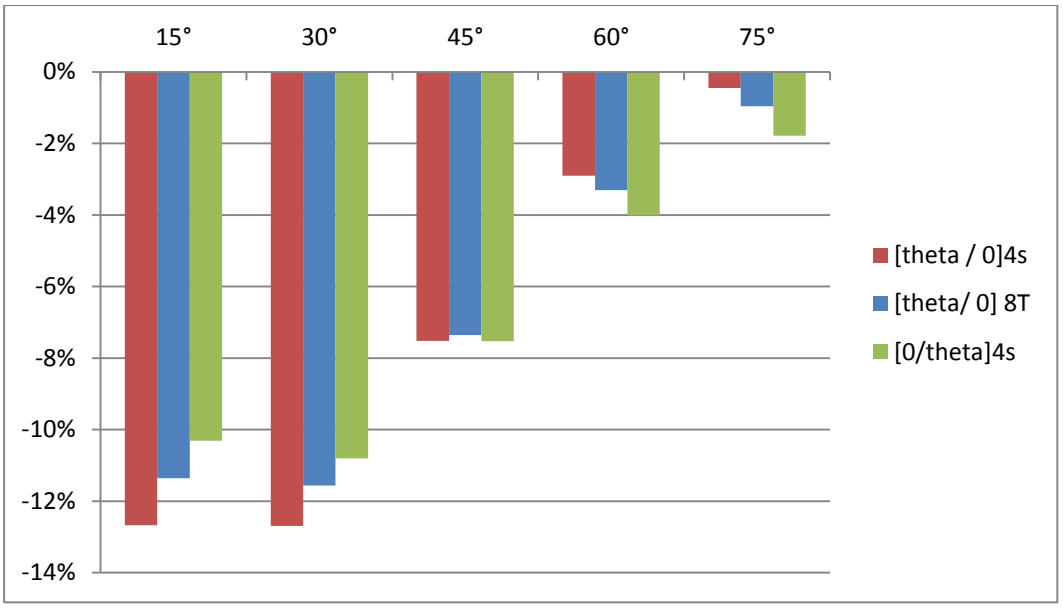

Figure 4.33 Error % in Case 3 by Using Bending Stiffness in Case B

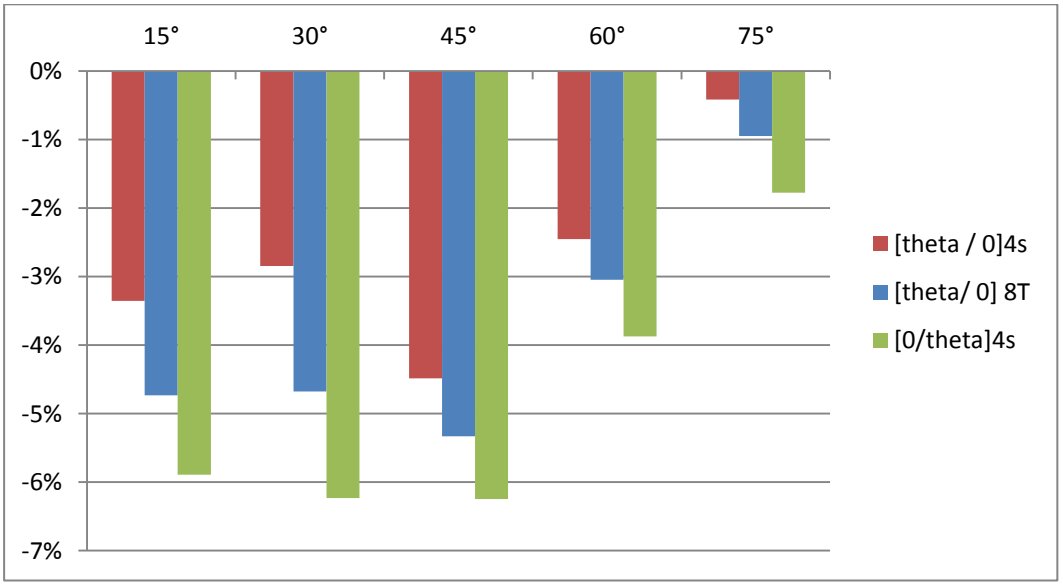

Figure 4.34 Error % in Case 3 by Using Bending Stiffness in Case A

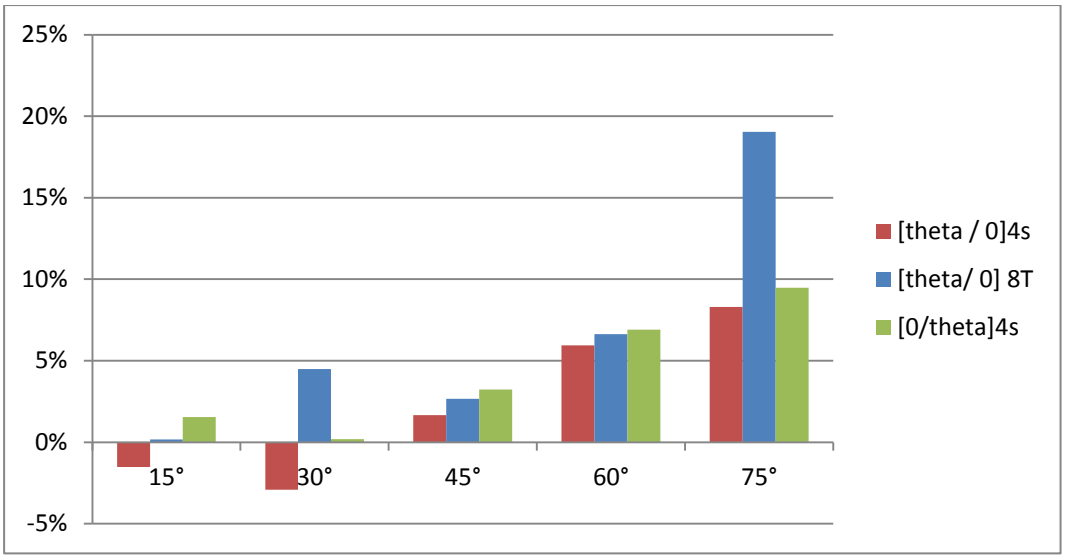

Figure 4.35 Error % in Case 4 by Using Bending Stiffness in Case B

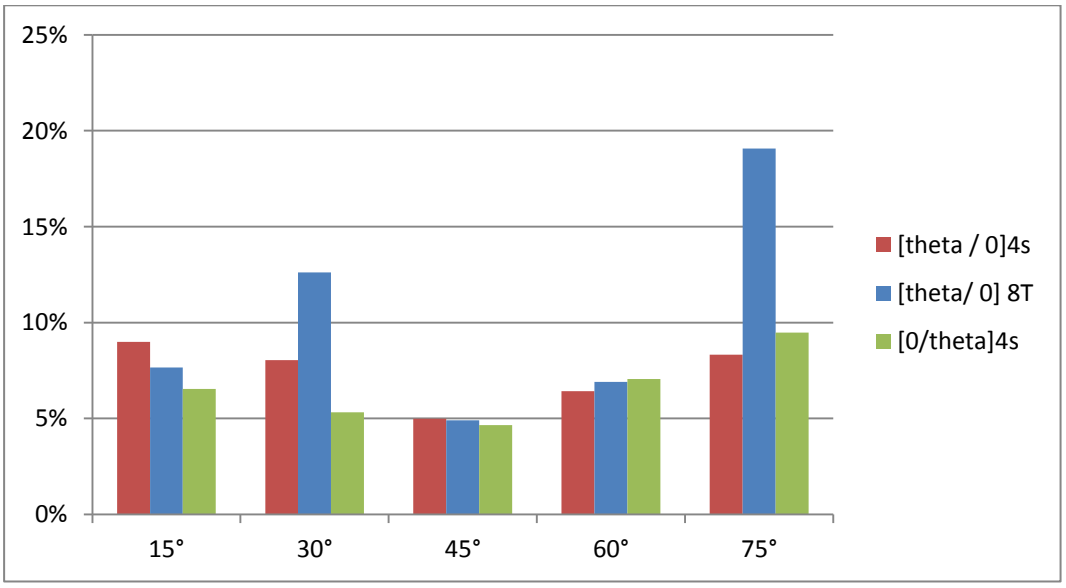

Figure 4.36 Error % in Case 4 by Using Bending Stiffness in Case A

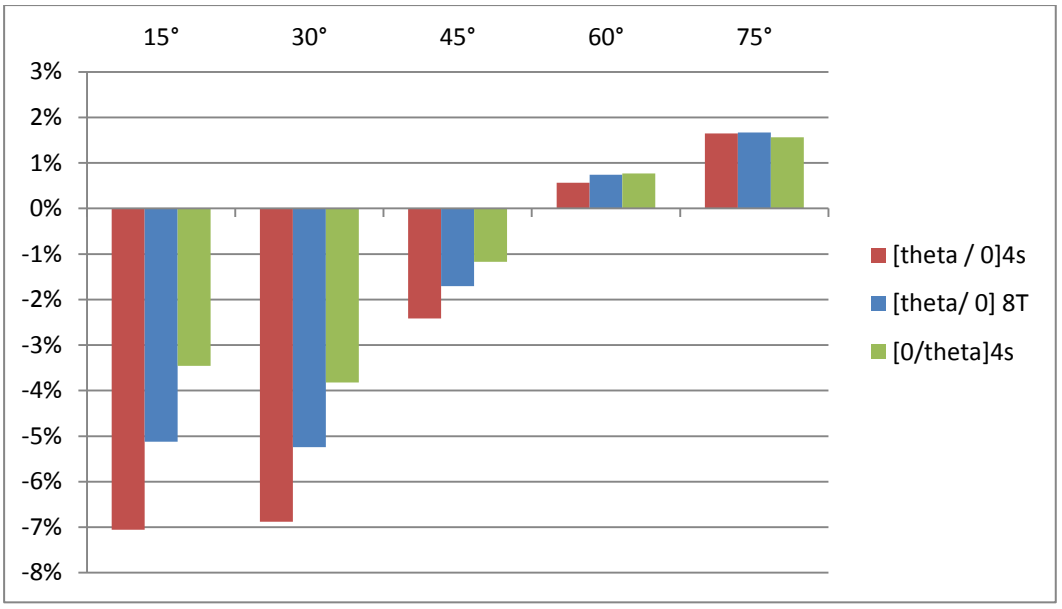

Figure 4.37 Error % in Case 5 by Using Bending Stiffness in Case B

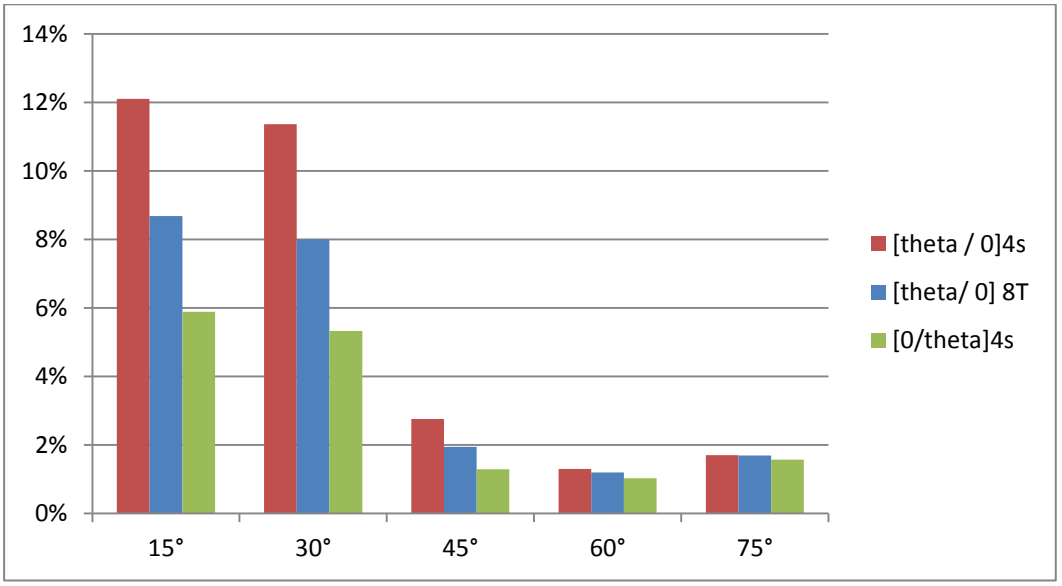

Figure 4.38 Error % in Case 5 by Using Bending Stiffness in Case A

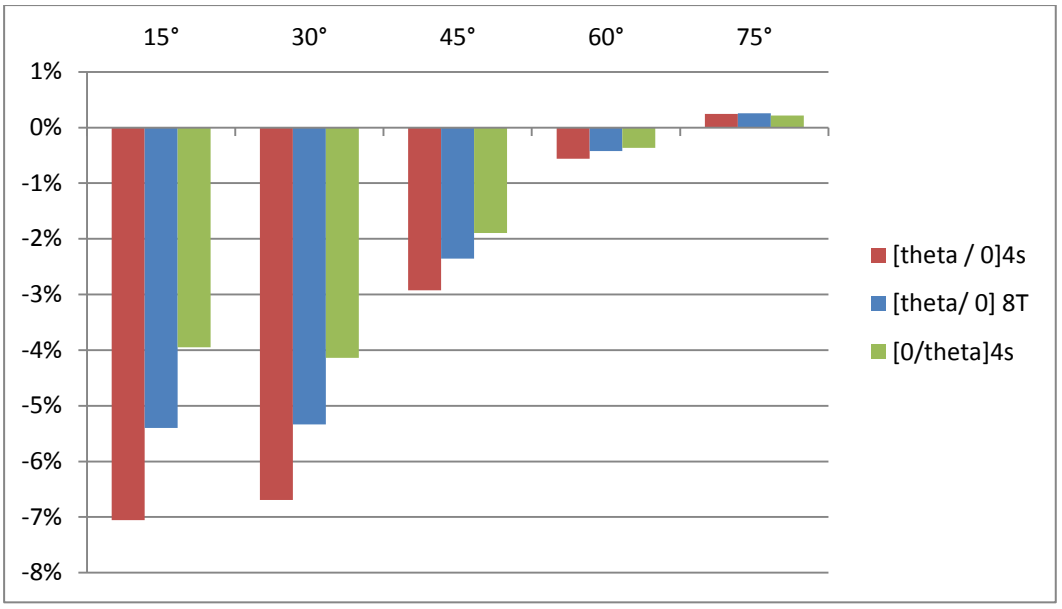

Figure 4.39 Error % in Case 6 by Using Bending Stiffness in Case B

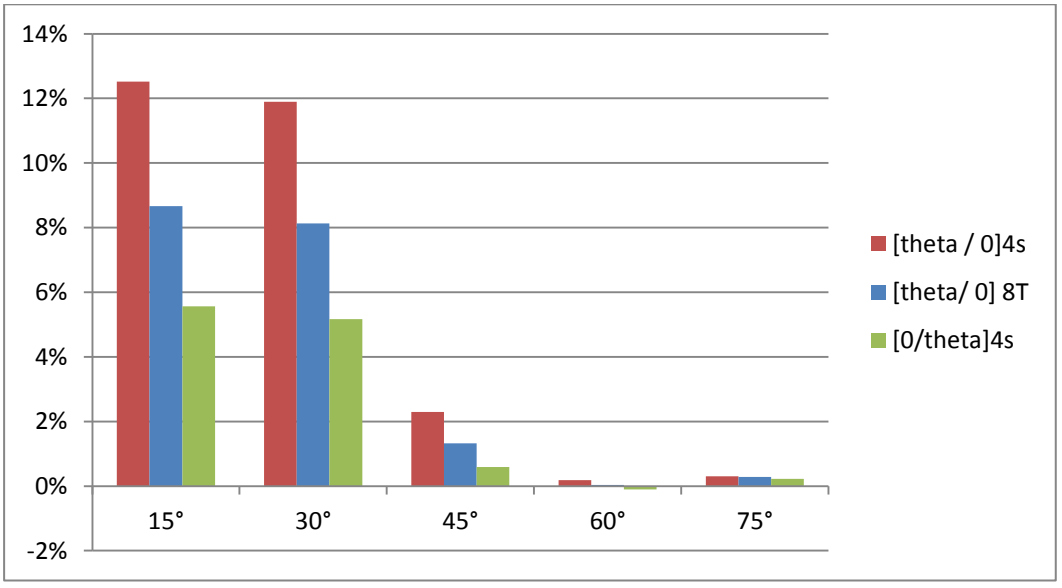

Figure 4.40 Error % in Case 6 by Using Bending Stiffness in Case A

Table 4.2 Comparison between Two Bending Stiffness for Laminate $[45/0]_{4s}$

$[45/0]_{4s}$									
		d_{11}				$\hat{d}_1$			
case	ANSYS	Wtotal	Wb	Ws	error %	Wtotal	Wb	Ws	error %
1	5.22E-5	5.49E-5	4.84E-5	6.50E-6	-4.82	5.23E-5	4.58E-5	6.50E-6	-0.14
3	1.50E-5	1.62E-5	9.67E-6	6.50E-6	-7.52	1.57E-5	9.16E-6	6.50E-6	-4.48
5	4.78E-4	4.90E-4	4.64E-4	2.60E-5	-2.42	4.66E-4	4.40E-4	2.60E-5	2.75
case	ANSYS	Wtotal	Wb	Ws	error	Wtotal	Wb	Ws	error %
2	8.78E-5	9.04E-5	7.74E-5	1.30E-5	-2.91	8.63E-5	7.33E-5	1.30E-5	1.72
4	3.29E-5	3.24E-5	1.93E-5	1.30E-5	1.66	3.13E-5	1.83E-5	1.30E-5	4.99
6	1.25E-3	1.29E-3	1.24E-3	5.20E-5	-2.93	1.22E-3	1.17E-3	5.20E-5	2.29

unit: inch

Table 4.3 Comparison between Two Bending Stiffness for Laminate $[45/0]_{8T}$

$[45/0]_{8T}$									
		d_{11}				$\hat{d}_1$			
case	ANSYS	Wtotal	Wb	Ws	error %	Wtotal	Wb	Ws	error %
1	4.63E-5	4.80E-5	4.15E-5	6.50E-6	-3.57	4.64E-5	3.99E-5	6.50E-6	-0.28
3	1.37E-5	1.48E-5	8.30E-6	6.50E-6	-7.36	1.45E-5	7.99E-6	6.50E-6	-5.33
5	4.17E-4	4.25E-4	3.99E-4	2.60E-5	-1.70	4.09E-4	3.83E-4	2.60E-5	1.95
case	ANSYS	Wtotal	Wb	Ws	error %	Wtotal	Wb	Ws	error %
2	7.78E-5	7.94E-5	6.64E-5	1.30E-5	-2.02	7.69E-5	6.39E-5	1.30E-5	1.21
4	3.04E-5	2.96E-5	1.66E-5	1.30E-5	2.67	2.90E-5	1.60E-5	1.30E-5	4.91
6	1.09E-3	1.12E-3	1.06E-3	5.20E-5	-2.36	1.07E-3	1.02E-3	5.20E-5	1.33

unit: inch

Observations:

1. $\hat{d}_1$ takes twisting curvature into account and d_{11} allow laminate twist. Once suppressing the curvaturek_{xy}, an extra moment M_{xy} will be induced. Thus, $\hat{d}_1$=$d_{11} - \frac{{d_{16}}^2}{d_{66}}$ takes shear coupling terms into account. The bending stiffness in case A is stiffer than case B, resulting in stiffer laminates. The stiffness increases with suppressingk_{xy}. Therefore, even though some cases' results are better by using bending stiffness in case B, in general, case A is more acceptable.

Chapter 5

Conclusion

Analytical methods are developed for determining deflection of composite beams under transverse load with various boundary conditions and laminate configurations. A closed form expression of 1-D equivalent bending stiffness with and without presence of twisting curvature is formulated and used for investigating the beam deflection. Finite element analysis of 3-D ANSYS models is conducted by using Solid186 elements to obtain the beam deflection used for comparing with analytical calculation. .

First of all, for boundary condition and loading effects, cases in concentrated load will have larger shear deformation than cases in uniformly distributed load. Cantilever beam cases will have larger total deflections than other cases. However, cases 3 and 4 (beam fixed at both ends with uniformly distributed and concentrated load, respectively) have larger shear percentage $\frac{W_s}{W_{total}}$ than other cases.

Secondly, for stack sequence effects, shear deformation on beam deflection due to stacking sequence is insignificant regardless of the type of loading. However, bending deformations are different because equivalent bending stiffness changes with changing stack sequences.

Thirdly, for fiber orientation effects, shear deformation increases with increasing fiber orientations. In addition, bending deformation increases with increasing fiber orientations. $\frac{W_s}{W_{total}}$ is maximum when fiber orientation is equal to $15°$ at which $\eta_{xy,x}$ reaches its maximum value.

Lastly, using bending stiffness of the beam with induced twisting curvature (Case A) for calculating beam deflection results in a better correlation with ANSYS results compared with the case of bending stiffness without twisting suppression (Case B).

However, some beam cases, using Case B expression is fitted better than using Case A. The future work is needed to find the shear correction factor by investigating patterns of shear stress τ_{xz} and experimental validation on the present analytical model.

Appendix A

Derived Moments for Different Boundary Conditions presented in Chapter 2

Derived Moments from Free Body Diagram in each Cases.

Case 1

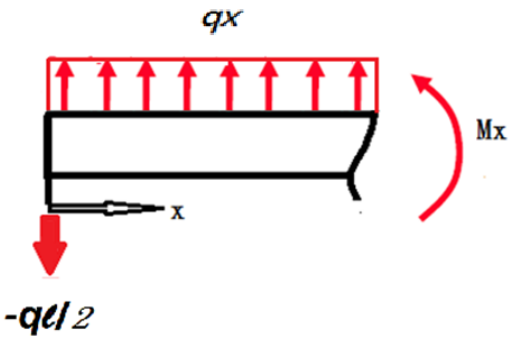

$$\mathrm{M} = -\frac{\mathrm{q}\ell}{2b}x + qx\frac{x}{2b}$$

$$= \frac{-\mathrm{q}\ell\mathrm{x}}{2b} + \frac{qx^2}{2b}$$

$$= -\frac{qx}{2b}(\ell - \mathrm{x}) \qquad (2.50)$$

Case 2

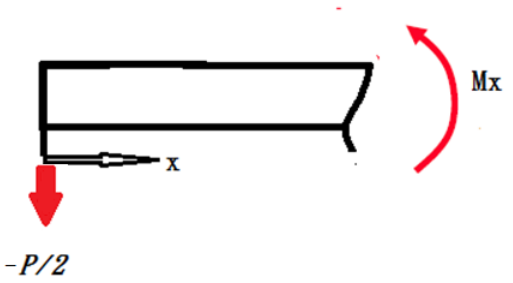

$$\mathrm{M} = \frac{-P}{2b}x = \frac{-Px}{2b} \qquad (2.51)$$

Case 3

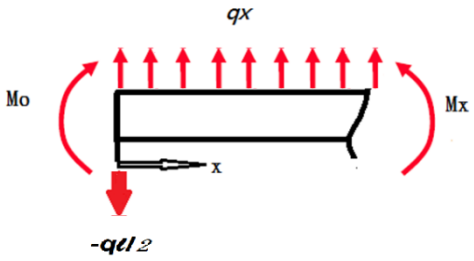

$$M_x = M_0 - \frac{q\ell}{2b}x + qx\frac{x}{2b}$$

$$\theta = \frac{\partial U_b}{\partial M_0} = \frac{\partial}{\partial M_0}\int_0^{\ell} 2\frac{{M_x}^2}{2EI}dx$$

Therefore,

$$\theta = 2\int_o^{\ell}\frac{\partial M_x}{\partial M_0}\frac{M_x}{EI}dx$$

$$= \frac{2}{EI}\int_0^{\ell} 1\left(M_0 - \frac{q\ell}{2b}x + qx\frac{x}{2b}\right)dx$$

$$= \frac{2}{EI}\left(M_0\ell - \frac{q\ell^3}{4b} + \frac{q\ell^3}{6b}\right) \qquad (2.53)$$

Substituting the boundary condition $\theta = 0$ at the fix end into equation,

$$M_0 = \frac{q\ell^2}{12b} \qquad (2.54)$$

Substituting Equation (2.54) into Equation (2.53), the bending moment along x-axis becomes

$$M_x = -\frac{q}{12b}(6\ell x - \ell^2 - 6x^2) \qquad (2.55)$$

Case 4

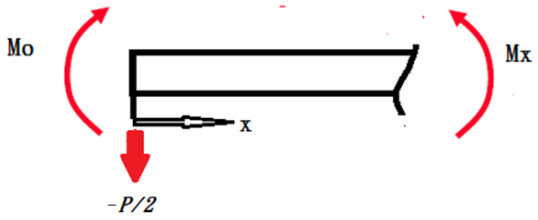

$$M_x = M_0 - \frac{\mathrm{P}}{2b}x$$

$$\theta = \frac{\partial U_b}{\partial M_0} = \frac{\partial}{\partial M_0}\int_0^{\ell/2} 2\frac{{M_x}^2}{2EI}dx$$

Therefore,

$$\theta = 2\int_o^{\ell}\frac{\partial M_x}{\partial M_0}\frac{M_x}{EI}dx$$

$$= \frac{2}{EI}\int_0^{\ell/2} 1\left(M_0 - \frac{\mathrm{P}}{2b}x\right)dx$$

$$= \frac{2}{EI}\left(\frac{M_0\ell}{2} - \frac{P\ell^2}{16b}\right) \qquad (2.56)$$

Substituting the boundary condition $\theta = 0$ at the fix end into equation,

$$M_0 = \frac{P\ell}{8b} \qquad (2.57)$$

Substituting Equation (2.57) into Equation (2.56), the bending moment along x-axis becomes

$$M_x = -\frac{P}{8b}(4x - \ell) \qquad (2.58)$$

Case 5

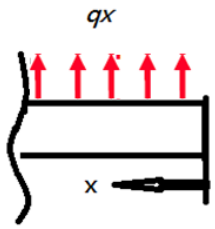

$$M_x = -qx\frac{x}{2b} = \frac{-qx^2}{2b} \tag{2.59}$$

Case 6

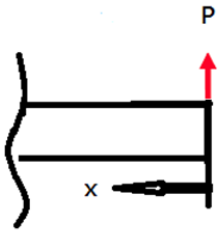

$$M_x = -Px \tag{2.60}$$

Appendix B

Derived Beam Equations from Case 2 to Case 6

Case 2 Simply Support Beam – Concentrated Load at Center

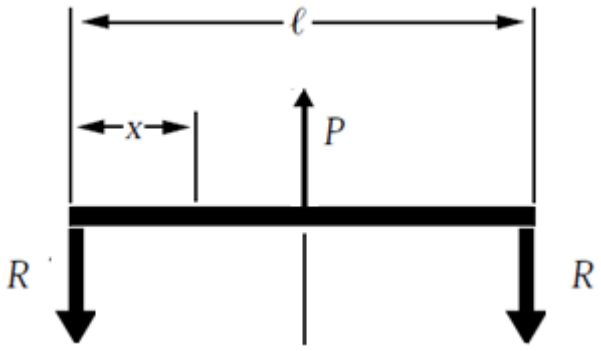

Figure 2

The bending moment in the left half of the beam is

$$M_x = \frac{-Px}{2b}, \qquad when\ x < \frac{\ell}{2} \tag{2.61}$$

where b is the width.

Thus, substituting Equations (2.25) and (2.33) into Equation (2.61) yields

$$\frac{d\psi_x}{dx} = d_{11}\frac{Px}{2b} \tag{2.62}$$

which integrates to

$$\psi_x(x) = d_{11}\frac{Px^2}{4b} + C_3 \tag{2.63}$$

The boundary condition, $\psi_x\left(\frac{\ell}{2}\right) = 0$, provides the constant of integration

$$C_3 = -d_{11}\frac{P\ell^2}{16b} \tag{2.64}$$

Thus, the rotation of cross-section originally perpendicular to the x axis ψ_x becomes

$$\psi_x(x) = d_{11}\frac{Px^2}{4b} - d_{11}\frac{P\ell^2}{16b} \tag{2.65}$$

Substituting of Equation (2.65) into Equation (2.35), yields

$$\frac{dw}{dx} = -d_{11}\frac{Px^2}{4b} + d_{11}\frac{P\ell^2}{16b} + \frac{kP}{2A\overline{G_{xz}}} \tag{2.66}$$

where A is the cross-section area of the beam. (*A*=*bh*)

The displacement *w* can be integrated from Equation (2.66).

$$w = -d_{11}\frac{Px^3}{12b} + d_{11}\frac{P\ell^2 x}{16b} + \frac{kPx}{2A\overline{G_{xz}}} + C_4 \tag{2.67}$$

The boundary condition *w* (0) = 0, provides the constant of integration

$$C_4 = 0 \tag{2.68}$$

Hence, the beam deflection is given by

$$\mathrm{w} = -d_{11}\frac{Px^3}{12b} + d_{11}\frac{P\ell^2 x}{16b} + \frac{kPx}{2A\overline{G_{xz}}} \tag{2.69}$$

In this case, the magnitude of deflection of the beam at the point of load application is of particular interest

$$\delta = |w(\ell/2)| = \frac{1}{48}\frac{d_{11}P\ell^3}{b} + \frac{kP\ell}{4A\overline{G_{xz}}} \tag{2.70}$$

where δ is the deflection of the beam.

When the bending moment distribution along the x-direction is known, the deflection may be obtained. The total deflection is the combination of bending and shear deformation. For the case of simply beam under concentrated load at center,

$$w^B = \frac{1}{48}\frac{d_{11}P\ell^3}{b} \tag{2.71}$$

$$w^S = \frac{kP\ell}{4A\overline{G_{xz}}} \tag{2.72}$$

$$\frac{w^B}{w^S} = \frac{d_{11}\ell^2 A\overline{G_{xz}}}{12bk} \tag{2.73}$$

Case 3 Bean Fixed at Both Ends – Uniform Distributed Load

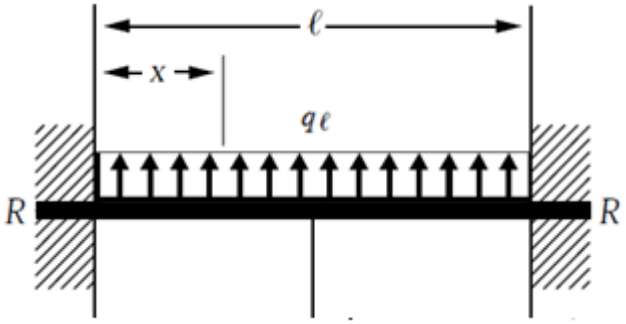

Figure 3

The bending moment in the left half of the beam is

$$M_x = \frac{-q}{12b}(6\ell x - \ell^2 - 6x^2) \qquad (2.74)$$

where b is the width, and ℓ is the length of the beam.

Thus, substituting Equations (2.25) and (2.33) into Equation (2.74) yields

$$\frac{d\psi_x}{dx} = d_{11}\frac{q}{12b}(6\ell x - \ell^2 - 6x^2) \qquad (2.75)$$

which integrates to

$$\psi_x(x) = d_{11}\frac{q}{12b}(3\ell x^2 - \ell^2 x - 2x^3) + C_5 \qquad (2.76)$$

The boundary condition, $\psi_x(0) = 0$, provides the constant of integration

$$C_5 = 0 \tag{2.77}$$

Thus, the rotation of cross-section originally perpendicular to the x axis ψ_x becomes

$$\psi_x(x) = d_{11}\frac{q}{12b}(3\ell x^2 - \ell^2 x - 2x^3) \tag{2.78}$$

Substituting of Equation (2.78) into Equation (2.35), yields

$$\frac{dw}{dx} = -d_{11}\frac{q}{12b}(3\ell x^2 - \ell^2 x - 2x^3) + \frac{kq}{12A\overline{G_{xz}}}(6\ell - 12x) \tag{2.79}$$

where A is the cross-section area of the beam. (*A*=*bh*)

The displacement *w* can be integrated from Equation (2.79).

$$w = -d_{11}\frac{q}{12b}(\ell x^3 - \frac{\ell^2 x^2}{2} - \frac{x^4}{2}) + \frac{kq}{12A\overline{G_{xz}}}(6\ell x - 6x^2) + C_6 \tag{2.80}$$

The boundary condition *w* (0) = 0, provides the constant of integration

$$C_6 = 0 \tag{2.81}$$

Hence, the beam deflection is given by

$$\mathrm{w} = -d_{11}\frac{q}{12b}(\ell x^3 - \frac{\ell^2 x^2}{2} - \frac{x^4}{2}) + \frac{kq}{12A\overline{G_{xz}}}(6\ell x - 6x^2) \tag{2.82}$$

In this case, the magnitude of deflection of the beam at the point of load application is of particular interest

$$\delta = |w(\ell/2)| = \frac{1}{384}\frac{d_{11}q\ell^4}{b} + \frac{kq\ell^2}{8A\overline{G_{xz}}} \tag{2.83}$$

where δ is the deflection of the beam.

When the bending moment distribution along the x-direction is known, the deflection may be obtained. The total deflection is the combination of bending and shear deformation. For the case of beam fixed at both ends with uniform distributed load,

$$w^B = \frac{1}{384}\frac{d_{11}q\ell^4}{b} \tag{2.84}$$

$$w^S = \frac{kq\ell^2}{8A\overline{G_{xz}}} \tag{2.84}$$

$$\frac{w^B}{w^S} = \frac{d_{11}\ell^2 A\overline{G_{xz}}}{48bk} \tag{2.86}$$

Case 4 Bean Fixed at Both Ends – Concentrated Load at Center

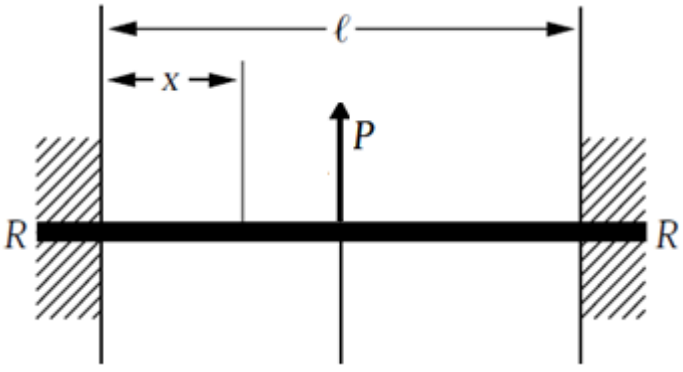

Figure 4

The bending moment in the left half of the beam is

$$M_x = -\frac{P}{8b}(4x - \ell) \tag{2.87}$$

where b is the width.

Thus, substituting Equations (2.25) and (2.33) into Equation (2.87) yields

$$\frac{d\psi_x}{dx} = d_{11}\frac{P}{8b}(4x - \ell) \tag{2.88}$$

which integrates to

$$\psi_x(x) = d_{11}\frac{P}{8b}(2x^2 - \ell x) + C_7 \tag{2.89}$$

The boundary condition, $\psi_x(0) = 0$, provides the constant of integration

$$C_7 = 0 \tag{2.90}$$

Thus, the rotation of cross-section originally perpendicular to the x axis ψ_x becomes

$$\psi_x(x) = d_{11}\frac{P}{8b}(2x^2 - \ell x) \tag{2.91}$$

Substituting of Equation (2.91) into Equation (2.35), yields

$$\frac{dw}{dx} = -d_{11}\frac{P}{8b}(2x^2 - \ell x) + \frac{k4P}{8A\overline{G_{xz}}} \qquad (2.92)$$

where A is the cross-section area of the beam. (*A*=*bh*)

The displacement *w* can be integrated from Equation (2.92).

$$w = -d_{11}\frac{P}{8b}\left(\frac{2x^3}{3} - \frac{\ell x^2}{2}\right) + \frac{4kPx}{8A\overline{G_{xz}}} + C_8 \qquad (2.93)$$

The boundary condition *w* (0) = 0, provides the constant of integration

$$C_8 = 0 \qquad (2.94)$$

Hence, the beam deflection is given by

$$\mathrm{w} = -d_{11}\frac{P}{8b}\left(\frac{2x^3}{3} - \frac{\ell x^2}{2}\right) + \frac{4kPx}{8A\overline{G_{xz}}} \qquad (2.95)$$

In this case, the magnitude of deflection of the beam at the point of load application is of particular interest

$$\delta = |w(\ell/2)| = \frac{1}{192}\frac{d_{11}P\ell^3}{b} + \frac{kP\ell}{4A\overline{G_{xz}}} \qquad (2.96)$$

where δ is the deflection of the beam.

When the bending moment distribution along the x-direction is known, the deflection may be obtained. The total deflection is the combination of bending and shear deformation. For the case of beam fixed at both ends with concentrated load at center,

$$w^B = \frac{1}{192}\frac{d_{11}P\ell^3}{b} \tag{2.97}$$

$$w^S = \frac{kP\ell}{4A\overline{G_{xz}}} \tag{2.98}$$

$$\frac{w^B}{w^S} = \frac{d_{11}\ell^2 A\overline{G_{xz}}}{48bk} \tag{2.99}$$

Case 5 Cantilever Beam – Uniform Distributed Load

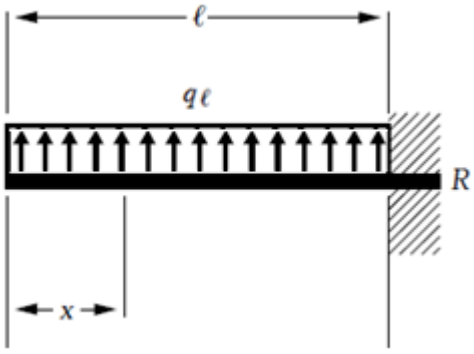

Figure 5

The bending moment in the right half of the beam is

$$M_x = -\frac{qx^2}{2b} \tag{2.100}$$

where b is the width.

Thus, substituting Equations (2.25) and (2.33) into Equation (2.100) yields

$$\frac{d\psi_x}{dx} = d_{11}\frac{qx^2}{2b} \tag{2.101}$$

which integrates to

$$\psi_x(x) = d_{11}\frac{qx^3}{6b} + C_9 \tag{2.102}$$

The boundary condition, $\psi_x(\ell) = 0$, provides the constant of integration

$$C_9 = -d_{11}\frac{q\ell^3}{6b} \tag{2.103}$$

Thus, the rotation of cross-section originally perpendicular to the x axis ψ_x becomes

$$\psi_x(x) = d_{11}\frac{qx^3}{6b} - d_{11}\frac{q\ell^3}{6b} \tag{2.104}$$

Substituting of Equation (2.104) into Equation (2.35), yields

$$\frac{dw}{dx} = -d_{11}\frac{qx^3}{6b} + d_{11}\frac{q\ell^3}{6b} + \frac{kqx}{A\overline{G_{xz}}} \tag{2.105}$$

where A is the cross-section area of the beam. (*A*=*bh*)

The displacement *w* can be integrated from Equation (2.105).

$$w = -d_{11}\frac{qx^4}{24b} + d_{11}\frac{q\ell^3 x}{6b} + \frac{kqx^2}{A\overline{G_{xz}}} + C_{10} \qquad (2.106)$$

The boundary condition $w(\ell) = 0$, provides the constant of integration

$$C_{10} = -d_{11}\frac{q\ell^4}{8b} - \frac{kq\ell^2}{2A\overline{G_{xz}}} \qquad (2.107)$$

Hence, the beam deflection is given by

$$\mathrm{w} = -d_{11}\frac{qx^4}{24b} + d_{11}\frac{q\ell^3 x}{6b} + \frac{kqx^2}{A\overline{G_{xz}}} - d_{11}\frac{q\ell^4}{8b} - \frac{kq\ell^2}{2A\overline{G_{xz}}} \qquad (2.108)$$

In this case, the magnitude of deflection of the beam at the point of load application is of particular interest

$$\delta = |w(0)| = d_{11}\frac{q\ell^4}{8b} + \frac{kq\ell^2}{2A\overline{G_{xz}}} \qquad (2.109)$$

where δ is the deflection of the beam.

When the bending moment distribution along the x-direction is known, the deflection may be obtained. The total deflection is the combination of bending and shear deformation. For the case of cantilever beam under uniform distributed load,

$$w^B = d_{11}\frac{q\ell^4}{8b} \qquad (2.110)$$

$$w^s = \frac{kq\ell^2}{2A\overline{G_{xz}}} \tag{2.111}$$

$$\frac{w^B}{w^s} = \frac{d_{11}\ell^2 A\overline{G_{xz}}}{4bk} \tag{2.112}$$

Case 6 Cantilever Beam – Concentrated Load at Center

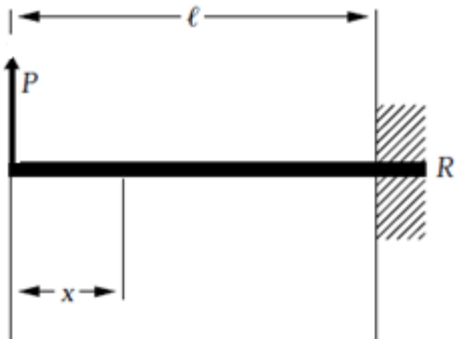

Figure 6

The bending moment of the beam is

$$M_x = -Px \tag{2.113}$$

where b is the width.

Thus, substituting Equations (2.25) and (2.33) into Equation (2.113) yields

$$\frac{d\psi_x}{dx} = d_{11}\frac{Px}{b} \tag{2.114}$$

which integrates to

$$\psi_x(x) = d_{11}\frac{Px^2}{2b} + C_{11} \tag{2.115}$$

The boundary condition, $\psi_x(\ell) = 0$, provides the constant of integration

$$C_{11} = -d_{11}\frac{P\ell^2}{2b} \tag{2.116}$$

Thus, the rotation of cross-section originally perpendicular to the x axis ψ_x becomes

$$\psi_x(x) = d_{11}\frac{Px^2}{2b} - d_{11}\frac{P\ell^2}{2b} \tag{2.117}$$

Substituting of Equation (2.117) into Equation (2.35), yields

$$\frac{dw}{dx} = -d_{11}\frac{Px^2}{2b} + d_{11}\frac{P\ell^2}{2b} + \frac{kP}{A\overline{G_{xz}}} \tag{2.118}$$

where A is the cross-section area of the beam. (*A*=*bh*)

The displacement *w* can be integrated from Equation (2.118).

$$w = -d_{11}\frac{Px^3}{6b} + d_{11}\frac{P\ell^2 x}{2b} + \frac{kPx}{A\overline{G_{xz}}} + C_{12} \tag{2.119}$$

The boundary condition *w* (ℓ) = 0, provides the constant of integration

$$C_{12} = -d_{11}\frac{P\ell^3}{3b} - \frac{P\ell}{A\overline{G_{xz}}} \tag{2.120}$$

Hence, the beam deflection is given by

$$\mathrm{w} = -d_{11}\frac{Px^3}{6b} + d_{11}\frac{P\ell^2 x}{2b} + \frac{kPx}{A\overline{G_{xz}}} - d_{11}\frac{P\ell^3}{3b} - \frac{kP\ell}{A\overline{G_{xz}}} \tag{2.121}$$

In this case, the magnitude of deflection of the beam at the point of load application is of particular interest

$$\delta = |w(0)| = \frac{1}{3}\frac{d_{11}P\ell^3}{b} + \frac{kP\ell}{A\overline{G_{xz}}} \tag{2.122}$$

where δ is the deflection of the beam.

When the bending moment distribution along the x-direction is known, the deflection may be obtained. The total deflection is the combination of bending and shear deformation. For the case of cantilever beam under concentrated load at tip end,

$$w^B = \frac{1}{3}\frac{d_{11}P\ell^3}{b} \tag{2.123}$$

$$w^S = \frac{kP\ell}{A\overline{G_{xz}}} \tag{2.124}$$

$$\frac{w^B}{w^S} = \frac{d_{11}\ell^2 A\overline{G_{xz}}}{3bk} \tag{2.125}$$

Appendix C

Data

Case 1 ($\frac{b}{a_{11}}$)

L=0.72, b=0.24, h=0.08, P=1lb unit : 10^{-3} inch
Node (middle)=10328

where W_b: deflection due to bending
Ws: deflection due to shear
W_{sb}: Ws/ W_b
W_{Total}: Ws + W_b
W_{sL} : Ws/ W_{Total}

Case 1		[15/0]4s	[30/0]4s	[45/0]4s
Theoretical	W_b	3.17E-02	4.26E-02	4.84E-02
	Ws	5.75E-03	6.08E-03	6.50E-03
	W_{sb}	1.81E-01	1.43E-01	1.34E-01
	W_{Total}	3.74E-02	4.87E-02	5.49E-02
	W_{sL}	1.54E-01	1.25E-01	1.19E-01
ANSYS	W10328	3.32E-02	4.31E-02	5.22E-02
Error %	E10328	-11.31	-11.43	-4.82

Case 1		[60/0]4s	[75/0]4s
Theoretical	W_b	5.08E-02	5.16E-02
	Ws	6.91E-03	7.20E-03
	W_{sb}	1.36E-01	1.40E-01
	W_{Total}	5.77E-02	5.88E-02
	W_{sL}	1.20E-01	1.23E-01
ANSYS	W10328	5.69E-02	5.86E-02
Error %	E10328	-1.40	-0.25

Case 1		[15/0]8T	[30/0]8T	[45/0]8T
Theoretical	W_b	2.95E-02	3.74E-02	4.15E-02
	Ws	5.75E-03	6.08E-03	6.50E-03
	W_{sb}	1.95E-01	1.62E-01	1.57E-01
	W_{Total}	3.52E-02	4.35E-02	4.80E-02
	W_{sL}	1.63E-01	1.40E-01	1.35E-01
ANSYS	W10328	3.23E-02	3.97E-02	4.63E-02
Error %	E10328	-8.39	-8.73	-3.57

Case 1		[60/0]8T	[75/0]8T
Theoretical	W_b	4.32E-02	4.37E-02
	Ws	6.91E-03	7.20E-03
	W_{sb}	1.60E-01	1.65E-01
	W_{Total}	5.01E-02	5.09E-02
	W_{sL}	1.38E-01	1.42E-01
ANSYS	W10328	4.97E-02	5.11E-02
Error %	E10328	-0.68	0.45

Case 1		[0/15]4s	[0/30]4s	[0/45]4s
Theoretical	W_b	2.76E-02	3.31E-02	3.59E-02
	Ws	5.75E-03	6.08E-03	6.50E-03
	W_{sb}	2.08E-01	1.83E-01	1.81E-01
	W_{Total}	3.34E-02	3.92E-02	4.24E-02
	W_{sL}	1.72E-01	1.55E-01	1.53E-01
ANSYS	W10328	0.31391E-01	0.36669E-01	0.41392E-01
Error %	E10328	-5.89	-6.43	-2.48

Case 1		[0/60]4s	[0/75]4s
Theoretical	W_b	3.70E-02	3.73E-02
	Ws	6.91E-03	7.20E-03
	W_{sb}	1.87E-01	1.93E-01
	W_{Total}	4.39E-02	4.45E-02
	W_{sL}	1.57E-01	1.62E-01
ANSYS	W10328	4.40E-02	4.51E-02
Error %	E10328	0.069	1.27

Case 1		[+-45/0/90]2s	[+-45/0/90]4T	[30/90/90/30]2s
Theoretical	W_b	6.65E-02	6.09E-02	1.32E-01
	Ws	7.31E-03	7.31E-03	8.03E-03
	W_{sb}	1.10E-01	1.20E-01	6.07E-02
	W_{Total}	7.38E-02	6.82E-02	1.40E-01
	W_{sL}	9.90E-02	1.07E-01	5.72E-02
ANSYS	W10328	7.40E-02	6.64E-02	1.02E-01
Error %	E10328	0.330	-2.54	-27.17

Case 2 $(\frac{b}{d_{11}})$

L=0.72, b=0.24, h=0.08, P=1*lb* unit : 10^{-3} inch

Node (middle)=10328

where W_b: deflection due to bending

Ws: deflection due to shear

W_{sb}: Ws/ W_b

W_{Total}: Ws + W_b

W_{sL} : Ws/ W_{Total}

Case 2		[15/0]4s	[30/0]4s	[45/0]4s
Theoretical	W_b	5.07E-02	6.81E-02	7.74E-02
	Ws	1.15E-02	1.22E-02	1.30E-02
	W_{sb}	2.27E-01	1.78E-01	1.68E-01
	W_{Total}	6.22E-02	8.03E-02	9.04E-02
	W_{sL}	1.85E-01	1.51E-01	1.44E-01
ANSYS	W10328	5.60E-02	7.25E-02	8.78E-02
Error %	E10328	-9.98	-9.67	-2.91

Case 2		[60/0]4s	[75/0]4s
Theoretical	W_b	8.12E-02	8.25E-02
	Ws	1.38E-02	1.44E-02
	W_{sb}	1.70E-01	1.75E-01
	W_{Total}	9.50E-02	9.69E-02
	W_{sL}	1.45E-01	1.49E-01
ANSYS	W10328	9.57E-02	9.89E-02
Error %	E10328	0.70	2.03

Case 2		[15/0]8T	[30/0]8T	[45/0]8T
Theoretical	W_b	4.72E-02	5.99E-02	6.64E-02
	Ws	1.15E-02	1.22E-02	1.30E-02
	W_{sb}	2.44E-01	2.03E-01	1.96E-01
	W_{Total}	5.87E-02	7.20E-02	7.94E-02
	W_{sL}	1.96E-01	1.69E-01	1.64E-01
ANSYS	W10328	5.44E-02	6.68E-02	7.78E-02
Error %	E10328	-7.27	-7.29	-2.02

Case 2		[60/0]8T	[75/0]8T
Theoretical	W_b	6.91E-02	6.99E-02
	Ws	1.38E-02	1.44E-02
	W_{sb}	2.00E-01	2.06E-01
	W_{Total}	8.29E-02	8.43E-02
	W_{sL}	1.67E-01	1.71E-01
ANSYS	W10328	8.37E-02	8.62E-02
Error %	E10328	1.04	2.33

Case 2		[0/15]4s	[0/30]4s	[0/45]4s
Theoretical	W_b	4.42E-02	5.30E-02	5.75E-02
	Ws	1.15E-02	1.22E-02	1.30E-02
	W_{sb}	2.60E-01	2.29E-01	2.26E-01
	W_{Total}	5.57E-02	6.51E-02	7.05E-02
	W_{sL}	2.07E-01	1.87E-01	1.84E-01
ANSYS	W10328	5.29E-02	6.17E-02	6.96E-02
Error %	E10328	-4.96	-5.32	-1.34

Case 2		[0/60]4s	[0/75]4s
Theoretical	W_b	5.92E-02	5.97E-02
	Ws	1.38E-02	1.44E-02
	W_{sb}	2.33E-01	2.41E-01
	W_{Total}	7.31E-02	7.41E-02
	W_{sL}	1.89E-01	1.94E-01
ANSYS	W10328	7.40E-02	7.60E-02
Error %	E10328	1.30	2.61

Case 2		[+-45/0/90]2s	[+-45/0/90]4T	[30/90/90/30]2s
Theoretical	W_b	1.06E-01	9.74E-02	2.12E-01
	Ws	1.46E-02	1.46E-02	1.61E-02
	W_{sb}	1.37E-01	1.50E-01	7.59E-02
	W_{Total}	1.21E-01	1.12E-01	2.28E-01
	W_{sL}	1.21E-01	1.30E-01	7.05E-02
ANSYS	W10328	1.24E-01	1.16E-01	1.73E-01
Error %	E10328	2.48	3.84	-23.94

Case 3 $(\frac{b}{d_{11}})$

L=0.72, b=0.24, h=0.08, P=1*lb* unit : 10^{-3} inch

Node (middle)=10328

where W_b: deflection due to bending

Ws: deflection due to shear

$W_{sb:}$ Ws/ W_b

$W_{Total:}$ Ws + W_b

W_{sL} : Ws/ W_{Total}

Case 3		[15/0]4s	[30/0]4s	[45/0]4s
Theoretical	W_b	6.34E-03	8.52E-03	9.67E-03
	Ws	5.75E-03	6.08E-03	6.50E-03
	W_{sb}	9.07E-01	7.13E-01	6.72E-01
	W_{Total}	1.21E-02	1.46E-02	1.62E-02
	W_{sL}	4.76E-01	4.16E-01	4.02E-01
ANSYS	W10328	1.06E-02	1.27E-02	1.50E-02
Error %	E10328	-12.67	-12.69	-7.52

Case 3		[60/0]4s	[75/0]4s
Theoretical	W_b	1.02E-02	1.03E-02
	Ws	6.91E-03	7.20E-03
	W_{sb}	6.81E-01	6.98E-01
	W_{Total}	1.71E-02	1.75E-02
	W_{sL}	4.05E-01	4.11E-01
ANSYS	W10328	1.66E-02	1.74E-02
Error %	E10328	-2.90	-0.45

Case 3		[15/0]8T	[30/0]8T	[45/0]8T
Theoretical	W_b	5.90E-03	7.49E-03	8.30E-03
	Ws	5.75E-03	6.08E-03	6.50E-03
	W_{sb}	9.74E-01	8.12E-01	7.83E-01
	W_{Total}	1.16E-02	1.36E-02	1.48E-02
	W_{sL}	4.93E-01	4.48E-01	4.39E-01
ANSYS	W10328	1.03E-02	1.20E-02	1.37E-02
Error %	E10328	-11.36	-11.56	-7.36

Case 3		[60/0]8T	[75/0]8T
Theoretical	W_b	8.63E-03	8.73E-03
	Ws	6.91E-03	7.20E-03
	W_{sb}	8.01E-01	8.25E-01
	W_{Total}	1.55E-02	1.59E-02
	W_{sL}	4.45E-01	4.52E-01
ANSYS	W10328	1.50E-02	1.58E-02
Error %	E10328	-3.31	-0.96

Case 3		[0/15]4s	[0/30]4s	[0/45]4s
Theoretical	W_b	5.52E-03	6.62E-03	7.19E-03
	Ws	5.75E-03	6.08E-03	6.50E-03
	W_{sb}	1.04E+00	9.17E-01	9.05E-01
	W_{Total}	1.13E-02	1.27E-02	1.37E-02
	W_{sL}	5.10E-01	4.78E-01	4.75E-01
ANSYS	W10328	1.01E-02	1.13E-02	1.27E-02
Error %	E10328	-10.31	-10.81	-7.53

Case 3		[0/60]4s	[0/75]4s
Theoretical	W_b	7.40E-03	7.46E-03
	Ws	6.91E-03	7.20E-03
	W_{sb}	9.34E-01	9.65E-01
	W_{Total}	1.43E-02	1.47E-02
	W_{sL}	4.83E-01	4.91E-01
ANSYS	W10328	1.37E-02	1.44E-02
Error %	E10328	-4.01	-1.78

Case 3		[+-45/0/90]2s	[+-45/0/90]4T	[30/90/90/30]2s
Theoretical	W_b	1.33E-02	1.22E-02	2.65E-02
	Ws	7.31E-03	7.31E-03	8.03E-03
	W_{sb}	5.49E-01	6.00E-01	3.03E-01
	W_{Total}	2.06E-02	1.95E-02	3.45E-02
	W_{sL}	3.55E-01	3.75E-01	2.33E-01
ANSYS	W10328	1.98E-02	1.85E-02	2.76E-02
Error %	E10328	-4.05	-5.19	-20.06

Case 4 $(\frac{b}{d_{11}})$

L=0.72, b=0.24, h=0.08, P=1*lb* unit : 10^{-3} inch

Node (middle)=10328

where W_b: deflection due to bending

Ws: deflection due to shear

$W_{sb:}$ Ws/ W_b

$W_{Total:}$ Ws + W_b

W_{sL} : Ws/ W_{Total}

Case 4		[15/0]4s	[30/0]4s	[45/0]4s
Theoretical	W_b	1.27E-02	1.70E-02	1.93E-02
	Ws	1.15E-02	1.22E-02	1.30E-02
	W_{sb}	9.07E-01	7.13E-01	6.72E-01
	W_{Total}	2.42E-02	2.92E-02	3.24E-02
	W_{sL}	4.76E-01	4.16E-01	4.02E-01
ANSYS	W10328	2.38E-02	2.83E-02	3.29E-02
Error %	E10328	-1.51	-2.90	1.66

Case 4		[60/0]4s	[75/0]4s
Theoretical	W_b	2.03E-02	2.06E-02
	Ws	1.38E-02	1.44E-02
	W_{sb}	6.81E-01	6.98E-01
	W_{Total}	3.41E-02	3.50E-02
	W_{sL}	4.05E-01	4.11E-01
ANSYS	W10328	3.62E-02	3.79E-02
Error %	E10328	5.93	8.30

Case 4		[15/0]8T	[30/0]8T	[45/0]8T
Theoretical	W_b	1.18E-02	1.50E-02	1.66E-02
	Ws	1.15E-02	1.22E-02	1.30E-02
	W_{sb}	9.74E-01	8.12E-01	7.83E-01
	W_{Total}	2.33E-02	2.71E-02	2.96E-02
	W_{sL}	4.93E-01	4.48E-01	4.39E-01
ANSYS	W10328	2.33E-02	2.83E-02	3.04E-02
Error %	E10328	0.17	4.49	2.67

Case 4		[60/0]8T	[75/0]8T
Theoretical	W_b	1.73E-02	1.75E-02
	Ws	1.38E-02	1.44E-02
	W_{sb}	8.01E-01	8.25E-01
	W_{Total}	3.11E-02	3.19E-02
	W_{sL}	4.45E-01	4.52E-01
ANSYS	W10328	3.32E-02	3.79E-02
Error %	E10328	6.62	19.05

Case 4		[0/15]4s	[0/30]4s	[0/45]4s
Theoretical	W_b	1.10E-02	1.32E-02	1.44E-02
	Ws	1.15E-02	1.22E-02	1.30E-02
	W_{sb}	1.04E+00	9.17E-01	9.05E-01
	W_{Total}	2.25E-02	2.54E-02	2.74E-02
	W_{sL}	5.10E-01	4.78E-01	4.75E-01
ANSYS	W10328	2.29E-02	2.54E-02	2.83E-02
Error %	E10328	1.54	0.18	3.23

Case 4		[0/60]4s	[0/75]4s
Theoretical	W_b	1.48E-02	1.49E-02
	Ws	1.38E-02	1.44E-02
	W_{sb}	9.34E-01	9.65E-01
	W_{Total}	2.86E-02	2.93E-02
	W_{sL}	4.83E-01	4.91E-01
ANSYS	W10328	3.06E-02	3.21E-02
Error %	E10328	6.91	9.48

Case 4		[+-45/0/90]2s	[+-45/0/90]4T	[30/90/90/30]2s
Theoretical	W_b	2.66E-02	2.43E-02	5.29E-02
	Ws	1.46E-02	1.46E-02	1.61E-02
	W_{sb}	5.49E-01	6.00E-01	3.03E-01
	W_{Total}	4.12E-02	3.90E-02	6.90E-02
	W_{sL}	3.55E-01	3.75E-01	2.33E-01
ANSYS	W10328	4.34E-02	4.21E-02	6.00E-02
Error %	E10328	5.38	8.06	-12.97

Case 5 $(\frac{b}{a_{11}})$

L=0.72, b=0.24, h=0.08, P=1*lb* unit : 10^{-3} inch

Node (middle)=9799

where W_b: deflection due to bending

Ws: deflection due to shear

W_{sb}: Ws/ W_b

W_{Total}: Ws + W_b

W_{sL} : Ws/ W_{Total}

Case 5		[15/0]4s	[30/0]4s	[45/0]4s
Theoretical	W_b	3.04E-01	4.09E-01	4.64E-01
	Ws	2.30E-02	2.43E-02	2.60E-02
	W_{sb}	7.56E-02	5.94E-02	5.60E-02
	W_{Total}	3.27E-01	4.33E-01	4.90E-01
	W_{sL}	7.03E-02	5.61E-02	5.31E-02
ANSYS	W9799	3.04E-01	4.03E-01	4.78E-01
Error %	E9799	-7.058	-6.88	-2.42

Case 5		[60/0]4s	[75/0]4s
Theoretical	W_b	4.87E-01	4.95E-01
	Ws	2.77E-02	2.88E-02
	W_{sb}	5.68E-02	5.82E-02
	W_{Total}	5.15E-01	5.24E-01
	W_{sL}	5.37E-02	5.50E-02
ANSYS	W9799	5.18E-01	5.33E-01
Error %	E9799	0.56	1.65

Case 5		[15/0]8T	[30/0]8T	[45/0]8T
Theoretical	W_b	2.83E-01	3.59E-01	3.99E-01
	Ws	2.30E-02	2.43E-02	2.60E-02
	W_{sb}	8.12E-02	6.76E-02	6.53E-02
	W_{Total}	3.06E-01	3.84E-01	4.25E-01
	W_{sL}	7.51E-02	6.33E-02	6.13E-02
ANSYS	W9799	2.91E-01	3.64E-01	4.17E-01
Error %	E9799	-5.12	-5.24	-1.70

Case 5		[60/0]8T	[75/0]8T
Theoretical	W_b	4.14E-01	4.19E-01
	Ws	2.77E-02	2.88E-02
	W_{sb}	6.67E-02	6.87E-02
	W_{Total}	4.42E-01	4.48E-01
	W_{sL}	6.26E-02	6.43E-02
ANSYS	W9799	4.45E-01	4.55E-01
Error %	E9799	0.74	1.67

Case 5		[0/15]4s	[0/30]4s	[0/45]4s
Theoretical	W_b	2.65E-01	3.18E-01	3.45E-01
	Ws	2.30E-02	2.43E-02	2.60E-02
	W_{sb}	8.67E-02	7.64E-02	7.54E-02
	W_{Total}	2.88E-01	3.42E-01	3.71E-01
	W_{sL}	7.98E-02	7.10E-02	7.01E-02
ANSYS	W9799	2.78E-01	3.29E-01	3.67E-01
Error %	E9799	-3.45	-3.82	-1.17

Case 5		[0/60]4s	[0/75]4s
Theoretical	W_b	3.55E-01	3.58E-01
	Ws	2.77E-02	2.88E-02
	W_{sb}	7.78E-02	8.05E-02
	W_{Total}	3.83E-01	3.87E-01
	W_{sL}	7.22E-02	7.45E-02
ANSYS	W9799	3.86E-01	3.93E-01
Error %	E9799	0.77	1.56

Case 5		[+-45/0/90]2s	[+-45/0/90]4T	[30/90/90/30]2s
Theoretical	W_b	6.38E-01	5.84E-01	1.27E+00
	Ws	2.92E-02	2.92E-02	3.21E-02
	W_{sb}	4.58E-02	5.00E-02	2.53E-02
	W_{Total}	6.68E-01	6.13E-01	1.30E+00
	W_{sL}	4.38E-02	4.76E-02	2.47E-02
ANSYS	W9799	6.65E-01	6.28E-01	1.16E+00
Error %	E9799	-0.43	2.30	-11.19

Case 6 $(\frac{b}{d_{11}})$

L=0.72, b=0.24, h=0.08, P=1*lb* unit : 10^{-3} inch

Node (middle)=9799

where W_b: deflection due to bending

Ws: deflection due to shear

$W_{sb:}$ Ws/ W_b

$W_{Total:}$ Ws + W_b

W_{sL} : Ws/ W_{Total}

Case 6		[15/0]4s	[30/0]4s	[45/0]4s
Theoretical	W_b	8.11E-01	1.09E+00	1.24E+00
	Ws	4.60E-02	4.86E-02	5.20E-02
	W_{sb}	5.67E-02	4.46E-02	4.20E-02
	W_{Total}	8.57E-01	1.14E+00	1.29E+00
	W_{sL}	5.37E-02	4.27E-02	4.03E-02
ANSYS	W9799	7.97E-01	1.06E+00	1.25E+00
Error %	E9799	-0.43	2.30	-11.19

Case 6		[60/0]4s	[75/0]4s
Theoretical	W_b	1.30E+00	1.32E+00
	Ws	5.53E-02	5.76E-02
	W_{sb}	4.26E-02	4.36E-02
	W_{Total}	1.35E+00	1.38E+00
	W_{sL}	4.08E-02	4.18E-02
ANSYS	W9799	1.35E+00	1.38E+00
Error %	E9799	-0.56	0.25

Case 6		[15/0]8T	[30/0]8T	[45/0]8T
Theoretical	W_b	7.55E-01	9.58E-01	1.06E+00
	Ws	4.60E-02	4.86E-02	5.20E-02
	W_{sb}	6.09E-02	5.07E-02	4.89E-02
	W_{Total}	8.01E-01	1.01E+00	1.12E+00
	W_{sL}	5.74E-02	4.83E-02	4.67E-02
ANSYS	W9799	7.58E-01	9.53E-01	1.09E+00
Error %	E9799	-5.40	-5.34	-2.36

Case 6		[60/0]8T	[75/0]8T
Theoretical	W_b	1.10E+00	1.12E+00
	Ws	5.53E-02	5.76E-02
	W_{sb}	5.01E-02	5.15E-02
	W_{Total}	1.16E+00	1.18E+00
	W_{sL}	4.77E-02	4.90E-02
ANSYS	W9799	1.16E+00	1.18E+00
Error %	E9799	-0.42	0.26

Case 6		[0/15]4s	[0/30]4s	[0/45]4s
Theoretical	W_b	7.07E-01	8.48E-01	9.20E-01
	Ws	4.60E-02	4.86E-02	5.20E-02
	W_{sb}	6.51E-02	5.73E-02	5.66E-02
	W_{Total}	7.53E-01	8.96E-01	9.72E-01
	W_{sL}	6.11E-02	5.42E-02	5.35E-02
ANSYS	W9799	7.23E-01	8.59E-01	9.54E-01
Error %	E9799	-3.95	-4.14	-1.90

Case 6		[0/60]4s	[0/75]4s
Theoretical	W_b	9.48E-01	9.55E-01
	Ws	5.53E-02	5.76E-02
	W_{sb}	5.84E-02	6.03E-02
	W_{Total}	1.00E+00	1.01E+00
	W_{sL}	5.52E-02	5.69E-02
ANSYS	W9799	9.99E-01	1.01E+00
Error %	E9799	-0.36	0.22

Case 6		[+-45/0/90]2s	[+-45/0/90]4T	[30/90/90/30]2s
Theoretical	W_b	1.70E+00	1.56E+00	3.39E+00
	Ws	5.84E-02	5.84E-02	6.42E-02
	W_{sb}	3.43E-02	3.75E-02	1.90E-02
	W_{Total}	1.76E+00	1.62E+00	3.45E+00
	W_{sL}	3.32E-02	3.62E-02	1.86E-02
ANSYS	W9799	1.75E+00	1.64E+00	3.10E+00
Error %	E9799	-0.84	1.42	-10.11

Case 1 ($\frac{b}{\bar{d}_1}$)

L=0.72, b=0.24, h=0.08, P=1*lb* unit : 10^{-3} inch

Node (middle)=10328

where W_b: deflection due to bending

Ws: deflection due to shear

W_{sb}: Ws/ W_b

W_{Total}: Ws + W_b

W_{sL} : Ws/ W_{Total}

Case 1		[15/0]4s	[30/0]4s	[45/0]4s
Theoretical	W_b	2.59E-02	3.52E-02	4.58E-02
	Ws	5.75E-03	6.08E-03	6.50E-03
	W_{sb}	2.22E-01	1.73E-01	1.42E-01
	W_{Total}	3.16E-02	4.13E-02	5.23E-02
	W_{sL}	1.82E-01	1.47E-01	1.24E-01
ANSYS	W10328	3.32E-02	4.31E-02	5.22E-02
Error %	E10328	5.03	4.44	-0.14

Case 1		[60/0]4s	[75/0]4s
Theoretical	W_b	5.04E-02	5.15E-02
	Ws	6.91E-03	7.20E-03
	W_{sb}	1.37E-01	1.40E-01
	W_{Total}	5.73E-02	5.87E-02
	W_{sL}	1.21E-01	1.23E-01
ANSYS	W10328	5.69E-02	5.86E-02
Error %	E10328	-0.73	-0.20

Case 1		[15/0]8T	[30/0]8T	[45/0]8T
Theoretical	W_b	2.55E-02	3.25E-02	3.99E-02
	Ws	5.75E-03	6.08E-03	6.50E-03
	W_{sb}	2.26E-01	1.87E-01	1.63E-01
	W_{Total}	3.12E-02	3.86E-02	4.64E-02
	W_{sL}	1.84E-01	1.57E-01	1.40E-01
ANSYS	W10328	3.23E-02	3.97E-02	4.63E-02
Error %	E10328	3.50	2.85	-0.28

Case 1		[60/0]8T	[75/0]8T
Theoretical	W_b	4.30E-02	4.37E-02
	Ws	6.91E-03	7.20E-03
	W_{sb}	1.61E-01	1.65E-01
	W_{Total}	4.99E-02	5.09E-02
	W_{sL}	1.39E-01	1.42E-01
ANSYS	W10328	4.97E-02	5.11E-02
Error %	E10328	-0.26	0.47

Case 1		[0/15]4s	[0/30]4s	[0/45]4s
Theoretical	W_b	2.50E-02	3.00E-02	3.50E-02
	Ws	5.75E-03	6.08E-03	6.50E-03
	W_{sb}	2.30E-01	2.02E-01	1.86E-01
	W_{Total}	3.07E-02	3.61E-02	4.15E-02
	W_{sL}	1.87E-01	1.68E-01	1.57E-01
ANSYS	W10328	3.14E-02	3.67E-02	4.14E-02
Error %	E10328	2.23	1.60	-0.27

Case 1		[0/60]4s	[0/75]4s
Theoretical	W_b	3.69E-02	3.73E-02
	Ws	6.91E-03	7.20E-03
	W_{sb}	1.87E-01	1.93E-01
	W_{Total}	4.38E-02	4.45E-02
	W_{sL}	1.58E-01	1.62E-01
ANSYS	W10328	4.40E-02	4.51E-02
Error %	E10328	0.31	1.28

Case 1		[+-45/0/90]2s	[+-45/0/90]4T	[30/90/90/30]2s
Theoretical	W_b	6.63E-02	6.09E-02	6.91E-02
	Ws	7.31E-03	7.31E-03	8.03E-03
	W_{sb}	1.10E-01	1.20E-01	1.16E-01
	W_{Total}	7.36E-02	6.82E-02	7.72E-02
	W_{sL}	9.93E-02	1.07E-01	1.04E-01
ANSYS	W10328	7.40E-02	6.64E-02	1.02E-01
Error %	E10328	0.63	-2.53	32.45

Case 2 ($\frac{b}{\bar{d}_1}$)

L=0.72, b=0.24, h=0.08, P=1*lb* unit : 10^{-3} inch

Node (middle)=10328

where W_b: deflection due to bending

Ws: deflection due to shear

$W_{sb:}$ Ws/ W_b

$W_{Total:}$ Ws + W_b

W_{sL} : Ws/ W_{Total}

Case 2		[15/0]4s	[30/0]4s	[45/0]4s
Theoretical	W_b	4.14E-02	5.63E-02	7.33E-02
	Ws	1.15E-02	1.22E-02	1.30E-02
	W_{sb}	2.78E-01	2.16E-01	1.78E-01
	W_{Total}	5.29E-02	6.85E-02	8.63E-02
	W_{sL}	2.17E-01	1.77E-01	1.51E-01
ANSYS	W10328	5.60E-02	7.25E-02	8.78E-02
Error %	E10328	5.89	5.93	1.72

Case 2		[60/0]4s	[75/0]4s
Theoretical	Wb	8.06E-02	8.25E-02
	Ws	1.38E-02	1.44E-02
	Wsb	1.72E-01	1.75E-01
	W	9.44E-02	9.69E-02
	WsL	1.46E-01	1.49E-01
ANSYS	W10328	9.57E-02	9.89E-02
Error %	E10328	1.37	2.08

Case 2		[15/0]8T	[30/0]8T	[45/0]8T
Theoretical	Wb	4.07E-02	5.21E-02	6.39E-02
	Ws	1.15E-02	1.22E-02	1.30E-02
	Wsb	2.82E-01	2.33E-01	2.04E-01
	W	5.22E-02	6.42E-02	7.69E-02
	WsL	2.20E-01	1.89E-01	1.69E-01
ANSYS	W10328	5.44E-02	6.68E-02	7.78E-02
Error %	E10328	4.24	4.02	1.21

Case 2		[60/0]8T	[75/0]8T
Theoretical	Wb	6.87E-02	6.98E-02
	Ws	1.38E-02	1.44E-02
	Wsb	2.01E-01	2.06E-01
	W	8.26E-02	8.42E-02
	WsL	1.68E-01	1.71E-01
ANSYS	W10328	8.37E-02	8.62E-02
Error %	E10328	1.45	2.35

Case 2		[0/15]4s	[0/30]4s	[0/45]4s
Theoretical	Wb	3.99E-02	4.80E-02	5.60E-02
	Ws	1.15E-02	1.22E-02	1.30E-02
	Wsb	2.88E-01	2.53E-01	2.32E-01
	W	5.14E-02	6.02E-02	6.90E-02
	WsL	2.24E-01	2.02E-01	1.89E-01
ANSYS	W10328	5.29E-02	6.17E-02	6.96E-02
Error %	E10328	2.87	2.48	0.81

Case 2		[0/60]4s	[0/75]4s
Theoretical	Wb	5.91E-02	5.97E-02
	Ws	1.38E-02	1.44E-02
	Wsb	2.34E-01	2.41E-01
	W	7.29E-02	7.41E-02
	WsL	1.90E-01	1.94E-01
ANSYS	W10328	7.40E-02	7.60E-02
Error %	E10328	1.53	2.62

Case 2		[+-45/0/90]2s	[+-45/0/90]4T	[30/90/90/30]2s
Theoretical	Wb	1.06E-01	9.74E-02	1.11E-01
	Ws	1.46E-02	1.46E-02	1.61E-02
	Wsb	1.38E-01	1.50E-01	1.45E-01
	W	1.21E-01	1.12E-01	1.27E-01
	WsL	1.21E-01	1.30E-01	1.27E-01
ANSYS	W10328	1.24E-01	1.16E-01	1.73E-01
Error %	E10328	2.78	3.84	36.74

Case 3 ($\frac{b}{\bar{d}_1}$)

L=0.72, b=0.24, h=0.08, P=1*lb* unit : 10^{-3} inch

Node (middle)=10328

where W_b: deflection due to bending

Ws: deflection due to shear

$W_{sb:}$ Ws/ W_b

$W_{Total:}$ Ws + W_b

W_{sL} : Ws/ W_{Total}

Case 3		[15/0]4s	[30/0]4s	[45/0]4s
Theoretical	Wb	5.17E-03	7.04E-03	9.16E-03
	Ws	5.75E-03	6.08E-03	6.50E-03
	Wsb	1.11E+00	8.63E-01	7.10E-01
	W	1.09E-02	1.31E-02	1.57E-02
	WsL	5.26E-01	4.63E-01	4.15E-01
ANSYS	W10328	1.06E-02	1.27E-02	1.50E-02
Error %	E10328	-3.35	-2.85	-4.48

Case 3		[60/0]4s	[75/0]4s
Theoretical	Wb	1.01E-02	1.03E-02
	Ws	6.91E-03	7.20E-03
	Wsb	6.86E-01	6.99E-01
	W	1.70E-02	1.75E-02
	WsL	4.07E-01	4.11E-01
ANSYS	W10328	1.66E-02	1.74E-02
Error %	E10328	-2.45	-0.42

Case 3		[15/0]8T	[30/0]8T	[45/0]8T
Theoretical	Wb	5.09E-03	6.51E-03	7.99E-03
	Ws	5.75E-03	6.08E-03	6.50E-03
	Wsb	1.13E+00	9.34E-01	8.14E-01
	W	1.08E-02	1.26E-02	1.45E-02
	WsL	5.30E-01	4.83E-01	4.49E-01
ANSYS	W10328	1.03E-02	1.20E-02	1.37E-02
Error %	E10328	-4.74	-4.68	-5.33

Case 3		[60/0]8T	[75/0]8T
Theoretical	Wb	8.59E-03	8.73E-03
	Ws	6.91E-03	7.20E-03
	Wsb	8.05E-01	8.25E-01
	W	1.55E-02	1.59E-02
	WsL	4.46E-01	4.52E-01
ANSYS	W10328	1.50E-02	1.58E-02
Error %	E10328	-3.05	-0.95

Case 3		[0/15]4s	[0/30]4s	[0/45]4s
Theoretical	Wb	4.99E-03	6.00E-03	7.00E-03
	Ws	5.75E-03	6.08E-03	6.50E-03
	Wsb	1.15E+00	1.01E+00	9.29E-01
	W	1.07E-02	1.21E-02	1.35E-02
	WsL	5.35E-01	5.03E-01	4.82E-01
ANSYS	W10328	1.01E-02	1.13E-02	1.27E-02
Error %	E10328	-5.90	-6.23	-6.25

Case 3		[0/60]4s	[0/75]4s
Theoretical	Wb	7.38E-03	7.46E-03
	Ws	6.91E-03	7.20E-03
	Wsb	9.37E-01	9.66E-01
	W	1.43E-02	1.47E-02
	WsL	4.84E-01	4.91E-01
ANSYS	W10328	1.37E-02	1.44E-02
Error %	E10328	-3.87	-1.78

Case 3		[+-45/0/90]2s	[+-45/0/90]4T	[30/90/90/30]2s
Theoretical	Wb	1.33E-02	1.22E-02	1.38E-02
	Ws	7.31E-03	7.31E-03	8.03E-03
	Wsb	5.51E-01	6.00E-01	5.81E-01
	WsL	2.06E-02	1.95E-02	2.19E-02
	W	3.55E-01	3.75E-01	3.67E-01
ANSYS	W10328	1.98E-02	1.85E-02	2.76E-02
Error %	E10328	-3.85	-5.16	26.14

Case 4 ($\frac{b}{\bar{d}_1}$)

L=0.72, b=0.24, h=0.08, P=1*lb* unit : 10^{-3} inch

Node (middle)=10328

where W_b: deflection due to bending

Ws: deflection due to shear

$W_{sb:}$ Ws/ W_b

$W_{Total:}$ Ws + W_b

W_{sL} : Ws/ W_{Total}

Case 4		[15/0]4s	[30/0]4s	[45/0]4s
Theoretical	Wb	1.03E-02	1.41E-02	1.83E-02
	Ws	1.15E-02	1.22E-02	1.30E-02
	Wsb	1.11E+00	8.63E-01	7.10E-01
	W	2.18E-02	2.62E-02	3.13E-02
	WsL	5.26E-01	4.63E-01	4.15E-01
ANSYS	W10328	2.38E-02	2.83E-02	3.29E-02
Error %	E10328	9.00	8.04	4.99

Case 4		[60/0]4s	[75/0]4s
Theoretical	Wb	2.01E-02	2.06E-02
	Ws	1.38E-02	1.44E-02
	Wsb	6.86E-01	6.99E-01
	W	3.40E-02	3.50E-02
	WsL	4.07E-01	4.11E-01
ANSYS	W10328	3.62E-02	3.79E-02
Error %	E10328	6.42	8.33

Case 4		[15/0]8T	[30/0]8T	[45/0]8T
Theoretical	Wb	1.02E-02	1.30E-02	1.60E-02
	Ws	1.15E-02	1.22E-02	1.30E-02
	Wsb	1.13E+00	9.34E-01	8.14E-01
	W	2.17E-02	2.52E-02	2.90E-02
	WsL	5.30E-01	4.83E-01	4.49E-01
ANSYS	W10328	2.33E-02	2.83E-02	3.04E-02
Error %	E10328	7.66	12.62	4.91

Case 4		[60/0]8T	[75/0]8T
Theoretical	Wb	1.72E-02	1.75E-02
	Ws	1.38E-02	1.44E-02
	Wsb	8.05E-01	8.25E-01
	W	3.10E-02	3.19E-02
	WsL	4.46E-01	4.52E-01
ANSYS	W10328	3.32E-02	3.79E-02
Error %	E10328	6.91	19.06

Case 4		[0/15]4s	[0/30]4s	[0/45]4s
Theoretical	Wb	9.98E-03	1.20E-02	1.40E-02
	Ws	1.15E-02	1.22E-02	1.30E-02
	Wsb	1.15E+00	1.01E+00	9.29E-01
	W	2.15E-02	2.42E-02	2.70E-02
	WsL	5.35E-01	5.03E-01	4.82E-01
ANSYS	W10328	2.29E-02	2.54E-02	2.83E-02
Error %	E10328	6.55	5.32	4.67

Case 4		[0/60]4s	[0/75]4s
Theoretical	Wb	1.48E-02	1.49E-02
	Ws	1.38E-02	1.44E-02
	Wsb	9.37E-01	9.66E-01
	W	2.86E-02	2.93E-02
	WsL	4.84E-01	4.91E-01
ANSYS	W10328	3.06E-02	3.21E-02
Error %	E10328	7.06	9.48

Case 4		[+-45/0/90]2s	[+-45/0/90]4T	[30/90/90/30]2s
Theoretical	Wb	2.65E-02	2.43E-02	2.77E-02
	Ws	1.46E-02	1.46E-02	1.61E-02
	Wsb	5.51E-01	6.00E-01	5.81E-01
	W	4.11E-02	3.90E-02	4.37E-02
	WsL	3.55E-01	3.75E-01	3.67E-01
ANSYS	W10328	4.34E-02	4.21E-02	6.00E-02
Error %	E10328	5.60	8.07	37.33

Case 5 ($\frac{b}{\bar{a}_1}$)

L=0.72, b=0.24, h=0.08, P=1*lb* unit : 10^{-3} inch

Node (middle)=9799

where W_b: deflection due to bending

Ws: deflection due to shear

$W_{sb:}$ Ws/ W_b

$W_{Total:}$ Ws + W_b

W_{sL} : Ws/ W_{Total}

Case 5		[15/0]4s	[30/0]4s	[45/0]4s
Theoretical	Wb	2.48E-01	3.38E-01	4.40E-01
	Ws	2.30E-02	2.43E-02	2.60E-02
	Wsb	9.26E-02	7.19E-02	5.92E-02
	W	2.71E-01	3.62E-01	4.66E-01
	WsL	8.48E-02	6.71E-02	5.59E-02
ANSYS	W9799	3.04E-01	4.03E-01	4.78E-01
Error %	E9799	12.10	11.36	2.75

Case 5		[60/0]4s	[75/0]4s
Theoretical	Wb	4.84E-01	4.95E-01
	Ws	2.77E-02	2.88E-02
	Wsb	5.72E-02	5.82E-02
	W	5.11E-01	5.24E-01
	WsL	5.41E-02	5.50E-02
ANSYS	W9799	5.18E-01	5.33E-01
Error %	E9799	1.30	1.70

Case 5		[15/0]8T	[30/0]8T	[45/0]8T
Theoretical	Wb	2.44E-01	3.12E-01	3.83E-01
	Ws	2.30E-02	2.43E-02	2.60E-02
	Wsb	9.41E-02	7.78E-02	6.79E-02
	W	2.67E-01	3.37E-01	4.09E-01
	WsL	8.60E-02	7.22E-02	6.35E-02
ANSYS	W9799	2.91E-01	3.64E-01	4.17E-01
Error %	E9799	8.68	7.99	1.95

Case 5		[60/0]8T	[75/0]8T
Theoretical	Wb	4.12E-01	4.19E-01
	Ws	2.77E-02	2.88E-02
	Wsb	6.71E-02	6.87E-02
	W	4.40E-01	4.48E-01
	WsL	6.29E-02	6.43E-02
ANSYS	W9799	4.45E-01	4.55E-01
Error %	E9799	1.20	1.69

Case 5		[0/15]4s	[0/30]4s	[0/45]4s
Theoretical	Wb	2.40E-01	2.88E-01	3.36E-01
	Ws	2.30E-02	2.43E-02	2.60E-02
	Wsb	9.60E-02	8.43E-02	7.74E-02
	W	2.63E-01	3.12E-01	3.62E-01
	WsL	8.76E-02	7.78E-02	7.19E-02
ANSYS	W9799	2.78E-01	3.29E-01	3.67E-01
Error %	E9799	5.89	5.33	1.29

Case 5		[0/60]4s	[0/75]4s
Theoretical	Wb	3.54E-01	3.58E-01
	Ws	2.77E-02	2.88E-02
	Wsb	7.80E-02	8.05E-02
	W	3.82E-01	3.87E-01
	WsL	7.24E-02	7.45E-02
ANSYS	W9799	3.86E-01	3.93E-01
Error %	E9799	1.03	1.57

Case 5		[+-45/0/90]2s	[+-45/0/90]4T	[30/90/90/30]2s
Theoretical	Wb	6.36E-01	5.84E-01	6.64E-01
	Ws	2.92E-02	2.92E-02	3.21E-02
	Wsb	4.59E-02	5.00E-02	4.84E-02
	W	6.65E-01	6.13E-01	6.96E-01
	WsL	4.39E-02	4.76E-02	4.62E-02
ANSYS	W9799	6.65E-01	6.28E-01	1.16E+00
Error %	E9799	-0.12	2.30	66.20

Case 6 ($\frac{b}{\bar{a}_1}$)

L=0.72, b=0.24, h=0.08, P=1lb unit : 10^{-3} inch

Node (middle)=10328

where W_b: deflection due to bending

Ws: deflection due to shear

$W_{sb:}$ Ws/ W_b

$W_{Total:}$ Ws + W_b

W_{sL} : Ws/ W_{Total}

Case 6		[15/0]4s	[30/0]4s	[45/0]4s
Theoretical	Wb	6.62E-01	9.01E-01	1.17E+00
	Ws	4.60E-02	4.86E-02	5.20E-02
	Wsb	6.95E-02	5.39E-02	4.44E-02
	W	7.08E-01	9.50E-01	1.22E+00
	WsL	6.50E-02	5.12E-02	4.25E-02
ANSYS	W9799	7.97E-01	1.06E+00	1.25E+00
Error %	E9799	12.52	11.90	2.29

Case 6		[60/0]4s	[75/0]4s
Theoretical	Wb	1.29E+00	1.32E+00
	Ws	5.53E-02	5.76E-02
	Wsb	4.29E-02	4.37E-02
	W	1.34E+00	1.38E+00
	WsL	4.11E-02	4.18E-02
ANSYS	W9799	1.35E+00	1.38E+00
Error %	E9799	0.18	0.30

Case 6		[15/0]8T	[30/0]8T	[45/0]8T
Theoretical	Wb	6.52E-01	8.33E-01	1.02E+00
	Ws	4.60E-02	4.86E-02	5.20E-02
	Wsb	7.06E-02	5.84E-02	5.09E-02
	W	6.98E-01	8.81E-01	1.07E+00
	WsL	6.59E-02	5.51E-02	4.84E-02
ANSYS	W9799	7.58E-01	9.53E-01	1.09E+00
Error %	E9799	8.67	8.13	1.33

Case 6		[60/0]8T	[75/0]8T
Theoretical	Wb	1.10E+00	1.12E+00
	Ws	5.53E-02	5.76E-02
	Wsb	5.03E-02	5.16E-02
	W	1.15E+00	1.18E+00
	WsL	4.79E-02	4.90E-02
ANSYS	W9799	1.16E+00	1.18E+00
Error %	E9799	0.034	0.28

Case 6		[0/15]4s	[0/30]4s	[0/45]4s
Theoretical	Wb	6.39E-01	7.68E-01	8.96E-01
	Ws	4.60E-02	4.86E-02	5.20E-02
	Wsb	7.20E-02	6.32E-02	5.81E-02
	W	6.85E-01	8.17E-01	9.48E-01
	WsL	6.71E-02	5.95E-02	5.49E-02
ANSYS	W9799	7.23E-01	8.59E-01	9.54E-01
Error %	E9799	5.56	5.17	0.59

Case 6		[0/60]4s	[0/75]4s
Theoretical	Wb	9.45E-01	9.55E-01
	Ws	5.53E-02	5.76E-02
	Wsb	5.85E-02	6.03E-02
	W	1.00E+00	1.01E+00
	WsL	5.53E-02	5.69E-02
ANSYS	W9798	9.99E-01	1.01E+00
Error %	E9799	-0.099	0.23

Case 6		[+-45/0/90]2s	[+-45/0/90]4T	[30/90/90/30]2s
Theoretical	Wb	1.70E+00	1.56E+00	1.77E+00
	Ws	5.84E-02	5.84E-02	6.42E-02
	Wsb	3.44E-02	3.75E-02	3.63E-02
	W	1.76E+00	1.62E+00	1.83E+00
	WsL	3.33E-02	3.62E-02	3.50E-02
ANSYS	W9799	1.75E+00	1.64E+00	3.10E+00
Error %	E9799	-0.53	1.43	69.14

Appendix D

ANSYS Code for Case 1

```
/UNITS,BIN ! inch/lb
/PREP7
/TRIAD,LBOT
! Define Parameter
L=0.72
b=0.24
thz=0.005
force=1000
! Define Key point
K,1,0,0,0
K,2,L,0,0
K,3,L,b,0
K,4,0,b,0
K,5,0,0,thz
K,6,L,0,thz
K,7,L,b,thz
K,8,0,b,thz
K,9,0,0,2*thz
K,10,L,0,2*thz
K,11,L,b,2*thz
K,12,0,b,2*thz
K,13,0,0,3*thz
K,14,L,0,3*thz
K,15,L,b,3*thz
K,16,0,b,3*thz
K,17,0,0,4*thz
K,18,L,0,4*thz
K,19,L,b,4*thz
K,20,0,b,4*thz
K,21,0,0,5*thz
K,22,L,0,5*thz
K,23,L,b,5*thz
K,24,0,b,5*thz
K,25,0,0,6*thz
K,26,L,0,6*thz
K,27,L,b,6*thz
K,28,0,b,6*thz
K,29,0,0,7*thz
K,30,L,0,7*thz
K,31,L,b,7*thz
K,32,0,b,7*thz
```

```
K,33,0,0,8*thz
K,34,L,0,8*thz
K,35,L,b,8*thz
K,36,0,b,8*thz
K,37,0,0,9*thz
K,38,L,0,9*thz
K,39,L,b,9*thz
K,40,0,b,9*thz
K,41,0,0,10*thz
K,42,L,0,10*thz
K,43,L,b,10*thz
K,44,0,b,10*thz
K,45,0,0,11*thz
K,46,L,0,11*thz
K,47,L,b,11*thz
K,48,0,b,11*thz
K,49,0,0,12*thz
K,50,L,0,12*thz
K,51,L,b,12*thz
K,52,0,b,12*thz
K,53,0,0,13*thz
K,54,L,0,13*thz
K,55,L,b,13*thz
K,56,0,b,13*thz
K,57,0,0,14*thz
K,58,L,0,14*thz
K,59,L,b,14*thz
K,60,0,b,14*thz
K,61,0,0,15*thz
K,62,L,0,15*thz
K,63,L,b,15*thz
K,64,0,b,15*thz
K,65,0,0,16*thz
K,66,L,0,16*thz
K,67,L,b,16*thz
K,68,0,b,16*thz
!Define Area
V,1,2,3,4,5,6,7,8
V,5,6,7,8,9,10,11,12
V,9,10,11,12,13,14,15,16
V,13,14,15,16,17,18,19,20
```

```
V,17,18,19,20,21,22,23,24
V,21,22,23,24,25,26,27,28
V,25,26,27,28,29,30,31,32
V,29,30,31,32,33,34,35,36
V,33,34,35,36,37,38,39,40
V,37,38,39,40,41,42,43,44
V,41,42,43,44,45,46,47,48
V,45,46,47,48,49,50,51,52
V,49,50,51,52,53,54,55,56
V,53,54,55,56,57,58,59,60
V,57,58,59,60,61,62,63,64
V,61,62,63,64,65,66,67,68
VGLUE,ALL
! Define Material Properties
ET,1,SOLID186
KEYOPT,1,2,0
KEYOPT,1,3,1
KEYOPT,1,6,1
MP,EX,1,20.3e6
MP,EY,1,1.5e6
MP,EZ,1,1.5e6
MP,PRXY,1,0.27
MP,PRYZ,1,0.54
MP,PRXZ,1,0.27
MP,GXY,1,1e6
MP,GYZ,1,0.54e6
MP,GXZ,1,1e6

local,26,,0,0,0,75
local,25,,0,0,0,-75
local,24,,0,0,0,75
local,23,,0,0,0,-75
local,22,,0,0,0,75
local,21,,0,0,0,-75
local,20,,0,0,0,75
local,19,,0,0,0,-75
local,18,,0,0,0,-75
local,17,,0,0,0,75
local,16,,0,0,0,-75
local,15,,0,0,0,75
local,14,,0,0,0,-75
```

```
local,13,,0,0,0,75
local,12,,0,0,0,-75
local,11,,0,0,0,75
CSYS,0
! Mesh Attribute & SIZE CONTROL & MESH
VSEL,S,VOLU,,1
VATT,1,,1,11,1

LSEL,S,LINE,,1
LSEL,A,LINE,,3
LSEL,A,LINE,,6
LSEL,A,LINE,,10
LESIZE,ALL,,,18,1

LSEL,S,LINE,,2
LSEL,A,LINE,,4
LSEL,A,LINE,,8
LSEL,A,LINE,,12
LESIZE,ALL,,,16,1

LSEL,S,LINE,,5
LSEL,A,LINE,,7
LSEL,A,LINE,,9
LSEL,A,LINE,,11
LESIZE,ALL,,,1,1
VMESH,ALL
VSEL,S,VOLU,,2
VATT,1,,1,12,2
LSEL,S,LINE,,6
LSEL,A,LINE,,10
LSEL,A,LINE,,14
LSEL,A,LINE,,18
LESIZE,ALL,,,18,1

LSEL,S,LINE,,8
LSEL,A,LINE,,12
LSEL,A,LINE,,16
LSEL,A,LINE,,20
LESIZE,ALL,,,16,1

LSEL,S,LINE,,13
```

```
LSEL,A,LINE,,15
LSEL,A,LINE,,17
LSEL,A,LINE,,19
LESIZE,ALL,,,1,1
VMESH,ALL

VSEL,S,VOLU,,3
VATT,1,,1,13,3
LSEL,S,LINE,,14
LSEL,A,LINE,,18
LSEL,A,LINE,,22
LSEL,A,LINE,,26
LESIZE,ALL,,,18,1

LSEL,S,LINE,,16
LSEL,A,LINE,,20
LSEL,A,LINE,,24
LSEL,A,LINE,,28
LESIZE,ALL,,,16,1

LSEL,S,LINE,,21
LSEL,A,LINE,,23
LSEL,A,LINE,,25
LSEL,A,LINE,,27
LESIZE,ALL,,,1,1
VMESH,ALL

VSEL,S,VOLU,,4
VATT,1,,1,14,4

LSEL,S,LINE,,22
LSEL,A,LINE,,26
LSEL,A,LINE,,30
LSEL,A,LINE,,34
LESIZE,ALL,,,18,1

LSEL,S,LINE,,24
LSEL,A,LINE,,28
LSEL,A,LINE,,32
LSEL,A,LINE,,36
LESIZE,ALL,,,16,1
```

```
LSEL,S,LINE,,29
LSEL,A,LINE,,31
LSEL,A,LINE,,33
LSEL,A,LINE,,35
LESIZE,ALL,,,1,1
VMESH,ALL

VSEL,S,VOLU,,5
VATT,1,,1,15,5

LSEL,S,LINE,,30
LSEL,A,LINE,,34
LSEL,A,LINE,,38
LSEL,A,LINE,,42
LESIZE,ALL,,,18,1

LSEL,S,LINE,,32
LSEL,A,LINE,,36
LSEL,A,LINE,,40
LSEL,A,LINE,,44
LESIZE,ALL,,,16,1

LSEL,S,LINE,,37
LSEL,A,LINE,,39
LSEL,A,LINE,,41
LSEL,A,LINE,,43
LESIZE,ALL,,,1,1
VMESH,ALL

VSEL,S,VOLU,,6
VATT,1,,1,16,6

LSEL,S,LINE,,38
LSEL,A,LINE,,42
LSEL,A,LINE,,46
LSEL,A,LINE,,50
LESIZE,ALL,,,18,1

LSEL,S,LINE,,40
LSEL,A,LINE,,42
```

```
LSEL,A,LINE,,48
LSEL,A,LINE,,52
LESIZE,ALL,,,16,1

LSEL,S,LINE,,45
LSEL,A,LINE,,47
LSEL,A,LINE,,49
LSEL,A,LINE,,51
LESIZE,ALL,,,1,1
VMESH,ALL

VSEL,S,VOLU,,7
VATT,1,,1,17,7

LSEL,S,LINE,,46
LSEL,A,LINE,,50
LSEL,A,LINE,,54
LSEL,A,LINE,,58
LESIZE,ALL,,,18,1

LSEL,S,LINE,,48
LSEL,A,LINE,,52
LSEL,A,LINE,,56
LSEL,A,LINE,,60
LESIZE,ALL,,,16,1

LSEL,S,LINE,,53
LSEL,A,LINE,,55
LSEL,A,LINE,,57
LSEL,A,LINE,,59
LESIZE,ALL,,,1,1
VMESH,ALL

VSEL,S,VOLU,,8
VATT,1,,1,18,8

LSEL,S,LINE,,54
LSEL,A,LINE,,58
LSEL,A,LINE,,62
LSEL,A,LINE,,66
LESIZE,ALL,,,18,1
```

```
LSEL,S,LINE,,56
LSEL,A,LINE,,60
LSEL,A,LINE,,64
LSEL,A,LINE,,68
LESIZE,ALL,,,16,1

LSEL,S,LINE,,61
LSEL,A,LINE,,63
LSEL,A,LINE,,65
LSEL,A,LINE,,67
LESIZE,ALL,,,1,1
VMESH,ALL

VSEL,S,VOLU,,9
VATT,1,,1,19,9

LSEL,S,LINE,,62
LSEL,A,LINE,,66
LSEL,A,LINE,,70
LSEL,A,LINE,,74
LESIZE,ALL,,,18,1

LSEL,S,LINE,,64
LSEL,A,LINE,,68
LSEL,A,LINE,,72
LSEL,A,LINE,,76
LESIZE,ALL,,,16,1

LSEL,S,LINE,,69
LSEL,A,LINE,,71
LSEL,A,LINE,,73
LSEL,A,LINE,,75
LESIZE,ALL,,,1,1
VMESH,ALL

VSEL,S,VOLU,,10
VATT,1,,1,20,10

LSEL,S,LINE,,70
LSEL,A,LINE,,74
```

```
LSEL,A,LINE,,78
LSEL,A,LINE,,82
LESIZE,ALL,,,18,1

LSEL,S,LINE,,72
LSEL,A,LINE,,76
LSEL,A,LINE,,80
LSEL,A,LINE,,84
LESIZE,ALL,,,16,1

LSEL,S,LINE,,77
LSEL,A,LINE,,79
LSEL,A,LINE,,81
LSEL,A,LINE,,83
LESIZE,ALL,,,1,1
VMESH,ALL

VSEL,S,VOLU,,11
VATT,1,,1,21,11

LSEL,S,LINE,,78
LSEL,A,LINE,,82
LSEL,A,LINE,,86
LSEL,A,LINE,,90
LESIZE,ALL,,,18,1

LSEL,S,LINE,,80
LSEL,A,LINE,,84
LSEL,A,LINE,,88
LSEL,A,LINE,,92
LESIZE,ALL,,,16,1

LSEL,S,LINE,,85
LSEL,A,LINE,,87
LSEL,A,LINE,,89
LSEL,A,LINE,,91
LESIZE,ALL,,,1,1
VMESH,ALL

VSEL,S,VOLU,,12
VATT,1,,1,22,12
```

```
LSEL,S,LINE,,86
LSEL,A,LINE,,90
LSEL,A,LINE,,94
LSEL,A,LINE,,98
LESIZE,ALL,,,18,1

LSEL,S,LINE,,88
LSEL,A,LINE,,92
LSEL,A,LINE,,96
LSEL,A,LINE,,100
LESIZE,ALL,,,16,1

LSEL,S,LINE,,93
LSEL,A,LINE,,95
LSEL,A,LINE,,97
LSEL,A,LINE,,99
LESIZE,ALL,,,1,1
VMESH,ALL

VSEL,S,VOLU,,13
VATT,1,,1,23,13

LSEL,S,LINE,,94
LSEL,A,LINE,,98
LSEL,A,LINE,,102
LSEL,A,LINE,,106
LESIZE,ALL,,,18,1

LSEL,S,LINE,,96
LSEL,A,LINE,,100
LSEL,A,LINE,,104
LSEL,A,LINE,,108
LESIZE,ALL,,,16,1

LSEL,S,LINE,,101
LSEL,A,LINE,,103
LSEL,A,LINE,,105
LSEL,A,LINE,,107
LESIZE,ALL,,,1,1
VMESH,ALL
```

```
VSEL,S,VOLU,,14
VATT,1,,1,24,14

LSEL,S,LINE,,102
LSEL,A,LINE,,106
LSEL,A,LINE,,110
LSEL,A,LINE,,114
LESIZE,ALL,,,18,1

LSEL,S,LINE,,104
LSEL,A,LINE,,108
LSEL,A,LINE,,112
LSEL,A,LINE,,116
LESIZE,ALL,,,16,1

LSEL,S,LINE,,109
LSEL,A,LINE,,111
LSEL,A,LINE,,113
LSEL,A,LINE,,115
LESIZE,ALL,,,1,1
VMESH,ALL

VSEL,S,VOLU,,15
VATT,1,,1,25,15

LSEL,S,LINE,,110
LSEL,A,LINE,,114
LSEL,A,LINE,,118
LSEL,A,LINE,,122
LESIZE,ALL,,,18,1

LSEL,S,LINE,,112
LSEL,A,LINE,,116
LSEL,A,LINE,,120
LSEL,A,LINE,,124
LESIZE,ALL,,,16,1

LSEL,S,LINE,,117
LSEL,A,LINE,,119
LSEL,A,LINE,,121
```

```
LSEL,A,LINE,,123
LESIZE,ALL,,,1,1
VMESH,ALL

VSEL,S,VOLU,,16
VATT,1,,1,26,16

LSEL,S,LINE,,118
LSEL,A,LINE,,122
LSEL,A,LINE,,126
LSEL,A,LINE,,130
LESIZE,ALL,,,18,1

LSEL,S,LINE,,120
LSEL,A,LINE,,124
LSEL,A,LINE,,128
LSEL,A,LINE,,132
LESIZE,ALL,,,16,1

LSEL,S,LINE,,125
LSEL,A,LINE,,127
LSEL,A,LINE,,129
LSEL,A,LINE,,131
LESIZE,ALL,,,1,1
VMESH,ALL



FLST,2,33,1,ORDE,4
FITEM,2,9726
FITEM,2,9782
FITEM,2,9784
FITEM,2,-9814
!*
/GO
D,P51X, ,0, , , ,UZ, , , , ,

FLST,2,33,1,ORDE,4
FITEM,2,9728
FITEM,2,9830
```

```
FITEM,2,9884
FITEM,2,-9914
!*
/GO
D,P51X, ,0, , , ,UX,UY,UZ, , ,



FLST,2,933,1,ORDE,12
FITEM,2,19774
FITEM,2,19776
FITEM,2,-19811
FITEM,2,19830
FITEM,2,19832
FITEM,2,-19862
FITEM,2,19878
FITEM,2,-19913
FITEM,2,19932
FITEM,2,-19962
FITEM,2,19978
FITEM,2,-20774
!*
/GO
F,P51X,FZ,force/933



/SOL
ANTYPE,STATIC
SOLVE
/REPLOT,RESIZE
WPSTYLE,,,,,,,,0
FINISH
/POST1
!*
PRNSOL,U,Z
```

Appendix E

MATLAB Code

```
% Composite Material
% PART 1 Equivalent ABD matrix
clear;
clc;
%input data
format long
E1=20.3e6;
E2=1.5e6;
E3=1.5e6;
v12=0.27;
v13=0.27;
v23=0.54;
G12=1e6;
G13=1e6;
G23=0.54e6;
tply=0.005;

% Dimensions
L=0.72;
bw=0.24;
layers=16;
h=tply*layers;
tply=0.005;
A=bw*(h);
P=1000;
thickness=16*tply;
Vf=1/16;
% Q
S=zeros(6,6);
S(1,1)=1/E1;
S(2,2)=1/E2;
S(3,3)=1/E3;
S(4,4)=1/G23;
S(5,5)=1/G13;
S(6,6)=1/G12;
S(1,2)=-v12./E1;
S(1,3)=-v13./E1;
S(2,1)=-v12./E1;
S(2,3)=-v23./E2;
S(3,1)=-v13./E1;
```

```
S(3,2)=-v23./E2;

% C matrix
C_bar=inv(S);
C44=C_bar(4,4);
C55=C_bar(5,5);

% C_bar@0deg rotate with z-axis
ANGLE_1=0;
A_1=ANGLE_1*pi/180;
m=cos(A_1);
n=sin(A_1);
Tstress=[m^2 n^2 0 0 0 2*m*n
   n^2 m^2 0 0 0 -2*m*n
         0 0 1 0 0 0
         0 0 0 m -n 0
         0 0 0 n m 0
   -m*n m*n 0 0 0 m^2-n^2];
Tstrain=[m^2 n^2 0 0 0 m*n
   n^2 m^2 0 0 0 -m*n
         0 0 1 0 0 0
         0 0 0 m -n 0
         0 0 0 n m 0
   -2*m*n 2*m*n 0 0 0 m^2-n^2];
C_bar_0=inv(Tstress)*C_bar*Tstrain;
C55_0=C_bar_0(5,5);  % C55=G13
c0=[C_bar_0(4,4) C_bar_0(4,5);
   C_bar_0(5,4) C_bar_0(5,5)];

% C_bar@15deg rotate with z-axis
ANGLE_1=15;
A_1=ANGLE_1*pi/180;
m=cos(A_1);
n=sin(A_1);
Tstress=[m^2 n^2 0 0 0 2*m*n
   n^2 m^2 0 0 0 -2*m*n
         0 0 1 0 0 0
         0 0 0 m -n 0
         0 0 0 n m 0
   -m*n m*n 0 0 0 m^2-n^2];
Tstrain=[m^2 n^2 0 0 0 m*n
```

```
   n^2 m^2 0 0 0 -m*n
         0 0 1 0 0 0
         0 0 0 m -n 0
         0 0 0 n m 0
   -2*m*n 2*m*n 0 0 0 m^2-n^2];
C_bar_15=inv(Tstress)*C_bar*Tstrain;
C55_15=C_bar_15(5,5); % C55=G13
C5515=(n^2)*C44+(m^2)*C55;
C4415=(m^2)*C44+(n^2)*C55;
C4515=(C55-C44)*m*n;
c15=[C_bar_15(4,4) C_bar_15(4,5);
    C_bar_15(5,4) C_bar_15(5,5)];

% C_bar@-15deg rotate with z-axis
ANGLE_1=-15;
A_1=ANGLE_1*pi/180;
m=cos(A_1);
n=sin(A_1);
Tstress=[m^2 n^2 0 0 0 2*m*n
   n^2 m^2 0 0 0 -2*m*n
         0 0 1 0 0 0
         0 0 0 m -n 0
         0 0 0 n m 0
   -m*n m*n 0 0 0 m^2-n^2];
Tstrain=[m^2 n^2 0 0 0 m*n
   n^2 m^2 0 0 0 -m*n
         0 0 1 0 0 0
         0 0 0 m -n 0
         0 0 0 n m 0
   -2*m*n 2*m*n 0 0 0 m^2-n^2];
C_bar_115=inv(Tstress)*C_bar*Tstrain;
C55_115=C_bar_115(5,5);  % C55=G13
c115=[C_bar_115(4,4) C_bar_115(4,5);
    C_bar_115(5,4) C_bar_115(5,5)];
% C_bar@30deg rotate with z-axis
ANGLE_1=30;
A_1=ANGLE_1*pi/180;
m=cos(A_1);
n=sin(A_1);
Tstress=[m^2 n^2 0 0 0 2*m*n
   n^2 m^2 0 0 0 -2*m*n
```

```
        0 0 1 0 0 0
        0 0 0 m -n 0
        0 0 0 n m 0
   -m*n m*n 0 0 0 m^2-n^2];
Tstrain=[m^2 n^2 0 0 0 m*n
   n^2 m^2 0 0 0 -m*n
        0 0 1 0 0 0
        0 0 0 m -n 0
        0 0 0 n m 0
   -2*m*n 2*m*n 0 0 0 m^2-n^2];
C_bar_30=inv(Tstress)*C_bar*Tstrain;
C55_30=C_bar_30(5,5);  % C55=G13
C5530=(n^2)*C44+(m^2)*C55;
c30=[C_bar_30(4,4) C_bar_30(4,5);
    C_bar_30(5,4) C_bar_30(5,5)];
% C_bar@-30deg rotate with z-axis
ANGLE_1=-30;
A_1=ANGLE_1*pi/180;
m=cos(A_1);
n=sin(A_1);
Tstress=[m^2 n^2 0 0 0 2*m*n
   n^2 m^2 0 0 0 -2*m*n
        0 0 1 0 0 0
        0 0 0 m -n 0
        0 0 0 n m 0
   -m*n m*n 0 0 0 m^2-n^2];
Tstrain=[m^2 n^2 0 0 0 m*n
   n^2 m^2 0 0 0 -m*n
        0 0 1 0 0 0
        0 0 0 m -n 0
        0 0 0 n m 0
   -2*m*n 2*m*n 0 0 0 m^2-n^2];
C_bar_330=inv(Tstress)*C_bar*Tstrain;
C55_330=C_bar_330(5,5);  % C55=G13
c330=[C_bar_330(4,4) C_bar_330(4,5);
    C_bar_330(5,4) C_bar_330(5,5)];

% C_bar@45deg rotate with z-axis
ANGLE_1=45;
A_1=ANGLE_1*pi/180;
m=cos(A_1);
```

```
n=sin(A_1);
Tstress=[m^2 n^2 0 0 0 2*m*n
   n^2 m^2 0 0 0 -2*m*n
         0 0 1 0 0 0
         0 0 0 m -n 0
         0 0 0 n m 0
   -m*n m*n 0 0 0 m^2-n^2];
Tstrain=[m^2 n^2 0 0 0 m*n
   n^2 m^2 0 0 0 -m*n
         0 0 1 0 0 0
         0 0 0 m -n 0
         0 0 0 n m 0
   -2*m*n 2*m*n 0 0 0 m^2-n^2];
C_bar_45=inv(Tstress)*C_bar*Tstrain;
C55_45=C_bar_45(5,5);  % C55=G13
c45=[C_bar_45(4,4) C_bar_45(4,5);
    C_bar_45(5,4) C_bar_45(5,5)];

% C_bar@-45deg rotate with z-axis
ANGLE_1=-45;
A_1=ANGLE_1*pi/180;
m=cos(A_1);
n=sin(A_1);
Tstress=[m^2 n^2 0 0 0 2*m*n
   n^2 m^2 0 0 0 -2*m*n
         0 0 1 0 0 0
         0 0 0 m -n 0
         0 0 0 n m 0
   -m*n m*n 0 0 0 m^2-n^2];
Tstrain=[m^2 n^2 0 0 0 m*n
   n^2 m^2 0 0 0 -m*n
         0 0 1 0 0 0
         0 0 0 m -n 0
         0 0 0 n m 0
   -2*m*n 2*m*n 0 0 0 m^2-n^2];
C_bar_445=inv(Tstress)*C_bar*Tstrain;
C55_445=C_bar_445(5,5);  % C55=G13
c445=[C_bar_445(4,4) C_bar_445(4,5);
    C_bar_445(5,4) C_bar_445(5,5)];

% C_bar@60deg rotate with z-axis
```

```
ANGLE_1=60;
A_1=ANGLE_1*pi/180;
m=cos(A_1);
n=sin(A_1);
Tstress=[m^2 n^2 0 0 0 2*m*n
   n^2 m^2 0 0 0 -2*m*n
         0 0 1 0 0 0
         0 0 0 m -n 0
         0 0 0 n m 0
   -m*n m*n 0 0 0 m^2-n^2];
Tstrain=[m^2 n^2 0 0 0 m*n
   n^2 m^2 0 0 0 -m*n
         0 0 1 0 0 0
         0 0 0 m -n 0
         0 0 0 n m 0
   -2*m*n 2*m*n 0 0 0 m^2-n^2];
C_bar_60=inv(Tstress)*C_bar*Tstrain;
C55_60=C_bar_60(5,5);  % C55=G13
c60=[C_bar_60(4,4) C_bar_60(4,5);
    C_bar_60(5,4) C_bar_60(5,5)];

% C_bar@-60deg rotate with z-axis
ANGLE_1=-60;
A_1=ANGLE_1*pi/180;
m=cos(A_1);
n=sin(A_1);
Tstress=[m^2 n^2 0 0 0 2*m*n
   n^2 m^2 0 0 0 -2*m*n
         0 0 1 0 0 0
         0 0 0 m -n 0
         0 0 0 n m 0
   -m*n m*n 0 0 0 m^2-n^2];
Tstrain=[m^2 n^2 0 0 0 m*n
   n^2 m^2 0 0 0 -m*n
         0 0 1 0 0 0
         0 0 0 m -n 0
         0 0 0 n m 0
   -2*m*n 2*m*n 0 0 0 m^2-n^2];
C_bar_660=inv(Tstress)*C_bar*Tstrain;
C55_660=C_bar_660(5,5);  % C55=G13
c660=[C_bar_660(4,4) C_bar_660(4,5);
```

```
    C_bar_660(5,4) C_bar_660(5,5)];

% C_bar@75deg rotate with z-axis
ANGLE_1=75;
A_1=ANGLE_1*pi/180;
m=cos(A_1);
n=sin(A_1);
Tstress=[m^2 n^2 0 0 0 2*m*n
   n^2 m^2 0 0 0 -2*m*n
         0 0 1 0 0 0
         0 0 0 m -n 0
         0 0 0 n m 0
   -m*n m*n 0 0 0 m^2-n^2];
Tstrain=[m^2 n^2 0 0 0 m*n
   n^2 m^2 0 0 0 -m*n
         0 0 1 0 0 0
         0 0 0 m -n 0
         0 0 0 n m 0
   -2*m*n 2*m*n 0 0 0 m^2-n^2];
C_bar_75=inv(Tstress)*C_bar*Tstrain;
C55_75=C_bar_75(5,5);  % C55=G13
c75=[C_bar_75(4,4) C_bar_75(4,5);
    C_bar_75(5,4) C_bar_75(5,5)];

% C_bar@-75deg rotate with z-axis
ANGLE_1=-75;
A_1=ANGLE_1*pi/180;
m=cos(A_1);
n=sin(A_1);
Tstress=[m^2 n^2 0 0 0 2*m*n
   n^2 m^2 0 0 0 -2*m*n
         0 0 1 0 0 0
         0 0 0 m -n 0
         0 0 0 n m 0
   -m*n m*n 0 0 0 m^2-n^2];
Tstrain=[m^2 n^2 0 0 0 m*n
   n^2 m^2 0 0 0 -m*n
         0 0 1 0 0 0
         0 0 0 m -n 0
         0 0 0 n m 0
   -2*m*n 2*m*n 0 0 0 m^2-n^2];
```

```
C_bar_775=inv(Tstress)*C_bar*Tstrain;
C55_775=C_bar_775(5,5);  % C55=G13
c775=[C_bar_775(4,4) C_bar_775(4,5);
    C_bar_775(5,4) C_bar_775(5,5)];

% C_bar@90deg rotate with z-axis
ANGLE_1=90;
A_1=ANGLE_1*pi/180;
m=cos(A_1);
n=sin(A_1);
Tstress=[m^2 n^2 0 0 0 2*m*n
   n^2 m^2 0 0 0 -2*m*n
         0 0 1 0 0 0
         0 0 0 m -n 0
         0 0 0 n m 0
   -m*n m*n 0 0 0 m^2-n^2];
Tstrain=[m^2 n^2 0 0 0 m*n
   n^2 m^2 0 0 0 -m*n
         0 0 1 0 0 0
         0 0 0 m -n 0
         0 0 0 n m 0
   -2*m*n 2*m*n 0 0 0 m^2-n^2];
C_bar_90=inv(Tstress)*C_bar*Tstrain;
C55_90=C_bar_90(5,5); % C55=G13
c90=[C_bar_90(4,4) C_bar_90(4,5);
    C_bar_90(5,4) C_bar_90(5,5)];

% C_bar@-90deg rotate with z-axis
ANGLE_1=-90;
A_1=ANGLE_1*pi/180;
m=cos(A_1);
n=sin(A_1);
Tstress=[m^2 n^2 0 0 0 2*m*n
   n^2 m^2 0 0 0 -2*m*n
         0 0 1 0 0 0
         0 0 0 m -n 0
         0 0 0 n m 0
   -m*n m*n 0 0 0 m^2-n^2];
Tstrain=[m^2 n^2 0 0 0 m*n
   n^2 m^2 0 0 0 -m*n
         0 0 1 0 0 0
```

```
        0 0 0 m -n 0
        0 0 0 n m 0
   -2*m*n 2*m*n 0 0 0 m^2-n^2];
C_bar_990=inv(Tstress)*C_bar*Tstrain;
C55_990=C_bar_990(5,5);  % C55=G13
c990=[C_bar_990(4,4) C_bar_990(4,5);
    C_bar_990(5,4) C_bar_990(5,5)];

%Laminate 1
h0=-8*tply;
h1=-7*tply;
h2=-6*tply;
h3=-5*tply;
h4=-4*tply;
h5=-3*tply;
h6=-2*tply;
h7=-1*tply;
h8=0*tply;
h9=1*tply;
h10=2*tply;
h11=3*tply;
h12=4*tply;
h13=5*tply;
h14=6*tply;
h15=7*tply;
h16=8*tply;

% Q
S=zeros(3,3);
S(1,1)=1/E1;
S(2,2)=1/E2;
S(3,3)=1/G12;
S(1,2)=-v12./E1;
S(2,1)=-v12./E1;
% Q matrix
Q_bar=inv(S);
% Q_bar@45deg
ANGLE_1=45;
A_1=ANGLE_1*pi/180;
m=cos(A_1);
n=sin(A_1);
```

```
Tstress=[m^2 n^2 2*m*n
   n^2 m^2 -2*m*n
   -m*n m*n m^2-n^2];
Tstrain=[m^2 n^2 m*n
   n^2 m^2 -m*n
   -2*m*n 2*m*n m^2-n^2];
Q_bar_45=inv(Tstress)*Q_bar*Tstrain;
% Q_bar@-45deg
ANGLE_1=-45;
A_1=ANGLE_1*pi/180;
m=cos(A_1);
n=sin(A_1);
Tstress=[m^2 n^2 2*m*n
   n^2 m^2 -2*m*n
   -m*n m*n m^2-n^2];
Tstrain=[m^2 n^2 m*n
   n^2 m^2 -m*n
   -2*m*n 2*m*n m^2-n^2];
Q_bar_445=inv(Tstress)*Q_bar*Tstrain;
% Q_bar@0deg
ANGLE_1=0;
A_1=ANGLE_1*pi/180;
m=cos(A_1);
n=sin(A_1);
Tstress=[m^2 n^2 2*m*n
   n^2 m^2 -2*m*n
   -m*n m*n m^2-n^2];
Tstrain=[m^2 n^2 m*n
   n^2 m^2 -m*n
   -2*m*n 2*m*n m^2-n^2];
Q_bar_0=inv(Tstress)*Q_bar*Tstrain;
% Q_bar@90deg
ANGLE_1=90;
A_1=ANGLE_1*pi/180;
m=cos(A_1);
n=sin(A_1);
Tstress=[m^2 n^2 2*m*n
   n^2 m^2 -2*m*n
   -m*n m*n m^2-n^2];
Tstrain=[m^2 n^2 m*n
   n^2 m^2 -m*n
```

```
   -2*m*n 2*m*n m^2-n^2];
Q_bar_90=inv(Tstress)*Q_bar*Tstrain;
% Q_bar@30deg
ANGLE_1=30;
A_1=ANGLE_1*pi/180;
m=cos(A_1);
n=sin(A_1);
Tstress=[m^2 n^2 2*m*n
   n^2 m^2 -2*m*n
   -m*n m*n m^2-n^2];
Tstrain=[m^2 n^2 m*n
   n^2 m^2 -m*n
   -2*m*n 2*m*n m^2-n^2];
Q_bar_30=inv(Tstress)*Q_bar*Tstrain;
% Q_bar@-30deg
ANGLE_1=-30;
A_1=ANGLE_1*pi/180;
m=cos(A_1);
n=sin(A_1);
Tstress=[m^2 n^2 2*m*n
   n^2 m^2 -2*m*n
   -m*n m*n m^2-n^2];
Tstrain=[m^2 n^2 m*n
   n^2 m^2 -m*n
   -2*m*n 2*m*n m^2-n^2];
Q_bar_330=inv(Tstress)*Q_bar*Tstrain;
% Q_bar@60deg
ANGLE_1=60;
A_1=ANGLE_1*pi/180;
m=cos(A_1);
n=sin(A_1);
Tstress=[m^2 n^2 2*m*n
   n^2 m^2 -2*m*n
   -m*n m*n m^2-n^2];
Tstrain=[m^2 n^2 m*n
   n^2 m^2 -m*n
   -2*m*n 2*m*n m^2-n^2];
Q_bar_60=inv(Tstress)*Q_bar*Tstrain;
% Q_bar@-60deg
ANGLE_1=-60;
A_1=ANGLE_1*pi/180;
```

```
m=cos(A_1);
n=sin(A_1);
Tstress=[m^2 n^2 2*m*n
   n^2 m^2 -2*m*n
   -m*n m*n m^2-n^2];
Tstrain=[m^2 n^2 m*n
   n^2 m^2 -m*n
   -2*m*n 2*m*n m^2-n^2];
Q_bar_660=inv(Tstress)*Q_bar*Tstrain;
% Q_bar@15deg
ANGLE_1=15;
A_1=ANGLE_1*pi/180;
m=cos(A_1);
n=sin(A_1);
Tstress=[m^2 n^2 2*m*n
   n^2 m^2 -2*m*n
   -m*n m*n m^2-n^2];
Tstrain=[m^2 n^2 m*n
   n^2 m^2 -m*n
   -2*m*n 2*m*n m^2-n^2];
Q_bar_15=inv(Tstress)*Q_bar*Tstrain;
% Q_bar@-15deg
ANGLE_1=-15;
A_1=ANGLE_1*pi/180;
m=cos(A_1);
n=sin(A_1);
Tstress=[m^2 n^2 2*m*n
   n^2 m^2 -2*m*n
   -m*n m*n m^2-n^2];
Tstrain=[m^2 n^2 m*n
   n^2 m^2 -m*n
   -2*m*n 2*m*n m^2-n^2];
Q_bar_115=inv(Tstress)*Q_bar*Tstrain;
% Q_bar@75deg
ANGLE_1=75;
A_1=ANGLE_1*pi/180;
m=cos(A_1);
n=sin(A_1);
Tstress=[m^2 n^2 2*m*n
   n^2 m^2 -2*m*n
   -m*n m*n m^2-n^2];
```

```
Tstrain=[m^2 n^2 m*n
   n^2 m^2 -m*n
   -2*m*n 2*m*n m^2-n^2];
Q_bar_75=inv(Tstress)*Q_bar*Tstrain;
% Q_bar@-75deg
ANGLE_1=-75;
A_1=ANGLE_1*pi/180;
m=cos(A_1);
n=sin(A_1);
Tstress=[m^2 n^2 2*m*n
   n^2 m^2 -2*m*n
   -m*n m*n m^2-n^2];
Tstrain=[m^2 n^2 m*n
   n^2 m^2 -m*n
   -2*m*n 2*m*n m^2-n^2];
Q_bar_775=inv(Tstress)*Q_bar*Tstrain;



%1 [+-45/0/90]4T      C_bar_90 C_bar_0 C_bar_445 C_bar_45 C_bar_90
C_bar_0 C_bar_445 C_bar_45 C_bar_90 C_bar_0 C_bar_445 C_bar_45
C_bar_90 C_bar_0 C_bar_445 C_bar_45
%                Q_bar_90 Q_bar_0 Q_bar_445 Q_bar_45 Q_bar_90 Q_bar_0
Q_bar_445 Q_bar_45 Q_bar_90 Q_bar_0 Q_bar_445 Q_bar_45 Q_bar_90
Q_bar_0 Q_bar_445 Q_bar_45
%2 [+-45/0/90]2T      C_bar_90 C_bar_0 C_bar_445 C_bar_45 C_bar_90
C_bar_0 C_bar_445 C_bar_45
%                Q_bar_90 Q_bar_0 Q_bar_445 Q_bar_45 Q_bar_90 Q_bar_0
Q_bar_445 Q_bar_45
%3 [+-45/0/90]T       C_bar_90 C_bar_0 C_bar_445 C_bar_45
%                Q_bar_90 Q_bar_0 Q_bar_445 Q_bar_45

%4 [0/+-45/90]4T      C_bar_90 C_bar_445 C_bar_45 C_bar_0 C_bar_90
C_bar_445 C_bar_45 C_bar_0 C_bar_90 C_bar_445 C_bar_45 C_bar_0
C_bar_90 C_bar_445 C_bar_45 C_bar_0
%                Q_bar_90 Q_bar_445 Q_bar_45 Q_bar_0 Q_bar_90 Q_bar_445
Q_bar_45 Q_bar_0 Q_bar_90 Q_bar_445 Q_bar_45 Q_bar_0 Q_bar_90
Q_bar_445 Q_bar_45 Q_bar_0
%5 [0/+-45/90]2T      C_bar_90 C_bar_445 C_bar_45 C_bar_0 C_bar_90
C_bar_445 C_bar_45 C_bar_0
```

% Q_bar_90 Q_bar_445 Q_bar_45 Q_bar_0 Q_bar_90 Q_bar_445 Q_bar_45 Q_bar_0
%6 [0/+-45/90]T C_bar_90 C_bar_445 C_bar_45 C_bar_0
% Q_bar_90 Q_bar_445 Q_bar_45 Q_bar_0

%7 [+-45/0/90]2s C_bar_45 C_bar_445 C_bar_0 C_bar_90 C_bar_45 C_bar_445 C_bar_0 C_bar_90 C_bar_90 C_bar_0 C_bar_445 C_bar_45 C_bar_90 C_bar_0 C_bar_445 C_bar_45
% Q_bar_45 Q_bar_445 Q_bar_0 Q_bar_90 Q_bar_45 Q_bar_445 Q_bar_0 Q_bar_90 Q_bar_90 Q_bar_0 Q_bar_445 Q_bar_45 Q_bar_90 Q_bar_0 Q_bar_445 Q_bar_45
%8 [+-45/0/90]s C_bar_45 C_bar_445 C_bar_0 C_bar_90 C_bar_90 C_bar_0 C_bar_445 C_bar_45
% Q_bar_45 Q_bar_445 Q_bar_0 Q_bar_90 Q_bar_90 Q_bar_0 Q_bar_445 Q_bar_45

%9 [0/+-45/90]2s C_bar_0 C_bar_45 C_bar_445 C_bar_90 C_bar_0 C_bar_45 C_bar_445 C_bar_90 C_bar_90 C_bar_445 C_bar_45 C_bar_0 C_bar_90 C_bar_445 C_bar_45 C_bar_0
% Q_bar_0 Q_bar_45 Q_bar_445 Q_bar_90 Q_bar_0 Q_bar_45 Q_bar_445 Q_bar_90 Q_bar_90 Q_bar_445 Q_bar_45 Q_bar_0 Q_bar_90 Q_bar_445 Q_bar_45 Q_bar_0
%10 [0/+-45/90]2s C_bar_0 C_bar_45 C_bar_445 C_bar_90 C_bar_90 C_bar_445 C_bar_45 C_bar_0
% Q_bar_0 Q_bar_45 Q_bar_445 Q_bar_90 Q_bar_90 Q_bar_445 Q_bar_45 Q_bar_0

%11 [45/0]8T C_bar_0 C_bar_45 C_bar_0 C_bar_45 C_bar_0 C_bar_45 C_bar_0 C_bar_45 C_bar_0 C_bar_45 C_bar_0 C_bar_45 C_bar_0 C_bar_45 C_bar_0 C_bar_45
% Q_bar_0 Q_bar_45 Q_bar_0 Q_bar_45 Q_bar_0 Q_bar_45 Q_bar_0 Q_bar_45 Q_bar_0 Q_bar_45 Q_bar_0 Q_bar_45 Q_bar_0 Q_bar_45 Q_bar_0 Q_bar_45
%12 [45/0]4T C_bar_0 C_bar_45 C_bar_0 C_bar_45 C_bar_0 C_bar_45 C_bar_0 C_bar_45
% Q_bar_0 Q_bar_45 Q_bar_0 Q_bar_45 Q_bar_0 Q_bar_45 Q_bar_0 Q_bar_45
%13 [45/0]2T C_bar_0 C_bar_45 C_bar_0 C_bar_45
% Q_bar_0 Q_bar_45 Q_bar_0 Q_bar_45
%14 [45/0]T C_bar_0 C_bar_45
% Q_bar_0 Q_bar_45

%15 [0/45]8T C_bar_45 C_bar_0 C_bar_45 C_bar_0 C_bar_45 C_bar_0 C_bar_45 C_bar_0 C_bar_45 C_bar_0 C_bar_45 C_bar_0 C_bar_45 C_bar_0 C_bar_45 C_bar_0
% Q_bar_45 Q_bar_0 Q_bar_45 Q_bar_0 Q_bar_45 Q_bar_0 Q_bar_45 Q_bar_0 Q_bar_45 Q_bar_0 Q_bar_45 Q_bar_0 Q_bar_45 Q_bar_0 Q_bar_45 Q_bar_0
%16 [0/45]4T C_bar_45 C_bar_0 C_bar_45 C_bar_0 C_bar_45 C_bar_0 C_bar_45 C_bar_0
% Q_bar_45 Q_bar_0 Q_bar_45 Q_bar_0 Q_bar_45 Q_bar_0 Q_bar_45 Q_bar_0
%17 [0/45]2T C_bar_45 C_bar_0 C_bar_45 C_bar_0
% Q_bar_45 Q_bar_0 Q_bar_45 Q_bar_0
%18 [0/45]T C_bar_45 C_bar_0
% Q_bar_45 Q_bar_0

%19 [45/0]4s C_bar_45 C_bar_0 C_bar_45 C_bar_0 C_bar_45 C_bar_0 C_bar_45 C_bar_0 C_bar_0 C_bar_45 C_bar_0 C_bar_45 C_bar_0 C_bar_45 C_bar_0 C_bar_45
% Q_bar_45 Q_bar_0 Q_bar_45 Q_bar_0 Q_bar_45 Q_bar_0 Q_bar_45 Q_bar_0 Q_bar_0 Q_bar_45 Q_bar_0 Q_bar_45 Q_bar_0 Q_bar_45 Q_bar_0 Q_bar_45
%20 [45/0]2s C_bar_45 C_bar_0 C_bar_45 C_bar_0 C_bar_0 C_bar_45 C_bar_0 C_bar_45
% Q_bar_45 Q_bar_0 Q_bar_45 Q_bar_0 Q_bar_0 Q_bar_45 Q_bar_0 Q_bar_45
%21 [45/0]s C_bar_45 C_bar_0 C_bar_0 C_bar_45
% Q_bar_45 Q_bar_0 Q_bar_0 Q_bar_45

%22 [0/45]4s C_bar_0 C_bar_45 C_bar_0 C_bar_45 C_bar_0 C_bar_45 C_bar_0 C_bar_45 C_bar_45 C_bar_0 C_bar_45 C_bar_0 C_bar_45 C_bar_0 C_bar_45 C_bar_0
% Q_bar_0 Q_bar_45 Q_bar_0 Q_bar_45 Q_bar_0 Q_bar_45 Q_bar_0 Q_bar_45 Q_bar_45 Q_bar_0 Q_bar_45 Q_bar_0 Q_bar_45 Q_bar_0 Q_bar_45 Q_bar_0
%23 [0/45]2s C_bar_0 C_bar_45 C_bar_0 C_bar_45 C_bar_45 C_bar_0 C_bar_45 C_bar_0
% Q_bar_0 Q_bar_45 Q_bar_0 Q_bar_45 Q_bar_45 Q_bar_0 Q_bar_45 Q_bar_0
%24 [0/45]s C_bar_0 C_bar_45 C_bar_45 C_bar_0
% Q_bar_0 Q_bar_45 Q_bar_45 Q_bar_0

% [15/0]4s C_bar_15 C_bar_0 C_bar_15 C_bar_0 C_bar_15 C_bar_0 C_bar_15 C_bar_0 C_bar_0 C_bar_15 C_bar_0 C_bar_15 C_bar_0 C_bar_15 C_bar_0 C_bar_15
% Q_bar_15 Q_bar_0 Q_bar_15 Q_bar_0 Q_bar_15 Q_bar_0 Q_bar_15 Q_bar_0 Q_bar_0 Q_bar_15 Q_bar_0 Q_bar_15 Q_bar_0 Q_bar_15 Q_bar_0 Q_bar_15
% [30/0]4s C_bar_30 C_bar_0 C_bar_30 C_bar_0 C_bar_30 C_bar_0 C_bar_30 C_bar_0 C_bar_0 C_bar_30 C_bar_0 C_bar_30 C_bar_0 C_bar_30 C_bar_0 C_bar_30
% Q_bar_30 Q_bar_0 Q_bar_30 Q_bar_0 Q_bar_30 Q_bar_0 Q_bar_30 Q_bar_0 Q_bar_0 Q_bar_30 Q_bar_0 Q_bar_30 Q_bar_0 Q_bar_30 Q_bar_0 Q_bar_30
% [45/0]4s C_bar_45 C_bar_0 C_bar_45 C_bar_0 C_bar_45 C_bar_0 C_bar_45 C_bar_0 C_bar_0 C_bar_45 C_bar_0 C_bar_45 C_bar_0 C_bar_45 C_bar_0 C_bar_45
% Q_bar_45 Q_bar_0 Q_bar_45 Q_bar_0 Q_bar_45 Q_bar_0 Q_bar_45 Q_bar_0 Q_bar_0 Q_bar_45 Q_bar_0 Q_bar_45 Q_bar_0 Q_bar_45 Q_bar_0 Q_bar_45
% [60/0]4s C_bar_60 C_bar_0 C_bar_60 C_bar_0 C_bar_60 C_bar_0 C_bar_60 C_bar_0 C_bar_0 C_bar_60 C_bar_0 C_bar_60 C_bar_0 C_bar_60 C_bar_0 C_bar_60
% Q_bar_60 Q_bar_0 Q_bar_60 Q_bar_0 Q_bar_60 Q_bar_0 Q_bar_60 Q_bar_0 Q_bar_0 Q_bar_60 Q_bar_0 Q_bar_60 Q_bar_0 Q_bar_60 Q_bar_0 Q_bar_60
% [75/0]4s C_bar_75 C_bar_0 C_bar_75 C_bar_0 C_bar_75 C_bar_0 C_bar_75 C_bar_0 C_bar_0 C_bar_75 C_bar_0 C_bar_75 C_bar_0 C_bar_75 C_bar_0 C_bar_75
% Q_bar_75 Q_bar_0 Q_bar_75 Q_bar_0 Q_bar_75 Q_bar_0 Q_bar_75 Q_bar_0 Q_bar_0 Q_bar_75 Q_bar_0 Q_bar_75 Q_bar_0 Q_bar_75 Q_bar_0 Q_bar_75

% [15/0]8T C_bar_0 C_bar_15 C_bar_0 C_bar_15 C_bar_0 C_bar_15 C_bar_0 C_bar_15 C_bar_0 C_bar_15 C_bar_0 C_bar_15 C_bar_0 C_bar_15 C_bar_0 C_bar_15
% Q_bar_0 Q_bar_15 Q_bar_0 Q_bar_15 Q_bar_0 Q_bar_15 Q_bar_0 Q_bar_15 Q_bar_0 Q_bar_15 Q_bar_0 Q_bar_15 Q_bar_0 Q_bar_15 Q_bar_0 Q_bar_15

% [30/0]8T C_bar_0 C_bar_30 C_bar_0 C_bar_30 C_bar_0 C_bar_30 C_bar_0 C_bar_30 C_bar_0 C_bar_30 C_bar_0 C_bar_30 C_bar_0 C_bar_30 C_bar_0 C_bar_30
% Q_bar_0 Q_bar_30 Q_bar_0 Q_bar_30 Q_bar_0 Q_bar_30 Q_bar_0 Q_bar_30 Q_bar_0 Q_bar_30 Q_bar_0 Q_bar_30 Q_bar_0 Q_bar_30 Q_bar_0 Q_bar_30
% [45/0]8T C_bar_0 C_bar_45 C_bar_0 C_bar_45 C_bar_0 C_bar_45 C_bar_0 C_bar_45 C_bar_0 C_bar_45 C_bar_0 C_bar_45 C_bar_0 C_bar_45 C_bar_0 C_bar_45
% Q_bar_0 Q_bar_45 Q_bar_0 Q_bar_45 Q_bar_0 Q_bar_45 Q_bar_0 Q_bar_45 Q_bar_0 Q_bar_45 Q_bar_0 Q_bar_45 Q_bar_0 Q_bar_45 Q_bar_0 Q_bar_45
% [60/0]8T C_bar_0 C_bar_60 C_bar_0 C_bar_60 C_bar_0 C_bar_60 C_bar_0 C_bar_60 C_bar_0 C_bar_60 C_bar_0 C_bar_60 C_bar_0 C_bar_60 C_bar_0 C_bar_60
% Q_bar_0 Q_bar_60 Q_bar_0 Q_bar_60 Q_bar_0 Q_bar_60 Q_bar_0 Q_bar_60 Q_bar_0 Q_bar_60 Q_bar_0 Q_bar_60 Q_bar_0 Q_bar_60 Q_bar_0 Q_bar_60
% [75/0]8T C_bar_0 C_bar_75 C_bar_0 C_bar_75 C_bar_0 C_bar_75 C_bar_0 C_bar_75 C_bar_0 C_bar_75 C_bar_0 C_bar_75 C_bar_0 C_bar_75 C_bar_0 C_bar_75
% Q_bar_0 Q_bar_75 Q_bar_0 Q_bar_75 Q_bar_0 Q_bar_75 Q_bar_0 Q_bar_75 Q_bar_0 Q_bar_75 Q_bar_0 Q_bar_75 Q_bar_0 Q_bar_75 Q_bar_0 Q_bar_75

% [0/15]4s C_bar_0 C_bar_15 C_bar_0 C_bar_15 C_bar_0 C_bar_15 C_bar_0 C_bar_15 C_bar_15 C_bar_0 C_bar_15 C_bar_0 C_bar_15 C_bar_0 C_bar_15 C_bar_0
% Q_bar_0 Q_bar_15 Q_bar_0 Q_bar_15 Q_bar_0 Q_bar_15 Q_bar_0 Q_bar_15 Q_bar_15 Q_bar_0 Q_bar_15 Q_bar_0 Q_bar_15 Q_bar_0 Q_bar_15 Q_bar_0
% [0/30]4s C_bar_0 C_bar_30 C_bar_0 C_bar_30 C_bar_0 C_bar_30 C_bar_0 C_bar_30 C_bar_30 C_bar_0 C_bar_30 C_bar_0 C_bar_30 C_bar_0 C_bar_30 C_bar_0
% Q_bar_0 Q_bar_30 Q_bar_0 Q_bar_30 Q_bar_0 Q_bar_30 Q_bar_0 Q_bar_30 Q_bar_30 Q_bar_0 Q_bar_30 Q_bar_0 Q_bar_30 Q_bar_0 Q_bar_30 Q_bar_0
% [0/45]4s C_bar_0 C_bar_45 C_bar_0 C_bar_45 C_bar_0 C_bar_45 C_bar_0 C_bar_45 C_bar_45 C_bar_0 C_bar_45 C_bar_0 C_bar_45 C_bar_0 C_bar_45 C_bar_0

% Q_bar_0 Q_bar_45 Q_bar_0 Q_bar_45 Q_bar_0 Q_bar_45 Q_bar_0 Q_bar_45 Q_bar_45 Q_bar_0 Q_bar_45 Q_bar_0 Q_bar_45 Q_bar_0 Q_bar_45 Q_bar_0

% [0/60]4s C_bar_0 C_bar_60 C_bar_0 C_bar_60 C_bar_0 C_bar_60 C_bar_0 C_bar_60 C_bar_60 C_bar_0 C_bar_60 C_bar_0 C_bar_60 C_bar_0 C_bar_60 C_bar_0

% Q_bar_0 Q_bar_60 Q_bar_0 Q_bar_60 Q_bar_0 Q_bar_60 Q_bar_0 Q_bar_60 Q_bar_60 Q_bar_0 Q_bar_60 Q_bar_0 Q_bar_60 Q_bar_0 Q_bar_60 Q_bar_0

% [0/75]4s C_bar_0 C_bar_75 C_bar_0 C_bar_75 C_bar_0 C_bar_75 C_bar_0 C_bar_75 C_bar_75 C_bar_0 C_bar_75 C_bar_0 C_bar_75 C_bar_0 C_bar_75 C_bar_0

% Q_bar_0 Q_bar_75 Q_bar_0 Q_bar_75 Q_bar_0 Q_bar_75 Q_bar_0 Q_bar_75 Q_bar_75 Q_bar_0 Q_bar_75 Q_bar_0 Q_bar_75 Q_bar_0 Q_bar_75 Q_bar_0

% [0/15]8T C_bar_15 C_bar_0 C_bar_15 C_bar_0 C_bar_15 C_bar_0 C_bar_15 C_bar_0 C_bar_15 C_bar_0 C_bar_15 C_bar_0 C_bar_15 C_bar_0 C_bar_15 C_bar_0

% Q_bar_15 Q_bar_0 Q_bar_15 Q_bar_0 Q_bar_15 Q_bar_0 Q_bar_15 Q_bar_0 Q_bar_15 Q_bar_0 Q_bar_15 Q_bar_0 Q_bar_15 Q_bar_0 Q_bar_15 Q_bar_0

% [0/30]8T C_bar_30 C_bar_0 C_bar_30 C_bar_0 C_bar_30 C_bar_0 C_bar_30 C_bar_0 C_bar_30 C_bar_0 C_bar_30 C_bar_0 C_bar_30 C_bar_0 C_bar_30 C_bar_0

% Q_bar_30 Q_bar_0 Q_bar_30 Q_bar_0 Q_bar_30 Q_bar_0 Q_bar_30 Q_bar_0 Q_bar_30 Q_bar_0 Q_bar_30 Q_bar_0 Q_bar_30 Q_bar_0 Q_bar_30 Q_bar_0

% [0/45]8T C_bar_45 C_bar_0 C_bar_45 C_bar_0 C_bar_45 C_bar_0 C_bar_45 C_bar_0 C_bar_45 C_bar_0 C_bar_45 C_bar_0 C_bar_45 C_bar_0 C_bar_45 C_bar_0

% Q_bar_45 Q_bar_0 Q_bar_45 Q_bar_0 Q_bar_45 Q_bar_0 Q_bar_45 Q_bar_0 Q_bar_45 Q_bar_0 Q_bar_45 Q_bar_0 Q_bar_45 Q_bar_0 Q_bar_45 Q_bar_0

% [0/60]8T C_bar_60 C_bar_0 C_bar_60 C_bar_0 C_bar_60 C_bar_0 C_bar_60 C_bar_0 C_bar_60 C_bar_0 C_bar_60 C_bar_0 C_bar_60 C_bar_0 C_bar_60 C_bar_0

% Q_bar_60 Q_bar_0 Q_bar_60 Q_bar_0 Q_bar_60 Q_bar_0 Q_bar_60 Q_bar_0 Q_bar_60 Q_bar_0 Q_bar_60 Q_bar_0 Q_bar_60 Q_bar_0 Q_bar_60 Q_bar_0

% [0/75]8T C_bar_75 C_bar_0 C_bar_75 C_bar_0 C_bar_75 C_bar_0 C_bar_75 C_bar_0 C_bar_75 C_bar_0 C_bar_75 C_bar_0 C_bar_75 C_bar_0 C_bar_75 C_bar_0
% Q_bar_75 Q_bar_0 Q_bar_75 Q_bar_0 Q_bar_75 Q_bar_0 Q_bar_75 Q_bar_0 Q_bar_75 Q_bar_0 Q_bar_75 Q_bar_0 Q_bar_75 Q_bar_0 Q_bar_75 Q_bar_0

% Teacher Stacking sequence study

% [+-15/0/0]2s C_bar_15 C_bar_115 C_bar_0 C_bar_0 C_bar_15 C_bar_115 C_bar_0 C_bar_0 C_bar_0 C_bar_0 C_bar_115 C_bar_15 C_bar_0 C_bar_0 C_bar_115 C_bar_15
% Q_bar_15 Q_bar_115 Q_bar_0 Q_bar_0 Q_bar_15 Q_bar_115 Q_bar_0 Q_bar_0 Q_bar_0 Q_bar_0 Q_bar_115 Q_bar_15 Q_bar_0 Q_bar_0 Q_bar_115 Q_bar_15
% [+-30/0/0]2s C_bar_30 C_bar_330 C_bar_0 C_bar_0 C_bar_30 C_bar_330 C_bar_0 C_bar_0 C_bar_0 C_bar_0 C_bar_330 C_bar_30 C_bar_0 C_bar_0 C_bar_330 C_bar_30
% Q_bar_30 Q_bar_330 Q_bar_0 Q_bar_0 Q_bar_30 Q_bar_330 Q_bar_0 Q_bar_0 Q_bar_0 Q_bar_0 Q_bar_330 Q_bar_30 Q_bar_0 Q_bar_0 Q_bar_330 Q_bar_30
% [+-45/0/0]2s C_bar_45 C_bar_445 C_bar_0 C_bar_0 C_bar_45 C_bar_445 C_bar_0 C_bar_0 C_bar_0 C_bar_0 C_bar_445 C_bar_45 C_bar_0 C_bar_0 C_bar_445 C_bar_45
% Q_bar_45 Q_bar_445 Q_bar_0 Q_bar_0 Q_bar_45 Q_bar_445 Q_bar_0 Q_bar_0 Q_bar_0 Q_bar_0 Q_bar_445 Q_bar_45 Q_bar_0 Q_bar_0 Q_bar_445 Q_bar_45
% [+-60/0/0]2s C_bar_60 C_bar_660 C_bar_0 C_bar_0 C_bar_60 C_bar_660 C_bar_0 C_bar_0 C_bar_0 C_bar_0 C_bar_660 C_bar_60 C_bar_0 C_bar_0 C_bar_660 C_bar_60
% Q_bar_60 Q_bar_660 Q_bar_0 Q_bar_0 Q_bar_60 Q_bar_660 Q_bar_0 Q_bar_0 Q_bar_0 Q_bar_0 Q_bar_660 Q_bar_60 Q_bar_0 Q_bar_0 Q_bar_660 Q_bar_60
% [+-75/0/0]2s C_bar_75 C_bar_775 C_bar_0 C_bar_0 C_bar_75 C_bar_775 C_bar_0 C_bar_0 C_bar_0 C_bar_0 C_bar_775 C_bar_75 C_bar_0 C_bar_0 C_bar_775 C_bar_75
% Q_bar_75 Q_bar_775 Q_bar_0 Q_bar_0 Q_bar_75 Q_bar_775 Q_bar_0 Q_bar_0 Q_bar_0 Q_bar_0 Q_bar_775 Q_bar_75 Q_bar_0 Q_bar_0 Q_bar_775 Q_bar_75

% [+-15/0/0]4T C_bar_0 C_bar_0 C_bar_115 C_bar_15 C_bar_0 C_bar_0 C_bar_115 C_bar_15 C_bar_0 C_bar_0 C_bar_115 C_bar_15 C_bar_0 C_bar_0 C_bar_115 C_bar_15
% Q_bar_0 Q_bar_0 Q_bar_115 Q_bar_15 Q_bar_0 Q_bar_0 Q_bar_115 Q_bar_15 Q_bar_0 Q_bar_0 Q_bar_115 Q_bar_15 Q_bar_0 Q_bar_0 Q_bar_115 Q_bar_15
% [+-30/0/0]4T C_bar_0 C_bar_0 C_bar_330 C_bar_30 C_bar_0 C_bar_0 C_bar_330 C_bar_30 C_bar_0 C_bar_0 C_bar_330 C_bar_30 C_bar_0 C_bar_0 C_bar_330 C_bar_30
% Q_bar_0 Q_bar_0 Q_bar_330 Q_bar_30 Q_bar_0 Q_bar_0 Q_bar_330 Q_bar_30 Q_bar_0 Q_bar_0 Q_bar_330 Q_bar_30 Q_bar_0 Q_bar_0 Q_bar_330 Q_bar_30
% [+-45/0/0]4T C_bar_0 C_bar_0 C_bar_445 C_bar_45 C_bar_0 C_bar_0 C_bar_445 C_bar_45 C_bar_0 C_bar_0 C_bar_445 C_bar_45 C_bar_0 C_bar_0 C_bar_445 C_bar_45
% Q_bar_0 Q_bar_0 Q_bar_445 Q_bar_45 Q_bar_0 Q_bar_0 Q_bar_445 Q_bar_45 Q_bar_0 Q_bar_0 Q_bar_445 Q_bar_45 Q_bar_0 Q_bar_0 Q_bar_445 Q_bar_45
% [+-60/0/0]4T C_bar_0 C_bar_0 C_bar_660 C_bar_60 C_bar_0 C_bar_0 C_bar_660 C_bar_60 C_bar_0 C_bar_0 C_bar_660 C_bar_60 C_bar_0 C_bar_0 C_bar_660 C_bar_60
% Q_bar_0 Q_bar_0 Q_bar_660 Q_bar_60 Q_bar_0 Q_bar_0 Q_bar_660 Q_bar_60 Q_bar_0 Q_bar_0 Q_bar_660 Q_bar_60 Q_bar_0 Q_bar_0 Q_bar_660 Q_bar_60
% [+-75/0/0]4T C_bar_0 C_bar_0 C_bar_775 C_bar_75 C_bar_0 C_bar_0 C_bar_775 C_bar_75 C_bar_0 C_bar_0 C_bar_775 C_bar_75 C_bar_0 C_bar_0 C_bar_775 C_bar_75
% Q_bar_0 Q_bar_0 Q_bar_775 Q_bar_75 Q_bar_0 Q_bar_0 Q_bar_775 Q_bar_75 Q_bar_0 Q_bar_0 Q_bar_775 Q_bar_75 Q_bar_0 Q_bar_0 Q_bar_775 Q_bar_75

% [0/0/+-15]2s C_bar_0 C_bar_0 C_bar_15 C_bar_115 C_bar_0 C_bar_0 C_bar_15 C_bar_115 C_bar_115 C_bar_15 C_bar_0 C_bar_0 C_bar_115 C_bar_15 C_bar_0 C_bar_0
% Q_bar_0 Q_bar_0 Q_bar_15 Q_bar_115 Q_bar_0 Q_bar_0 Q_bar_15 Q_bar_115 Q_bar_115 Q_bar_15 Q_bar_0 Q_bar_0 Q_bar_115 Q_bar_15 Q_bar_0 Q_bar_0
% [0/0/+-30]2s C_bar_0 C_bar_0 C_bar_30 C_bar_330 C_bar_0 C_bar_0 C_bar_30 C_bar_330 C_bar_330 C_bar_30 C_bar_0 C_bar_0 C_bar_330 C_bar_30 C_bar_0 C_bar_0

% Q_bar_0 Q_bar_0 Q_bar_30 Q_bar_330 Q_bar_0 Q_bar_0
Q_bar_30 Q_bar_330 Q_bar_330 Q_bar_30 Q_bar_0 Q_bar_0 Q_bar_330
Q_bar_30 Q_bar_0 Q_bar_0
% [0/0/+-45]2s C_bar_0 C_bar_0 C_bar_45 C_bar_445 C_bar_0 C_bar_0
C_bar_45 C_bar_445 C_bar_445 C_bar_45 C_bar_0 C_bar_0 C_bar_445
C_bar_45 C_bar_0 C_bar_0
% Q_bar_0 Q_bar_0 Q_bar_45 Q_bar_445 Q_bar_0 Q_bar_0
Q_bar_45 Q_bar_445 Q_bar_445 Q_bar_45 Q_bar_0 Q_bar_0 Q_bar_445
Q_bar_45 Q_bar_0 Q_bar_0
% [0/0/+-60]2s C_bar_0 C_bar_0 C_bar_60 C_bar_660 C_bar_0 C_bar_0
C_bar_60 C_bar_660 C_bar_660 C_bar_60 C_bar_0 C_bar_0 C_bar_660
C_bar_60 C_bar_0 C_bar_0
% Q_bar_0 Q_bar_0 Q_bar_60 Q_bar_660 Q_bar_0 Q_bar_0
Q_bar_60 Q_bar_660 Q_bar_660 Q_bar_60 Q_bar_0 Q_bar_0 Q_bar_660
Q_bar_60 Q_bar_0 Q_bar_0
% [0/0/+-75]2s C_bar_0 C_bar_0 C_bar_75 C_bar_775 C_bar_0 C_bar_0
C_bar_75 C_bar_775 C_bar_775 C_bar_75 C_bar_0 C_bar_0 C_bar_775
C_bar_75 C_bar_0 C_bar_0
% Q_bar_0 Q_bar_0 Q_bar_75 Q_bar_775 Q_bar_0 Q_bar_0
Q_bar_75 Q_bar_775 Q_bar_775 Q_bar_75 Q_bar_0 Q_bar_0 Q_bar_775
Q_bar_75 Q_bar_0 Q_bar_0

% [15/0/0/-15]2s C_bar_15 C_bar_0 C_bar_0 C_bar_115 C_bar_15 C_bar_0
C_bar_0 C_bar_115 C_bar_115 C_bar_0 C_bar_0 C_bar_15 C_bar_115 C_bar_0
C_bar_0 C_bar_15
% Q_bar_15 Q_bar_0 Q_bar_0 Q_bar_115 Q_bar_15 Q_bar_0
Q_bar_0 Q_bar_115 Q_bar_115 Q_bar_0 Q_bar_0 Q_bar_15 Q_bar_115
Q_bar_0 Q_bar_0 Q_bar_15
% [30/0/0/-30]2s C_bar_30 C_bar_0 C_bar_0 C_bar_330 C_bar_30 C_bar_0
C_bar_0 C_bar_330 C_bar_330 C_bar_0 C_bar_0 C_bar_30 C_bar_330 C_bar_0
C_bar_0 C_bar_30
% Q_bar_30 Q_bar_0 Q_bar_0 Q_bar_330 Q_bar_30 Q_bar_0
Q_bar_0 Q_bar_330 Q_bar_330 Q_bar_0 Q_bar_0 Q_bar_30 Q_bar_330
Q_bar_0 Q_bar_0 Q_bar_30
% [45/0/0/-45]2s C_bar_45 C_bar_0 C_bar_0 C_bar_445 C_bar_45 C_bar_0
C_bar_0 C_bar_445 C_bar_445 C_bar_0 C_bar_0 C_bar_45 C_bar_445 C_bar_0
C_bar_0 C_bar_45
% Q_bar_45 Q_bar_0 Q_bar_0 Q_bar_445 Q_bar_45 Q_bar_0
Q_bar_0 Q_bar_445 Q_bar_445 Q_bar_0 Q_bar_0 Q_bar_45 Q_bar_445
Q_bar_0 Q_bar_0 Q_bar_45

% [60/0/0/-60]2s C_bar_60 C_bar_0 C_bar_0 C_bar_660 C_bar_60 C_bar_0 C_bar_0 C_bar_660 C_bar_660 C_bar_0 C_bar_0 C_bar_60 C_bar_660 C_bar_0 C_bar_0 C_bar_0 C_bar_60
% Q_bar_60 Q_bar_0 Q_bar_0 Q_bar_660 Q_bar_60 Q_bar_0 Q_bar_0 Q_bar_660 Q_bar_660 Q_bar_0 Q_bar_0 Q_bar_60 Q_bar_660 Q_bar_0 Q_bar_0 Q_bar_60
% [75/0/0/-75]2s C_bar_75 C_bar_0 C_bar_0 C_bar_775 C_bar_75 C_bar_0 C_bar_0 C_bar_775 C_bar_775 C_bar_0 C_bar_0 C_bar_75 C_bar_775 C_bar_0 C_bar_0 C_bar_0 C_bar_75
% Q_bar_75 Q_bar_0 Q_bar_0 Q_bar_775 Q_bar_75 Q_bar_0 Q_bar_0 Q_bar_775 Q_bar_775 Q_bar_0 Q_bar_0 Q_bar_75 Q_bar_775 Q_bar_0 Q_bar_0 Q_bar_0 Q_bar_75

% [15/0/0/-15]4T C_bar_115 C_bar_0 C_bar_0 C_bar_15 C_bar_115 C_bar_0 C_bar_0 C_bar_15 C_bar_115 C_bar_0 C_bar_0 C_bar_15 C_bar_115 C_bar_0 C_bar_0 C_bar_0 C_bar_15
% Q_bar_115 Q_bar_0 Q_bar_0 Q_bar_15 Q_bar_115 Q_bar_0 Q_bar_0 Q_bar_15 Q_bar_115 Q_bar_0 Q_bar_0 Q_bar_15 Q_bar_115 Q_bar_0 Q_bar_0 Q_bar_0 Q_bar_15
% [30/0/0/-30]4T C_bar_330 C_bar_0 C_bar_0 C_bar_30 C_bar_330 C_bar_0 C_bar_0 C_bar_30 C_bar_330 C_bar_0 C_bar_0 C_bar_30 C_bar_330 C_bar_0 C_bar_0 C_bar_0 C_bar_30
% Q_bar_330 Q_bar_0 Q_bar_0 Q_bar_30 Q_bar_330 Q_bar_0 Q_bar_0 Q_bar_30 Q_bar_330 Q_bar_0 Q_bar_0 Q_bar_30 Q_bar_330 Q_bar_0 Q_bar_0 Q_bar_0 Q_bar_30
% [45/0/0/-45]4T C_bar_445 C_bar_0 C_bar_0 C_bar_45 C_bar_445 C_bar_0 C_bar_0 C_bar_45 C_bar_445 C_bar_0 C_bar_0 C_bar_45 C_bar_445 C_bar_0 C_bar_0 C_bar_0 C_bar_45
% Q_bar_445 Q_bar_0 Q_bar_0 Q_bar_45 Q_bar_445 Q_bar_0 Q_bar_0 Q_bar_45 Q_bar_445 Q_bar_0 Q_bar_0 Q_bar_45 Q_bar_445 Q_bar_0 Q_bar_0 Q_bar_0 Q_bar_45
% [60/0/0/-60]4T C_bar_660 C_bar_0 C_bar_0 C_bar_60 C_bar_660 C_bar_0 C_bar_0 C_bar_60 C_bar_660 C_bar_0 C_bar_0 C_bar_60 C_bar_660 C_bar_0 C_bar_0 C_bar_0 C_bar_60
% Q_bar_660 Q_bar_0 Q_bar_0 Q_bar_60 Q_bar_660 Q_bar_0 Q_bar_0 Q_bar_60 Q_bar_660 Q_bar_0 Q_bar_0 Q_bar_60 Q_bar_660 Q_bar_0 Q_bar_0 Q_bar_0 Q_bar_60
% [75/0/0/-75]4T C_bar_775 C_bar_0 C_bar_0 C_bar_75 C_bar_775 C_bar_0 C_bar_0 C_bar_75 C_bar_775 C_bar_0 C_bar_0 C_bar_75 C_bar_775 C_bar_0 C_bar_0 C_bar_0 C_bar_75

```
%                   Q_bar_775 Q_bar_0 Q_bar_0 Q_bar_75 Q_bar_775 Q_bar_0
Q_bar_0 Q_bar_75 Q_bar_775 Q_bar_0 Q_bar_0 Q_bar_75 Q_bar_775 Q_bar_0
Q_bar_0 Q_bar_75

%   [30/90/90/30]2s    C_bar_30 C_bar_90 C_bar_90 C_bar_30 C_bar_30
C_bar_90 C_bar_90 C_bar_30 C_bar_30 C_bar_90 C_bar_90 C_bar_30
C_bar_30 C_bar_90 C_bar_90 C_bar_30
%                   Q_bar_30 Q_bar_90 Q_bar_90 Q_bar_30 Q_bar_30 Q_bar_90
Q_bar_90 Q_bar_30 Q_bar_30 Q_bar_90 Q_bar_90 Q_bar_30 Q_bar_30
Q_bar_90 Q_bar_90 Q_bar_30



C1=[C_bar_30 C_bar_90 C_bar_90 C_bar_30 C_bar_30 C_bar_90 C_bar_90
C_bar_30 C_bar_30 C_bar_90 C_bar_90 C_bar_30 C_bar_30 C_bar_90
C_bar_90 C_bar_30];
Q1=[Q_bar_30 Q_bar_90 Q_bar_90 Q_bar_30 Q_bar_30 Q_bar_90 Q_bar_90
Q_bar_30 Q_bar_30 Q_bar_90 Q_bar_90 Q_bar_30 Q_bar_30 Q_bar_90
Q_bar_90 Q_bar_30];
t1=[h0 h1 h2 h3 h4 h5 h6 h7 h8 h9 h10 h11 h12 h13 h14 h15 h16];
C2=[C1(4:5,[4 5]) C1(4:5,[10 11]) C1(4:5,[16 17]) C1(4:5,[22 23]) C1(4:5,[28
29]) C1(4:5,[34 35]) C1(4:5,[40 41]) C1(4:5,[46 47]) C1(4:5,[52 53]) C1(4:5,[58
59]) C1(4:5,[64 65]) C1(4:5,[70 71]) C1(4:5,[76 77]) C1(4:5,[82 83]) C1(4:5,[88
89]) C1(4:5,[94 95])];



F1=zeros(2,2);
for ie=1:16
        t1ie=t1(ie+1)-t1(ie);
   C2ie=[C2(:,ie*2-1) C2(:,ie*2)] ;
   F1ie=C2ie+t1ie;
   F1=F1+F1ie;
end
F1;
FF=F1*tply;
Fstar=inv(FF);
F55=FF(2,2)/thickness;
F55star=Fstar(2,2);
```

```
Gxz_from_theoretical=1/(F55star*thickness)  %F55=Gxz
Sbar=Gxz_from_theoretical; % sbar=shear stiffness


A1=zeros(3,3);
for ie=1:16
   t1ie=t1(ie+1)-t1(ie);
   Q1ie=[Q1(:,ie*3-2) Q1(:,ie*3-1) Q1(:,ie*3)];
   A1ie=Q1ie*t1ie;
   A1=A1+A1ie;
end
A1;

B1=zeros(3,3);
for ie=1:16
   t1ie=t1(ie+1)^2-t1(ie)^2;
   Q1ie=[Q1(:,ie*3-2) Q1(:,ie*3-1) Q1(:,ie*3)];
   B1ie=1/2*(Q1ie*t1ie);
   B1=B1+B1ie;
end
B1;

D1=zeros(3,3);
for ie=1:16
   t1ie=t1(ie+1)^3-t1(ie)^3;
   Q1ie=[Q1(:,ie*3-2) Q1(:,ie*3-1) Q1(:,ie*3)];
   D1ie=1/3*(Q1ie*t1ie);
   D1=D1+D1ie;
end
D1;


mat=[A1 B1
   B1 D1];
INV=inv(mat);
a=INV(1:3,[1 2 3]);
b=INV(1:3,[4 5 6]);
bT=INV(4:6,[1 2 3]);
d=INV(4:6,[4 5 6]);
a11=a(1,1);
a12=a(1,2);
```

```
a16=a(1,3);
a21=a(2,1);
a22=a(2,2);
a26=a(2,3);
a61=a(3,1);
a62=a(3,2);
a66=a(3,3);

b11=b(1,1);
b12=b(1,2);
b16=b(1,3);
b21=b(2,1);
b22=b(2,2);
b26=b(2,3);
b61=b(3,1);
b62=b(3,2);
b66=b(3,3);

d11=d(1,1);
d12=d(1,2);
d16=d(1,3);
d21=d(2,1);
d22=d(2,2);
d26=d(2,3);
d61=d(3,1);
d62=d(3,2);
d66=d(3,3);

% use narrow beam effect to find bending rigidity
a1star=a11-(b16^2)/d66;
b1star=b11-(b16*d16/d66);
d1star=d11-(d16^2)/d66;

EI=bw/d1star;
q=P/L;

Sbar=Gxz_from_theoretical*A; % sbar=shear stiffness


% Case 1
WB1=(5/384)*((q*(L^4)))/EI       % WB=deflection due to bending
```

```
WS1=1.2*(q*(L^2))/(8*Sbar)          % WS=deflection due to shear
WBS1=WS1/WB1
W1=WB1+WS1
WSL1=WS1/W1
% Case 2
WB2=(1/48)*((P*(L^3)))/EI
WS2=1.2*(P*(L))/(4*Sbar)
WBS2=WS2/WB2
W2=WB2+WS2
WSL2=WS2/W2
% Case 3
WB3=(1/384)*((q*(L^4)))/EI
WS3=1.2*(q*(L^2))/(8*Sbar)
WBS3=WS3/WB3
W3=WB3+WS3
WSL3=WS3/W3
% Case 4
WB4=(1/192)*((P*(L^3)))/EI
WS4=1.2*(P*(L))/(4*Sbar)
WBS4=WS4/WB4
W4=WB4+WS4
WSL4=WS4/W4
% Case 5
WB5=(1/8)*((q*(L^4)))/EI
WS5=1.2*(q*(L^2))/(2*Sbar)
WBS5=WS5/WB5
W5=WB5+WS5
WSL5=WS5/W5
% Case 6
WB6=(1/3)*((P*(L^3)))/EI
WS6=1.2*(P*(L))/(Sbar)
WBS6=WS6/WB6
W6=WB6+WS6
WSL6=WS6/W6
```

References

1. Skudra, A. M., Kruklinsh, A. A., Bulavs, F. Y. and Gurvich, M. R. (1991). Structural Analysis of Composite Beam Systems, Technomic, Lancaster, PA.
2. Vasiliev, V. V. and Jones, R. M. (1993). Chapter 4 in Mechanics of Composite Structures, Taylor & Francis, Washington, DC.
3. Barbero, E.J., (1998). Chapter 8 in Introduction to Composite Materials Design, Taylor & Francis, Washington, DC.
4. Chen, D. J. and Chan, W. S. (1996). "Use of Composite Effective Moduli for Lumping Layers in Finite Element Analysis", Proceedings of the 37TH AIAA SDM Conference, Salt Lake City, Utah, April 15-17, 1996.
5. Chan, W. S., Lin, C. Y., Liang Y. C. and Hwu., C., (2006). "Equivalent Thermal Expansion Coefficient of Lumped Layer in Laminated Composites", Composites Science and Technology 66 2402–2408
6. Hu, J. (1995). Analysis of laminated composite cantilever beams (Master thesis, Department of Aerospace Engineering, University of Texas at Arlington
7. Drummond, J. A., and Chan, W. S. (1999). "Fabrication, Analysis, and Experimentation of a Practically Constructed Laminated Composite I-Beam under Pure Bending", Journal of Thermoplastic Composite Materials, volume 12, May 1999, pp. 177-187.
8. Parambil, J. C., Chan, W.S., Lawrence, K. L., and Sanghavi, V.M., (2011). "Stress Analysis for Composite I-Beams by a Non-Conventional Method", Proceedings of the 25th Technical Conference of American Society for Composites, Paper No. 1027.
9. Sanghavi, V. M. S. and Chan, W. S. (2013). "Torsional Analysis of a Composite I-beam", Proceedings of the American Society for Composites 28th Technical Conference.
10. Karama, M., Afaq, K. S., and Mistou, S. (2003). "Mechanical behavior of laminated composite beam by the new multi-layered laminated composite structures model with

transverse shear stress continuity." *International Journal of Solids and Structures* 40, no. 6, 1525-1546.

11. Akavci, S., Seren, H. R. Yerli, and Dogan, A. (2007). "The first order shear deformation theory for symmetrically laminated composite plates on elastic foundation." *Arabian Journal for Science and Engineering* 32, no. 2, 341.
12. Schnabl, S., Miran, S., Goran, T., and Igor, P. (2007). "Analytical solution of two-layer beam taking into account interlayer slip and shear deformation. "*Journal of structural engineering* 133, no. 6, 886-894.
13. Ascione, L., Feo, L., and Mancusi, G., (2000). “On the statical behaviour of fiber-reinforcedpolymer thin-walled beams”, ELSEVIER, Composites, Part B, vol. 3,, pp. 643-654.
14. Wu, X. and Sun, C. T. (1992). “Simplified Theory for Composite Thin-Walled Beams”, AIAA Journal, Vol. 30. PP2945-2952.
15. Berthelot, J. M. (2012). *Composite materials: mechanical behavior and structural analysis*. Springer Science & Business Media.
16. Carlsson, L. A., & Kardomateas, G. A. (2011). *Structural and failure mechanics of sandwich composites* (Vol. 121). Springer Science & Business Media.
17. Daniel, I. M., Ishai, O., Daniel, I. M., & Daniel, I. (1994). *Engineering mechanics of composite materials* (Vol. 3). New York: Oxford university press.
18. Becker, A. A. (2004). An introductory guide to finite element analysis. New York, NY: The American Society of Mechanical Engineers.

BIOGRAPHICAL INFORMATION

Wei-Tsen Lu received his B.S in aerospace engineering from Tamkang University. His academic interest lies in composite analysis, design, and modeling. He further plans to pursue PhD in UTA to learn more about composite materials and related fields.